

**UCSF**

**UC San Francisco Electronic Theses and Dissertations**

**Title**

Electrophysiologic and pharmacologic properties of mammalian sensory neurons

**Permalink**

<https://escholarship.org/uc/item/0vr511fq>

**Author**

Jaffe, Richard Andrew

**Publication Date**

1977

Peer reviewed|Thesis/dissertation

ELECTROPHYSIOLOGIC AND PHARMACOLOGIC PROPERTIES  
OF MAMMALIAN SENSORY NEURONS

by

Richard Andrew Jaffe  
A.B. University of California Berkeley 1969  
M.A. California State University Hayward 1971

DISSERTATION

Submitted in partial satisfaction of the requirements for the degree of

DOCTOR OF PHILOSOPHY

in

Physiology

in the

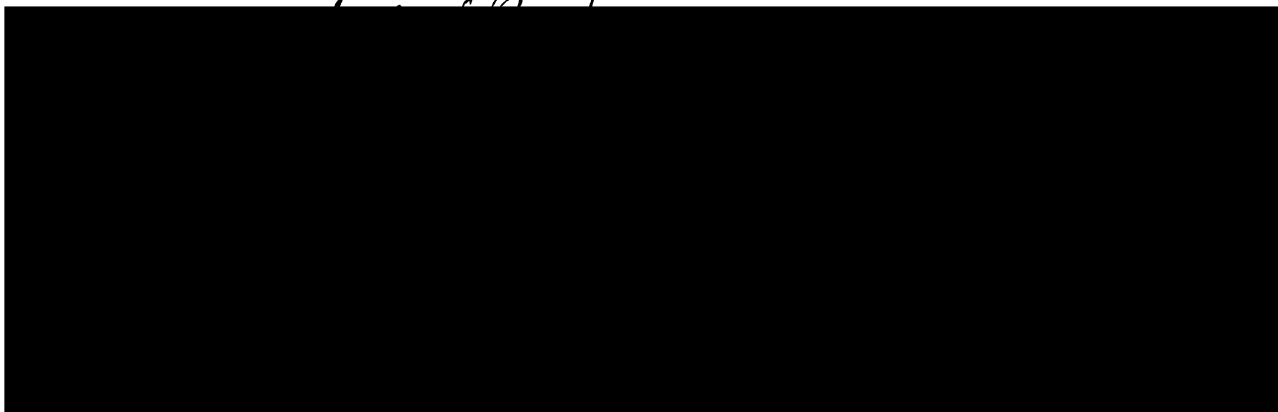
GRADUATE DIVISION

(San Francisco)

of the

UNIVERSITY OF CALIFORNIA

*1-2-77*



Date

Librarian

JAN 2 1977

Degree Conferred: .....

## ELECTROPHYSIOLOGIC AND PHARMACOLOGIC PROPERTIES OF MAMMALIAN SENSORY NEURONS

## ABSTRACT

Passive and active electrical properties of the soma membrane of neurons in nodose ganglia removed from cats and rabbits were studied. The ganglia were maintained in vitro and were superfused at 37°C with a solution formulated to approximate the extracellular fluid of each species. The solution was buffered to pH 7.34, continuously equilibrated with 95% O<sub>2</sub> and 5% CO<sub>2</sub>, and contained dialyzed calf serum and glucose. These properties were also examined in nodose ganglion neurons in vivo. Intracellular recordings were obtained with glass micropipettes filled with either 3 M KCl or 5 M K acetate. Mean values ( $\pm$ SEM) for the resting membrane potential ( $-49 \pm 0.4$  mV;  $-52 \pm 0.4$  mV), input resistance ( $21 \pm 0.9$  M $\Omega$ ;  $18 \pm 0.4$  M $\Omega$ ), time constant ( $3.6 \pm 0.16$  msec;  $3.0 \pm 0.14$  msec) and action potential amplitude ( $78 \pm 0.7$  mV;  $87 \pm 0.36$  mV), duration ( $1.7 \pm 0.05$  msec;  $1.7 \pm 0.02$  msec), rate of rise ( $151 \pm 10$  V/sec;  $217 \pm 3$  V/sec), rate of fall ( $72 \pm 2$  V/sec;  $75 \pm 2$  V/sec) and afterhyperpolarization ( $18 \pm 0.5$  mV;  $15 \pm 0.2$  mV) were determined for both rabbit and cat nodose ganglion neurons respectively. Values obtained in vitro did not differ significantly from those obtained in vivo. Based on a comparison of electrophysiologic properties of the soma membrane, neurons in the nodose ganglion appear to be a uniform population, despite the different sensory modalities conveyed by the afferent fibers. Many neurons, both in vitro and in vivo developed a persistent hyperpolarization when repetitive action potentials occurred in the soma. This hyperpolarization was apparent at frequencies as low as 1-2 Hz, persisted

for up to 5 s after the occurrence of the last somatic spike, and sometimes caused failure of somatic spikes to be generated. Neurons in both species differed in their responses to supra-threshold depolarization applied through the recording electrode. Some neurons produced a train of action potentials which lasted for the duration of the depolarizing pulse, the frequency of the train being related to the magnitude of depolarization. Other neurons responded with only a single spike or brief burst of action potentials at the beginning of depolarization to threshold. It is suggested that the adaptive properties of the soma membrane of a peripheral sensory neuron are similar to those of its sensory ending, and that electrophysiological studies of the soma membrane may provide an opportunity to examine mechanisms of receptor adaptation. The ionic contributions to the resting and action potentials in neurons in cat nodose ganglia were studied. The maximum slope of the potassium-potential curve (25 mV/decade), however, was significantly less than the Nernst predicted value of 61 mV/decade. The amplitude of the afterhyperpolarization in these cat sensory neurons was less affected by changes in external potassium concentration than was the resting potential. The membrane potential depolarized when the external sodium concentration was reduced. This is in marked contrast to findings in similar studies in other species which reported either no change or slight hyperpolarization of the resting potential upon removal of extracellular sodium. A small rise in external chloride ion concentration increased the resting membrane potential while significantly reducing the membrane resistance.

Membrane resistance was also significantly affected by changes in external calcium concentration. Measurements of the specific ion contributions to the resting and action potentials have revealed several differences between these mammalian neurons and the neurons of nonmammalian species. These differences need to be studied in more detail before any definitive conclusions can be reached. The pharmacologic actions of a variety of drugs were tested on neurons in cat and rabbit nodose ganglia. Results suggest that the cell bodies possess receptors for drugs, and that drug-induced effects may result in the initiation of action potentials or the modification of pre-existing activity. Thus, the nodose ganglion may be an important site of action for the autonomic effects of some drugs.

## ACKNOWLEDGEMENT

I thank the members of my Dissertation Committee, Dr. H. M. Coleridge, Dr. E. Mayeri, and the Chairman and my advisor Dr. S. R. Sampson, for their critical advice in the preparation of this thesis. I am particularly grateful to Dr. Sampson for providing me with laboratory facilities, and for his encouragement and collaboration in this study. I am also grateful to Mr. E. Mentzer, Mr. J. R. Wall, and Mr. S. G. Winston for their invaluable advice and assistance on technical matters. Finally, I am grateful to Professor W. F. Ganong for his generous support, and Professor L. L. Bennett for his constant advice and encouragement.

"...Are we nearly there?" Alice managed to pant out at last.

"Nearly there!" the Queen repeated. "Why, we passed it ten minutes ago! Faster!"

"Through the  
Looking Glass"

- Lewis Carroll

## TABLE OF CONTENTS

<u>ACKNOWLEDGEMENT</u> . . . . .	2
<u>LIST OF TABLES.</u> . . . . .	6
<u>LIST OF FIGURES</u> . . . . .	7
<u>INTRODUCTION.</u> . . . . .	9
I. Statement of the Problem. . . . .	9
II. Historical Background . . . . .	10
A. Introduction . . . . .	10
B. Electrophysiologic Properties of Vertebrate Neurons. . . . .	15
C. Roles of Extracellular Ions. . . . .	26
1. Potassium . . . . .	26
2. Sodium. . . . .	28
3. Calcium . . . . .	34
4. Chloride. . . . .	36
III. The Nodose Ganglion of the Vagus Nerve. . . . .	38
A. Cellular Structure and Function. . . . .	38
B. Pharmacology . . . . .	39
C. The Nodose Ganglion: A Possible Model for the Study of Drug Action . . . . .	40
<u>METHODS</u> . . . . .	44
I. Intracellular Recording <u>In Vivo</u> . . . . .	44
II. Intracellular Recording <u>In Vitro</u> . . . . .	47



III.	Superfusion Media for <u>In Vitro</u> Experiments. . . . .	49
IV.	The Recording Chamber . . . . .	52
V.	Intracellular Recording Apparatus . . . . .	55
VI.	Data Analysis . . . . .	58
VII.	Ionic Contributions to Passive and Active Properties. . . . .	63
VIII.	Pharmacological Techniques. . . . .	64
<u>RESULTS</u> . . . . .		67
I.	Superfusion Media Selection . . . . .	68
II.	Passive Electrophysiologic Properties . . . . .	69
A.	Resting Membrane Potentials. . . . .	69
B.	Membrane Resistance. . . . .	70
C.	Membrane Time Constant . . . . .	73
D.	Membrane Capacitance . . . . .	74
E.	Specific Membrane Resistance . . . . .	74
III.	Active Electrophysiologic Properties. . . . .	77
A.	Spontaneous and Repetitive Activity. . . . .	77
B.	The Action Potential . . . . .	78
C.	Effects of Depolarizing and Hyperpolarizing Currents . . . . .	81
D.	Repetitive Stimulation . . . . .	84
E.	Latency and Conduction Velocity. . . . .	85
IV.	Ionic Contributions . . . . .	86
A.	Potassium. . . . .	86
B.	Sodium . . . . .	88
C.	Calcium. . . . .	90
D.	Chloride . . . . .	92

V.	Pharmacologic Properties. . . . .	92
A.	Tetrodotoxin . . . . .	93
B.	Tetraethylammonium Ions. . . . .	94
C.	Ouabain. . . . .	94
D.	Metabolic Inhibitors . . . . .	95
E.	Local and General Anesthetics. . . . .	95
F.	Veratridine, Phenyldiguanide, and 5-Hydroxytryptamine. . . . .	96
<u>DISCUSSION.</u> . . . . .		98
I.	Passive Electrophysiologic Properties . . . . .	99
II.	Active Electrophysiologic Properties. . . . .	102
III.	Ionic Contributions . . . . .	109
IV.	Pharmacologic Properties. . . . .	120
<u>CONCLUSIONS</u> . . . . .		126
<u>SUMMARY</u> . . . . .		129

LIST OF TABLES

1.	Passive and Active Electrophysiologic Properties of Vertebrate Neurons. . . . .	17
2.	Comparison of Serum Values and Buffer Compositions . . . . .	50
3.	Composition of Extracellular Bathing Media Used in this Study . . . . .	53
4.	A Comparison of Preliminary Results Obtained <u>In Vitro</u> with Buffer Types I, II, and III. . . . .	68
5.	Passive and Active Electrophysiologic Properties of Neurons in Mammalian Nodose Ganglia . . . . .	75
6.	Intracellular Ionic Concentrations in Mammalian Neurons. . . . .	118

LIST OF FIGURES

1.	Diagram of Perfusion Chamber. . . . .	172
2.	The Effect of Current Passage on Electrode Resistance. . . . .	174
3.	Distribution of Resting Membrane Potentials . . . . .	176
4.	Responses to Intracellularly Applied Polarizing Current Pulses . . . . .	178
5.	Examples of Current-Voltage Relations . . . . .	180
6.	Input Resistance as a Function of Membrane Potential . . . . .	182
7.	Example of Rectifying Behavior. . . . .	184
8.	Examples of Intracellularly Recorded Action Potentials . . . . .	186
9.	Delay and Failure of Somatic Spike Generation . . . . .	188
10.	Example of Directly Evoked Action Potential . . . . .	190
11.	Adaptation Types. . . . .	192
12.	Adaptation in a Type IV Neuron. . . . .	194
13.	Blockade of Somatic Spike by Hyperpolarizing Current . . . . .	196

LIST OF FIGURES (continued)

14.	Influence of the Membrane Potential on the Afterhyperpolarization. . . . .	198
15.	Activity-Induced Hyperpolarization. . . . .	200
16.	Histogram of Latencies. . . . .	202
17.	Histogram Comparing Latency and Conduction Velocity Distributions. . . . .	204
18.	Plot of External Potassium Concentration Versus Membrane Potential, Resistance and Afterhyperpolarization. . . . .	206
19.	Effects of Low Sodium on the Action Potential Configuration . . . . .	208
20.	Effects of TEA. . . . .	210
21.	Effects of Lidocaine. . . . .	212
22.	Effects of Atropine . . . . .	214
23.	Effects of Veratridine. . . . .	216
24.	Veratridine Induced Action Potential Train. . . . .	218

## I. STATEMENT OF THE PROBLEM

Many of the generally accepted, basic principles of neurophysiology such as those used to explain the maintenance of the resting membrane potential, and the generation and propagation of the action potential have been derived primarily from the study of invertebrate giant axons and neurons, and frog skeletal muscle cells. The utility of, and significance of the data obtained from these preparations cannot be overestimated. In large part, however, they owe much of their importance to the fact that they are relatively easy to study with available techniques. In marked contrast to mammalian cells, these axons and neurons are often quite large and remarkably rugged, being able to maintain and generate, resting and action potentials long after they have been removed from the animal and, in some cases, even after the forcible extrusion of their cytoplasm. These simple systems, in addition to providing the foundations of presently accepted neurophysiologic principles, are being used to study the effects of a variety of pharmacologic agents and provide insight into their mechanisms of action. An implicit assumption is that observations on these simple systems, with perhaps minor modification, are directly applicable to all neurons. The universality of that assumption may be questioned.

Until now few adult mammalian nerve cell preparations have been available that allow the precise manipulation of the extracellular environment and the control of current passing through the membrane while recording the transmembrane electrical potential. The need

for this type of preparation becomes apparent if one accepts as an important goal of neurophysiology the elucidation of the fundamental mechanisms underlying mammalian neural functions. The purpose of this project, therefore, was to develop the procedures and techniques necessary for the short-term maintenance of adult mammalian nodose ganglion neurons in vitro. The primary goal was to characterize some of the basic electrophysiologic and pharmacologic properties of the soma membrane of these pseudounipolar sensory neurons with the use of intracellular microelectrode techniques.

## II. HISTORICAL BACKGROUND

### A. Introduction

In 1902, Burnstein (26) proposed an explanation for the potential difference observed between the intact surface of a nerve or muscle fiber and its cut surface. He suggested that the cell was surrounded by a specialized membrane which was selectively permeable to potassium ions but not to sodium ions. Moreover, he proposed that during the action potential, this selective permeability barrier broke down resulting in the elimination of the membrane potential. However, with the advent of intracellular recording techniques, it became apparent that the amplitude of the action potential was significantly greater than the resting potential. Hodgkin and Katz (111) proposed that the action potential was due to a large and selective increase in the permeability of the membrane to sodium and that the resulting

inward movement of sodium ions down their electrochemical gradient accounted for the overshoot of the action potential. According to Hodgkin and Katz, the membrane at rest was predominantly permeable to potassium and, thus, its potential approached the potassium equilibrium potential calculated from the Nernst equation (172).

The origin of the membrane potential is fundamental to the understanding of all neural phenomena. The Nernst equation describes the magnitude of the equilibrium potential as a function of the unequal distribution of an ion species on either side of a semipermeable membrane (172):

$$E = \frac{RT}{ZF} \ln \frac{C_1}{C_2}$$

where  $E$  = equilibrium potential,  $R$  = gas constant,  $T$  = absolute temperature,  $Z$  = ion valence,  $F$  = Faraday constant,  $C_1$  and  $C_2$  = concentrations or, more accurately, activities of the ion species on either side of the membrane. When the constants are combined at a temperature of  $37^\circ\text{C}$ , and for monovalent ions, the equation reduces to:  $E = 61 \log \frac{C_1}{C_2}$ . Thus, a 10-fold difference in concentration across a semipermeable membrane will result in a 61 mV change in potential. Measurements of intracellular and extracellular ionic concentrations have demonstrated that ions are unequally distributed on either side of the cell membrane. The unequal distribution of ions will result in a diffusion potential because of differences in mobilities of different ionic species as they diffuse



down their concentration gradients. The semipermeable membrane can enhance the differential mobilities to the extent that only one ion species may be able to permeate the membrane. It is in this case, that the Nernst equation can predict the membrane potential. This is a stable or equilibrium potential because continued diffusion of the permeant ion down its concentration gradient is prevented by its generation of an opposing electrical gradient. If the membrane were permeable to other ions, then the electrical and concentration gradients would eventually be eliminated. Large, impermeant organic anions are present within the cell and significantly contribute to the existence of an osmotic pressure gradient. The type of equilibrium characterized by the simultaneous existence of both osmotic and electrical gradients is called the Donnan equilibrium. The Donnan relation predicts that whenever a charged impermeant ion is present on one side of the membrane, an electrical potential will exist across that membrane. This potential may, in part, account for the unequal distribution of potassium and chloride ions.

If the resting membrane is permeable only to potassium, then changes in the external potassium concentration should cause precise and predictable changes in the membrane potential. The Nernst equation predicts a linear relationship between membrane potential and the logarithm of the external potassium concentration, having a slope of 61 mV per decade (58 mV per decade at 20°C). In fact, there is often considerable deviation of measured potentials from those predicted by

the Nernst equation in many systems. The observed, nonlinear nature of the relationship, especially at low potassium concentrations, as well as the usually decreased slope, has been attributed to the possibility that the resting membrane is permeable to other ions, or that changes in external potassium concentration may affect potassium conductance or indirectly alter the internal ionic composition (49,107,131,211,229).

The possibility that permeability to other ions may contribute to the resting membrane potential was considered by Goldman in his constant field theory (87). According to this theory, as modified by Hodgkin and Katz (111) the membrane potential could be predicted by a modified form of the Nernst equation relating permeability coefficients for the various ions to their concentration differences:

$$E = 61 \log \frac{P_K [K^+]_o + P_{Na} [Na^+]_o + P_{Cl} [Cl^-]_i}{P_K [K^+]_i + P_{Na} [Na^+]_i + P_{Cl} [Cl^-]_o} \text{ at } 37^\circ\text{C}$$

where  $[X]_o$  = specific ion concentrations (activity) outside,  $[X]_i$  = specific ion concentrations (activity) inside and  $P_x$  = specific ion permeability coefficients. Implicit in the Goldman equation are the requirements that ion permeation be a constant, linear, passive property of the membrane. Hodgkin and Horowicz (107) were able to account for the deviation from Nernst predicted values for resting potential in muscle fibers by assuming that the resting membrane was also permeable to sodium. The sodium permeability being about 0.01 of the potassium

permeability. Thus, in the resting state, potassium, and possibly chloride, permeabilities predominate and the membrane potential approaches the Nernst predicted potassium or chloride equilibrium potentials. According to the sodium hypothesis, however, during the action potential the sodium permeability becomes predominant and the membrane potential approaches the sodium equilibrium potential.

General support of the sodium hypothesis came with the development of voltage clamping techniques. The voltage clamp permits the imposition of a sudden change in the membrane potential and the simultaneous measurement of the magnitude and time course of the current necessary to cause and maintain the sudden change. Hence, it is possible to quantify directly the ionic current which flows across a nerve or muscle membrane. The particular ion species responsible for specific components of the total membrane current can be determined by examining the effects of variations in the ionic composition of the extracellular or intracellular medium on the changes in current. In the case of the squid giant axon, removal of the extracellular sodium ions has been shown to eliminate the early, transient inward current flow in response to a suprathreshold step depolarization. Reduction of the external sodium ion concentration had already been associated with a decrease in both the rate of rise and amplitude of the action potential in the squid axon (111). Direct evidence that the movement of potassium ions is responsible for the later steady current flow, observed under voltage clamp conditions, was provided by Hodgkin and Huxley (110) when they

reported a study on radioactive potassium tracer efflux during transmembrane current flow. Shortly thereafter, Hodgkin and Keynes (112) demonstrated that an active metabolic process was responsible for the maintenance of the ionic concentration gradients across the squid axon membrane. They raise the possibility that this active ionic transport may contribute to the resting membrane potential.

The temptation to generalize the sodium hypothesis and therefore other findings obtained from the study of giant axons must be tempered by the fact that in some neurons [including both molluscan (39,83) and mammalian (106)] it has been clearly demonstrated that inward calcium ion movement is responsible for a significant portion of the total transient depolarizing current flow. Furthermore, it has been shown that active transport of ions significantly contributes to the resting membrane potential in many systems (29,218), thus violating one of the principle requirements of the Goldman equation and the constant field theory.

#### B. Electrophysiologic Properties of Vertebrate Neurons

In 1949, Ling and Gerard (153) demonstrated that it was possible to produce glass capillary micropipettes with a tip diameter of less than  $1 \mu$  and that these microelectrodes could be used to penetrate a cell membrane without causing significant injury or leakage of the intracellular contents. They then used these electrodes to measure the transmembrane resting potential of frog muscle fibers. This event

signaled, perhaps, the single most important advance in neurophysiologic techniques. The intracellular microelectrode was to permit, for the first time, the direct measurement of transmembrane potentials in vertebrate neurons.

The first study to make use of the intracellular microelectrode, on vertebrate neurons, was published in 1951 by Svaetichin (212). He found the transmembrane resting potentials of neurons in dorsal root ganglia removed from frogs and a cat, to range between -50 and -90 mV with respect to an external reference electrode. He reported further that the action potential had no positive phase; that is, it had no overshoot. This study was quickly followed by others on the spinal motoneuron, neurons in sympathetic ganglia and sensory neurons. Table 1 is a compilation of all published research (excluding abstracts) in which intracellular microelectrodes were used to study the passive and active electrophysiological properties of the cell bodies of vertebrate neurons. Whereas a discussion of each individual report would involve much repetition of information not directly relevant to this project, a consideration of certain particular studies is in order.

Araki and Otani (6) were the first to make extensive use of a single microelectrode for both stimulating and recording. They were able to eliminate selectively the voltage drop produced by stimulating current flowing through the resistances of the microelectrodes, tissue and bathing medium, and to retain the ability to measure the voltage drop produced by the resistance of the cell membrane. This was

TABLE 1A. Passive Electrophysiologic Properties of Vertebrate Neurons

<i>Reference</i>	<i>Species</i>	$V_m$ (mV)	$R_m$ (M $\Omega$ )	$R'_m$ ( $\Omega/cm^2$ )	$C_m$ (nF)	$C'_m$ ( $\mu F/cm^2$ )	$\tau$ (msec)
<b>I. MOTONEURONS</b>							
226	cat	-50-80	-	-	-	-	-
23	cat	-70	-	-	-	-	-
7	toad	-40-50	-	-	-	-	-
6	toad	-40-50	4.5	269	1.05	17.5	4.3
42	cat	-70	0.4-1.3	500	-	8.0	4.0
72	cat	-	1.65	1000	-	-	1.08
40	cat	-64	-	-	-	-	-
189	cat	-	-	2000	-	2	4
62	cat	-62	-	-	-	-	-
94	cat	-40-50	-	-	-	-	-
41	cat	-55-80	1.2	600	2.5	5	3.1
168	cat	-	1	-	-	-	4.2
12	cat	-	-	1770	-	-	5.2
195	cat	-	2	-	-	-	3.2
114	mouse	-66	-	-	-	-	-
<b>II. SYMPATHETIC NEURONS</b>							
63	rabbit	-65-75	-	-	-	-	-
213	frog	-60-70*	-	-	-	-	-
175	frog	-65	20	456	-	24.4	10.6
16	frog	-54	-	-	-	-	-
116	frog	-48	100	5000	0.138	2.8	12.8
65	rabbit	-69	-	-	-	-	2.8-7.7
17	G. pig	-	55.5	1000	0.17	10	9.11
184	rat	-45-90	39.4	1800	0.071	1.6	2.7
184	G. pig	-45-90	40.6	2300	0.117	2.1	4.4
217	rabbit	-50-60	20-40	-	-	-	-
14	G. pig	-40-70	40-150	-	-	-	5-200
33	chick	-45	45	436	0.088	11	3.8
171	mouse	-42	30	-	0.75	-	1.8

$V_m$  - resting membrane potential

$R'_m$  - specific membrane resistance

$C'_m$  - specific membrane capacitance

\* - denotes that only maximum values were reported

$R_m$  - input resistance

$C_m$  - input capacitance

$\tau$  - membrane time constant

TABLE 1A. (Continued)

<u>Reference</u>	<u>Species</u>	<u>V<sub>m</sub></u> (mV)	<u>R<sub>m</sub></u> (MΩ)	<u>R'<sub>m</sub></u> (Ω/cm <sup>2</sup> )	<u>C<sub>m</sub></u> (nF)	<u>C'<sub>m</sub></u> (μF/cm <sup>2</sup> )	<u>τ</u> (msec)
<b>III. PERIPHERAL SENSORY NEURONS</b>							
212	frog	-50-90	-	-	-	-	-
212	cat	-50-90	-	-	-	-	-
43	chick	-50-65*	-	-	-	-	-
119	toad	-65	22.3	4030	0.207	1.18	4.63
199	cat	-30-80	-	-	-	-	-
203	chick	-40-55	-	-	-	-	-
214	frog	≈80	-	-	-	-	-
183	mouse	-51	-	-	-	-	-
59	cat	-57	5.6	-	-	-	-
223	chick	-50	-	-	-	-	-
<b>IV. OTHER NEURONS</b>							
215	fish mauthner	-60*	-	-	-	-	-
115	cat inter- neurons	-40-60	-	-	-	-	-
208,128	cat pyramidal	-52	13	-	-	-	9.9
157	chick ciliary	-50-70	-	-	-	-	-
121	cat Dieter's	-50-70	-	-	-	-	-
104	G. pig cortex	-50-70	-	-	-	-	-
155	cat Betz	-50-70	6.7	-	0.77	-	8.4
137	cat pyramidal	-56-74	-	-	-	-	-
69	chick spinal cord	-51.3	21.4	-	-	-	-
169	mouse cerebellum	-37	20	-	-	-	-
95	fish super- medullary	-60-70	0.6-2.5	0.4-1	8.0	5-15	4-6
200	cat pyramidal	-25-66	-	-	-	-	-
100	cat cerebellum	-50*	-	-	-	-	-
194	cat medulla	-60	7.2	-	-	-	-
69	chick spinal cord	-20-60	-	-	-	-	-

V<sub>m</sub> - resting membrane potential

R'<sub>m</sub> - specific membrane resistance

C'<sub>m</sub> - specific membrane capacitance

\* - denotes that only maximum values were reported

R<sub>m</sub> - input resistance

C<sub>m</sub> - input capacitance

τ - membrane time constant

TABLE 1B. Active Electrophysiologic Properties of Vertebrate Neurons

<u>Reference</u>	<u>Species</u>	<u>APA (mV)</u>	<u>OVST (mV)</u>	<u>APD (msec)</u>	<u>RT (V/sec)</u>	<u>FT (V/sec)</u>	<u>AFHYP (mV)</u>
<b>I. MOTONEURONS</b>							
226	cat	40-80	-	-	-	-	-
23	cat	90-100	20-30	-	400	250	-
7	toad	70*	20-30	-	-	-	-
24	cat	100	-	1.0	-	-	-
6	toad	40-65	-	-	218*	177*	-
72	cat	79	-	-	-	-	-
40	cat	78	14	-	-	-	-
195	cat	83	-	1.6	345	117	4.9
114	mouse	86	20	-	-	-	1.8
<b>II. SYMPATHETIC NEURONS</b>							
63	rabbit	75-85	-	4.7	-	-	20*
213	frog	70-85*	-	-	-	-	-
175	frog	90	25	3.0	160*	80*	25
16	frog	89	35	-	-	-	-
116	frog	76	28	-	-	-	-
65	rabbit	77	8	3.1	-	-	-
184	rat	75	-	3.6	230	-	21*
184	G. pig	76	-	3.0	155	-	21*
217	rabbit	-	-	-	262	-	-
14	G. pig	72	-	-	-	-	14
33	chick	65	20	4.0	60	-	-
171	mouse	-	-	-	24	-	-
<b>III. PERIPHERAL SENSORY NEURONS</b>							
212	frog	50-90	-	-	-	-	-
212	cat	50-90	-	-	-	-	-
43	chick	80-95*	30-40*	2.0-4.0	500*	70*	3-10
119	toad	100	35	2.8	319	161	1-6
199	cat	53	5-10	1.29	76	-	6.88
214	frog	~100	~20	-	~100	-	~10
183	mouse	--	-	-	144	-	-
59	cat	92	25	-	-	-	-
223	chick	65	15	-	-	-	-

APA - action potential amplitude  
 APD - action potential duration  
 FT - rate of fall

OVST - overshoot  
 RT - rate of rise of action potential  
 AFHYP - afterhyperpolarization

\* - denotes that only maximum values were reported



TABLE 1B. (Continued)

<u>Reference</u>	<u>Species</u>	<u>APA</u> (mV)	<u>OVST</u> (mV)	<u>APD</u> (msec)	<u>RT</u> (V/sec)	<u>FT</u> (V/sec)	<u>AFHYP</u> (mV)
IV. OTHER NEURONS							
215	fish Mauthner	-	-	1.0-1.5	-	-	-
115	cat inter- neurons	-	-	0.51	-	-	-
128	cat pyramidal	70	18	1.84	-	-	-
155	cat Betz	-	-	0.75	-	-	-
69	chick spinal cord	60	9.1	2.6	132	-	-
100	cat cerebellum	70*	20*	1.5-3.0	-	-	-
95	fish supra- medullary	80-100	-	6.0-7.0	-	-	13-20
104	G. pig cortex	27-70	-	-	-	-	-
200	cat pyramidal	10-56	-	0.5-2.0	-	-	-
121	cat Dieter's	80	10-30	-	-	-	-
194	cat medulla	62	2	1.6	211	104	4.1

APA - action potential amplitude

APD - action potential duration

FT - rate of fall

\* - denotes that only maximum values were reported

OVST - overshoot

RT - rate of rise of action potential

AFHYP - afterhyperpolarization

accomplished by inserting the microelectrode in one arm of a Wheatstone bridge. Theoretically the bridge was to be balanced (that is, all artifacts of a stimulus current flow were to be eliminated) with the tip of the electrode just extracellular, then on penetrating the membrane, the bridge would be thrown out of balance by the series addition of the membrane resistance in the stimulus current path. Thus, not only was it possible to inject current while simultaneously recording potentials with a single electrode, but it was also possible to measure the electrical resistance of the cell membrane. Resistance measurements were accomplished by measuring both the current flowing through the electrode and the voltage drop (bridge imbalance) which it caused. Then, with the application of Ohm's law:  $R = E \div I$ , where  $R$  = resistance,  $E$  = voltage drop, and  $I$  = current. Araki and Otani (6) calculated an average input resistance of  $4.5 \text{ M}\Omega$  and, assuming a surface area of  $6,000 \mu^2$ , a specific membrane resistance of  $269 \Omega/\text{cm}^2$ . Because the cell membrane can behave like a capacitor, a finite amount of time is taken to charge or discharge in response to an applied current. The time constant of the membrane can be determined by measuring the time it takes to change from its original level to  $1-1/e$  of its final level in response to an instantaneous current step. This assumes that the time course can be described by a simple exponential curve. Araki and Otani (6) reported time constants ranging from 1.5 to 8 msec. Membrane capacitance ( $C_m$ ) can be calculated from the membrane resistance ( $R_m$ ) and time constant ( $\tau$ ):  $C_m = R_m/\tau$ . Araki and Otani obtained an average value for input



capacitance of  $1.05 \times 10^{-9}$  F and a specific input capacitance of  $17.5 \mu\text{F}/\text{cm}^2$ . This was the first study to determine by direct measurement, the passive electrophysiologic properties of a vertebrate neuron.

Although nerve cells had been successfully maintained in culture, it was not until 1956 when Crain (43) published the results of a series of experiments which demonstrated for the first time, that nerve cells grown in tissue culture could retain their characteristic electrical function. He obtained records of resting and action potentials from over 60 neurons from dissociated embryonic chick spinal ganglia that had been maintained at least 7 days in vitro. Resting potentials were as high as -50 to -60 mV with overshoots of up to 40 mV, although frequently much smaller action potentials were recorded. The most distinctive advantage of Crain's preparation, in addition to the fact that it permitted direct observation of impaled neurons, was that the external environment of the neurons could be completely defined and experimentally controlled. Although the neurons were removed from 7-9 day chick embryos, it is quite possible that they already possessed, or were able to develop in culture, the features and characteristics of adult avian neurons.

The study by Ito (119), published in 1957, deserves special mention because it was at the time, and it still remains, the most complete characterization of the passive and active electrophysiologic properties of a vertebrate sensory neuron. Data for computation of mean values for resting potential and action potential amplitude (Table 1) were obtained

from 50 cells, and mean values for action potential duration and rates of rise and fall were calculated from a selected subpopulation of 25 cells. An analysis of the same spike configurations revealed similarities to action potentials generated in cat motoneurons. Thus, two inflection points were observed on the rising phase of the action potential and its multicomponent nature was demonstrated. The smallest component, called "M spike" had an amplitude of 4.2-7.6 mV and was believed to originate in the myelinated axon of the cell. The second component, called the "NM spike", had an amplitude ranging from 32-58 mV in different neurons and was believed to originate in the nonmyelinated, initial segment of the axon, near the axon hillock. These two components are exactly analogous to the M and NM spikes reported by Brock et al. (23,24) for cat motoneurons. The largest component had been called the "SD spike" by Brock et al. (23,24) indicating its origin in the soma and dendrites, Ito named this component the "S spike" in deference to the absence of dendrites from DRG neurons. The falling phase of the action potential was characterized by the presence of an afterhyperpolarization of 1-6 mV similar to the "after-positivity" observed following action potentials in squid axon (111) and toad motoneuron (6). Mean values for membrane resistance, capacitance and time constant were derived from measurements on only 6 neurons. It was found that membrane resistance was not a linear function of membrane potential. Slope resistance ( $dV/dI$ ) was 4-7  $M\Omega$  less when measured with depolarizing current pulses than when measured with hyperpolarizing

pulses. This type of rectification had also been observed in squid axon (37) but not cat motoneuron (42). An interesting type of behavior which had not previously been reported consisted of a time-dependent change in membrane resistance in response to a long polarizing current pulse. This delayed resistance change was most pronounced with hyperpolarizing current pulses greater than 0.5 nA, and it was suggested that it might be due to an increase in chloride conductance.

All data reported by Ito were obtained from large diameter (60-90  $\mu$ ) neurons which he believed were associated with myelinated axons (no conduction velocities were reported). On three occasions, however, data were obtained from small neurons with conduction velocities of about 0.3 M/sec. These cells had properties similar to those of the larger neurons except that their time constant and action potential duration were significantly longer. In addition, these small neurons did not exhibit a delayed decrease in membrane resistance during hyperpolarizing current pulses.

The basic electrophysiologic properties of mammalian sensory neurons had not been studied in any detail, and the possibility that they differed from those properties which had been measured in amphibian or invertebrate neurons deserved consideration. Sato and Austin (199), who studied cat dorsal root ganglia (DRG) in situ, were the first to present data that suggested that mammalian sensory neurons do indeed differ from neurons of other species. They reported values for action potential parameters which were significantly different from values reported

by Ito (119,120) in toad spinal ganglia. For example, the typical action potential in cat DRG neurons was found to have an amplitude of 52.6 mV and a duration of 1.29 msec compared with the 100 mV and 2.9 msec reported for toad sensory neurons. Similar differences for other parameters are shown in Table 1. Sato and Austin were unable to observe any inflections on the rising phase of the action potential. Spike failure was characterized by a gradual decrease in amplitude with no change in time course. In their discussion on the origin of the somatic action potential, they concluded that the threshold of the soma membrane is nearly as low as that of the nonmyelinated segment. Therefore, invasion of the soma could proceed without significant delay or blockage. An M spike was not observed because the distance between the myelinated - nonmyelinated junction was too great for effective electrotonic spread. The possibility that the complex nonmyelinated segment and the dense covering of satellite cells associated with each neuron may be of functional significance in the regulation of soma excitability was also discussed.

Several electrophysiologic studies on embryonic avian neurons in culture have been published (see Table 1). Comparable studies on mammalian neurons maintained in culture have not often been reported. Aside from the work of Hild and Tasaki (100), the only other published electrophysiologic study of cultured mammalian neurons is that of Peacock et al. in 1973 (183). They studied neurons from fetal mouse dorsal root ganglia and spinal cords, and demonstrated that the complex

differentiated electrical properties of mammalian neurons could be maintained in culture up to 14 weeks. They suggest that the cultured mammalian neuron will provide a unique opportunity to examine many of the problems of mammalian neurophysiology.

### C. Roles of Extracellular Ions

The nature of the ionic contributions to the resting and action potentials in vertebrate neurons has received comparatively little attention. It is generally agreed that the resting membrane potential is primarily determined by the ratio of internal to external potassium ion concentrations and the resting potassium permeability of the membrane. The action potential is most strongly affected by changes in sodium ion concentration, behaving as though the membrane were mainly permeable to sodium at the peak of the action potential.

1. Potassium. Huxley and Stämpfli in 1951 (117) were first to report on the specific contribution of potassium and sodium to the resting and action potentials in a vertebrate neuron. In general, the results of their studies in frog myelinated nerve in vitro, closely resembled those obtained from squid giant axon for the effect of potassium (Curtis and Cole, 47) and sodium (Hodgkin and Katz, 111). Huxley and Stämpfli made use of their newly developed oil-gap apparatus to measure the effects of alterations in the external ionic environment on resting membrane potentials and action potentials. Potassium concentration was altered by direct exchange with sodium. The magnitude of



the resting potential varied inversely with the external potassium concentration between 0 and 117 mM (normal = 2.5 mM). When the log of the external potassium concentration was plotted against the membrane potential, the relationship was linear only at potassium concentrations above 10 mM. The maximum change in membrane potential for a 10-fold change in external potassium concentration was found to be 51 mV. This was compared to the 56 mV per decade change observed in squid axon (37) and the 58 mV change predicted by the Nernst equation, if it is assumed that the membrane is permeable only to potassium. At potassium concentrations below 10 mM, the slope of the relation decreased markedly. These findings suggested that the membrane potential was not simply a diffusion potential for potassium. Indeed, Hodgkin and Katz (111) had already explained similar behavior in the squid axon by assuming that the resting membrane was permeable to both sodium and chloride as well as to potassium ions. Differences in the relative permeabilities for these three ions were suggested to account for the observed nonlinear relationship between membrane potential and log external potassium concentration. In the case of the frog myelinated nerve, it would appear that the relative contributions of the sodium and chloride permeabilities are of even greater significance. External potassium concentration was found to affect action potential overshoot, the action potential being blocked at potassium concentrations above 20 mM. Below 20 mM, the overshoot varied inversely with external potassium concentration. It was suggested that this was not a direct effect of

potassium on the overshoot, but rather it was an indirect effect of potassium acting through changes in the membrane potential.

2. Sodium. Huxley and Stämpfli (117) reported that the reduction of external sodium ion concentration (with equimolar choline substitution) caused a marked decrease in the overshoot and a slight increase in the resting potential (hyperpolarization) in frog myelinated nerve. They demonstrated that the overshoot changed approximately 58 mV per 10-fold change in external sodium concentration, and agreed with Hodgkin and Katz (111) that the overshoot represents a sudden large increase in the membrane permeability to sodium. Huxley and Stämpfli also noted that the rate of rise of the action potential was approximately proportional to the external sodium concentration. This provided further evidence that increased sodium permeability had a major role in the formation of the action potential. The replacement of sodium by lithium was almost without effect on either the resting potential, or amplitude and rate of rise of the action potential.

The extensive work by Frankenhaeuser and associates (21,74,78), using voltage clamp techniques on isolated frog myelinated nerve fibers, supported many of these findings. In addition, they have demonstrated that the initial inward current of the action potential was carried by sodium ions and the delayed outward current was carried primarily by potassium ions. In general, their data are remarkably similar to voltage clamp data obtained from squid giant axon (108), and they conclude that the ionic phenomena underlying the generation of the action potential are essentially identical in both species.

When one considers vertebrate nervous tissue other than frog myelinated nerve the similarities to squid giant axon become much harder to find and the overall complexity appears to be greatly increased. Blackman et al. (16) examined the effects of changes in ionic concentration on intracellularly recorded potentials from neurons in frog sympathetic ganglia. They found that a reduction in external potassium concentration, from its normal 2 mM to zero, had no effect on the resting membrane potential. Moreover, a 10-fold increase in external potassium concentration caused a maximum change in the membrane potential of only 43 mV, far less than the 59 mV predicted by the Nernst equation for their experimental temperature. Similarly, low values for the slope of the relation between external potassium and membrane potential have been reported by others (90,105,144,176). Thus, Koketsu et al. (139) reported a slope of 38 mV per decade change for the membrane potential recorded in frog dorsal root neurons, and Armett and Ritchie (8) reported a potassium-potential slope of 28 mV per decade with essentially no effect on the resting potential at potassium concentrations below 5 mM for nonmyelinated nerve fibers in the rabbit. These various authors suggested that the ratio of potassium to sodium permeability in vertebrate neurons must be significantly higher than the 0.01 reported for frog muscle fiber (107) or the 0.04 reported for squid giant axon (111). Using a sucrose-gap technique, Armett and Ritchie (8), in fact, reported a sodium-potassium permeability ratio of 0.25 for rabbit vagal C fibers and a value of 0.10 for cat hypogastric nerve.

The interpretation of the effects of changing extracellular potassium ion concentration is further complicated by studies indicating that glial cells may have an important role in regulating potassium concentration in the perineuronal space (99,219). Thus, it may well be impossible to determine accurately the composition of the ionic microenvironment around an individual neuron. It does, however, seem safe to conclude that potassium contributes significantly, but not exclusively, to the maintenance of the resting membrane potential in vertebrate neurons.

Blackman et al. (16) also examined the effects of changes in extracellular sodium ion concentration on the resting and action potentials. Because it had been demonstrated that the nerve membrane was not perfectly selective to potassium, a small but significant resting permeability to sodium was considered. In their experiments, Blackman et al. (16) substituted choline chloride, choline methylsulfate or sucrose for most of the sodium chloride in the extracellular medium. If, in fact, the membrane was permeable to sodium ions at rest, then replacement of sodium by an impermeant cation should cause hyperpolarization. They stated that "(hyperpolarization) was never observed: in the better experiments. . .there was no change in the resting potential of the cell." This would seem to imply that depolarization was often seen upon reduction of extracellular sodium, a finding subsequently confirmed by Hillman and Hydén (105) in experiments on isolated rabbit medullary neurons. They demonstrated that a reduction in extracellular

sodium ion concentration caused a significant reduction (depolarization) in the resting membrane potential, in spite of the fact that these neurons exhibited a maximum change in membrane potential of only 35 mV per 10-fold change in external potassium. Koketsu et al. (140) also reported that replacement of sodium chloride by either choline chloride or diethanol-dimethylammonium chloride caused a reduction in the membrane potential in frog dorsal root neurons. Effects on membrane resistance were not reported in any of these studies (16,105,140). Tashiro and Nishi (217) reported that no change occurred in membrane potential or resistance of rabbit sympathetic ganglion cells when TRIS was substituted for sodium in the extracellular environment. In studies where low external sodium induced hyperpolarization, it was characterized as small (<5 mV) and transient (96,176). Adrian and Freygang (2) offered some alternative explanations for the absence of the expected hyperpolarization. They suggested that the substituent cations (e.g., choline, TRIS) were not truly impermeant, although osmotic studies do not support that contention (98). They also suggested that there could be an imperfect seal around the tip of the microelectrode. Hyperpolarization was induced by other means during the course of these experiments, however, forcing one to assume the existence of a rather selective imperfection. A more satisfactory explanation can be postulated from recent studies (20,21) indicating that the permeability properties of a nerve membrane are, in part, dependent upon the ionic composition of the external medium. Voltage clamp experiments on frog

myelinated nerve (20) have demonstrated that membrane permeability to potassium can be decreased by decreasing external sodium concentration; but not by decreasing external calcium concentration. Other experiments in the same study have shown that the concentration of univalent ions or calcium can affect the voltage dependence of the sodium and potassium permeability changes. In another study on frog myelinated nerve (21) it was shown that sodium permeability was affected by changes in the external concentrations of sodium, potassium, or calcium. Sodium permeability being increased by simultaneously increasing both sodium and potassium concentration or by decreasing calcium concentration. Experiments on voltage-clamped molluscan neurons (35) showed that changes in hydrogen ion concentration as well as calcium concentration affected the membrane potential by a specific change in chloride conductance. Thus, the complex interactions between the ionic composition of the external medium and membrane permeability might result in membrane behavior that otherwise could not be predicted.

In summary, the origin of the resting membrane potential in mammalian peripheral sensory neurons has not been studied, but experiments on other mammalian neurons have demonstrated the importance of an unequal distribution of ions on either side of the selectively permeable nerve membrane. Several studies have shown that the mammalian nerve membrane, at rest, does not behave as a simple potassium electrode but must also be permeable to other ion species. A possible consequence of this increased permeability is that the internal ionic composition (see Table 6), and therefore the membrane potential determined by the transmembrane ionic distribution, differ from that measured in many

nonmammalian species. The analysis of experiments designed to elucidate specific ion contributions have been complicated by the existence of poorly understood interactions between membrane permeability and the concentration of certain ions in the external medium. The possibility that electrogenic ion pumps contribute to the resting potential, especially under conditions of altered ion concentrations, needs further consideration. Finally, many types of mammalian neurons are densely covered by glial cells, and if one hypothesizes that these cells, with their active ionic pumps, can act as a diffusion barrier, then the microenvironment surrounding each nerve cell may not reflect the composition of the external bathing medium, further complicating experimental analyses.

The effects of changes in sodium concentration on the action potential are more consistent and less difficult to interpret than those on the resting membrane potential. It has been shown that both the rate of rise and the amplitude of the action potential are reduced in sodium deficient media (16,90,139,140). According to the sodium hypothesis, the membrane permeability to sodium is predominant at the peak of the action potential. Thus, it is expected that the overshoot will vary with the sodium concentration as predicted by the Nernst equation, that is, the overshoot should decrease by 58 mV for a 10-fold change in external sodium concentration at 20°C. That this occurs in squid axon has been demonstrated by Hodgkin and Katz (111), however, changes of this magnitude in vertebrate neurons have not been observed (16,90,139,140,210). The possibility that, at the peak of the overshoot, the

active membrane is significantly permeable to other ions in addition to sodium has been considered. Hodgkin and Huxley (109) have shown that potassium permeability is increasing at the peak of the action potential and this may account for some deviation from predicted behavior. Hirst and Spence (106) reported that, at least in some mammalian peripheral neurons, complete blockade of both resting and active sodium permeability had little effect on the action potential. A reduction in extracellular sodium concentration to 25% of its normal value (sucrose replacement) had no effect on the action potential. Their experiments went on to demonstrate that a significant proportion of the inward depolarizing current was carried by calcium ions.

3. Calcium. The importance of calcium ions in the maintenance of membrane excitability and the regulation of membrane permeability is well known (1,29,48,73,138). The relation of calcium ions to the resting and action potential appears to be quite complex. In both frog dorsal root neurons and skeletal muscle fibers it has been shown that the resting potential varies directly with the external calcium concentration (138), presumably because the membrane permeability to sodium and potassium ions (but not to chloride ions) is directly affected by changes in the external calcium ion concentration (138,141, 142,143). External calcium also affects membrane permeability during the action potential. In frog dorsal root neurons it has been shown that the maximum rate of rise of the action potential can be affected by changes in calcium concentration (138). In addition to its ability to



regulate membrane permeability during both the resting and active states, calcium can also function as a charge carrier (138). Thus, intracellular calcium may be increased during activity. Krnjevic and Lisiewicz (149) reported that injections of calcium ions into cat motoneurons caused hyperpolarization and a decrease in membrane resistance. These effects were attributed to a calcium mediated increase in potassium conductance. The complex interrelationship between calcium and membrane permeability can make the interpretation of the effects observed during the manipulation of extracellular calcium concentration quite difficult.

Ichioka (118) published one of the first studies that described the effects of calcium on action potentials in vertebrate neurons. In calcium-free media the action potential amplitude was often reduced up to 50% but was occasionally unaffected or even increased. In high calcium media the action potential amplitude was usually reduced, but again, this effect was variable. Ichioka concluded that the effects of calcium were dependent on the fiber type and not simply on the concentration of calcium in the external medium. Subsequently, Hashimura and Wright (97) reported that removal of extracellular calcium had no significant effects on the resting membrane potential or configuration of the action potential in frog single nerve fibers. Koketsu and Koyama (141) reported that simple reduction of external calcium concentration for up to 3 hours was without effect on the resting potential or configuration of the action potential of neurons in frog dorsal root ganglia. When the calcium chelating agent EDTA was added to the

calcium-free solution, the resting membrane potential and input resistance decreased markedly within 15-30 min. Action potentials developed prolonged plateaus on their falling phase and eventually the neurons became inexcitable. The neurons were, however, capable of generating action potentials, provided that they were stimulated during a hyperpolarizing conditioning pulse. These action potentials were similar to those obtained under identical conditions of stimulation in high-potassium media. The need for a hyperpolarizing conditioning pulse suggests that sodium inactivation is a result of calcium removal. Whether or not this inactivation is a direct effect of calcium removal on the sodium "gates" or an indirect effect of zero calcium-induced conductance changes, and consequent membrane depolarization, remains to be tested.

In a recent study on isolated rat dorsal root nerve fibers (90), a calcium-free environment caused the resting membrane potential to be depolarized by about 3 mV, the action potential amplitude to be decreased by about 7 mV, and the membrane resistance to be reduced to about 70% of control. It was suggested that calcium may have a role in controlling sodium efflux in a manner similar to that demonstrated in squid axon (10).

4. Chloride. Chloride is the principle permeant anion in both extracellular and intracellular fluids. It is generally believed to be passively distributed according to the electrical gradient maintained by the active distribution of sodium and potassium ions. The existence of

a chloride pump, however, has been demonstrated in nerve cells as diverse as squid giant axon (131) and cat motoneuron (154). Thus, chloride is actively transported into squid axon resulting in an internal chloride concentration significantly higher than that predicted by the Nernst equation. The function of this high internal chloride concentration is not known although it has been suggested that it may reduce internal resistivity thereby increasing conduction velocity (29). Chloride appears to be actively transported out of cat motoneuron, but the function of this transport system is not clear. It has been suggested that this outwardly directed chloride pump may have a role in the generation of the chloride-dependent inhibitory post-synaptic potential (154).

If chloride ions contribute significantly to the membrane conductance, then the replacement of extracellular chloride ions by impermeant anions should cause a transient depolarization and, upon return to a chloride-containing media, a transient hyperpolarization (107). In this regard, Blackman et al. (16) found that reduction of extracellular chloride concentration (methylsulfate replacement) had no effects on frog sympathetic ganglion neurons, and they concluded that chloride ions do not contribute significantly to either resting or active membrane conductance. In contrast, Nishi et al. (176) reported that replacement of chloride by either sulfate or methylsulfate caused a 10 mV depolarization and a 30-70% decrease in membrane resistance in frog dorsal root neurons. Thus it would appear, at least in the case of these vertebrate

neurons, that chloride ions are not freely permeable and that changes in chloride concentration may affect total membrane conductance. The possibility that chloride conductance may be controlled by the extracellular concentration of other ions has been suggested (35). For example, some of the effects caused by changes in extracellular calcium concentration may be mediated through changes in chloride conductance.

In summary, several studies have shown that the resting membrane potential in mammalian neurons depends primarily on the unequal distribution of potassium across the selectively permeable nerve membrane. It appears, however, that the mammalian nerve membrane is not as selective for potassium as is the nerve membrane of nonmammalian species. Attempts to experimentally analyze the specific contributions of sodium, chloride and calcium, to the resting potential are considerably complicated by concentration-permeability interactions and other previously discussed factors. The generation of action potentials in many mammalian neurons is known to be the result of a sudden increase in sodium permeability. It has been shown, however, that at the peak of the action potential the membrane does not behave as a sodium electrode, implying significant contributions by other ions. Attempts to assess these contributions accurately have been frustrated by many of the same problems complicating the analysis of the resting potential.

### III. THE NODOSE GANGLION OF THE VAGUS NERVE

#### A. Cellular Structure and Function

The nodose ganglion is the principal sensory ganglion of the vagus nerve and contains the cell bodies of afferent fibers that innervate

nearly all of the thoracic and abdominal viscera (4,181). The neurons of the nodose ganglion are similar to pseudounipolar neurons found in dorsal root ganglia. However, a large proportion of neurons in the nodose ganglion are of a complex type in which the initial axon may be long and coiled or give rise to several roots to form a plexus near the cell body (190). The cell bodies range in diameter from 20-60  $\mu\text{m}$  and are devoid of dendrites and synapses (30,190). In addition to sensory neurons, small intensely fluorescent (SIF) cells have been identified in nodose ganglia of both cat and rabbit (89,125; M. Grillo, personal communication) but their function is unknown. The passive and active electrophysiological properties of vertebrate sensory neurons have not been characterized completely, although certain properties have been described for neurons in amphibian spinal ganglia (119,120,139,140, 212,213) and mammalian dorsal root ganglia both in vivo (59,68,199,213), and in tissue culture (43,183,223). The only published work on the nodose ganglion was by Mei (160), who studied its functional activity and organization with extracellular microelectrodes.

#### B. Pharmacology

Cell bodies of neurons in the peripheral craniospinal ganglia provide a trophic function for the afferent fibers and are not believed to play a role in modulation of afferent nerve activity. Recent studies, however, indicate that these cells possess receptors for drugs either to initiate action potentials or to modify activity, and that

these neurons have properties that may modify transmission of afferent impulses. Thus, the nodose ganglion of cat has been shown to be a site for the initiation of certain reflexes (apnea, bradycardia, hypotension, emesis) caused by 5-hydroxytryptamine (5-HT) and phenyl diguanide (125), veratrum alkaloids (18,19,31) and cardiac glycosides (32). It has been shown that 5-HT, phenyl diguanide or veratridine, administered by close intra-arterial injection, can cause some neurons in the nodose ganglion to generate action potentials, and that small doses of pentobarbital administered intravenously can depress the sensitivity of these neurons to 5-HT and veratridine (198). Finally, mammalian dorsal root ganglion cells are depolarized by drugs such as gamma-aminobutyric acid (54, 55,56) and the convulsant barbiturate 5-(2-cyclohexilidenethyl)-5-ethyl barbituric acid (59). The precise sites and mechanisms of action of these various agents in the sensory ganglia are unknown. With regard to mechanisms in craniospinal ganglia for modifying afferent impulse activity, Tagini and Camino (214), in a study of frog dorsal root ganglion cells, reported that trains of stimuli at frequencies of 20-100 Hz to the infraganglion nerve trunk produced action potentials in the dorsal root that exceeded the number of stimuli applied to the nerve. They attributed this increase to a delay in the generation of action potentials in the soma of the ganglion cells, which are brought to threshold level by an action potential in the initial segment. It thus appears likely that activity in afferent nerve fibers may be modified both pharmacologically and physiologically in craniospinal ganglia.

### C. The Nodose Ganglion: A Possible Model for the Study of Drug Action

The findings that peripheral sensory neurons are sensitive to the action of a number of drugs raise the possibility that these nerve cells may provide a useful model for studying the manner in which drugs may influence the basic electrophysiologic properties of mammalian neurons. Although there is a vast literature on the effects of drugs on the nervous system, there have been relatively few studies directed toward elucidating the mechanisms by which such drugs affect basic electrophysiologic properties of individual mammalian neurons. Crawford (45) reported that anesthetics reduced both spontaneous and drug induced activity of neurons in the cerebral cortex of cat, and Richens (192,193) found that volatile anesthetics depressed excitability of the membrane of motoneurons in the isolated superfused frog spinal cord. In neither of these studies was a detailed examination made of the effects of anesthetic agents on threshold and membrane resistance or on various properties of the action potential (amplitude, rise time, fall time, duration, after-potentials). Somjen and Gill (205) observed that thiopental and ether blocked the generation of orthodromic action potentials in spinal motoneurons of cat by causing an increase in threshold and a decrease in the amplitude of synaptic potentials, but they did not examine effects of these drugs on other passive or active electrical properties of the motoneuron. Moreover, in assessing such studies, it is difficult to determine whether the drug acts directly on the nerve cell under study or indirectly by causing changes in synaptic

(excitatory or inhibitory) input to the cell. Thus, for the study of drug effects on mammalian nerve membranes, a distinctive advantage is offered by the nerve cell bodies in cat and rabbit nodose ganglia, as they are known to lack both dendrites and synapses (30,190).

The effects of different agents on properties of mammalian peripheral nerves have also been examined. Kosterlitz and Wallis (145) reported that certain analgesics decreased the size of the compound action potential and slowed the conduction velocity of cat hypogastric and rabbit vagus nerves, and Julien and Halpern (127) found that the anticonvulsant diphenylhydantoin caused a significant shortening of the duration of the hyperpolarization induced in mammalian C-fibers by tetanic stimulation. Byck and Ritchie (27) observed that  $\Delta^9$ -tetrahydrocannabinol decreased the size of the compound action potential of mammalian C-fibers, an effect reduced by removal of extracellular chloride ion. Whereas studies such as these provide clues as to possible mechanisms of action of drugs on the mammalian nervous system, the techniques used do not allow for detailed examination of the basic phenomena underlying the described effects.

Experiments designed to elucidate precise mechanisms by which drugs alter normal neuronal behavior have been conducted on single neurons of several invertebrate species. Narahashi, Moore and Poston (166) using the squid axon, reported that dibucaine and pentobarbital caused reversible blockade of both peak transient and steady state components of changes in conductance and, sometimes, hyperpolarization of the membrane. Levitan and Barker (152) found that nonnarcotic analgesics



produced hyperpolarization and a fall in input resistance of neurons in the buccal ganglion of molluscs, effects which they attributed to changes in membrane permeability to potassium and chloride ions. Similarly, the mechanisms of action of pentylenetetrazol and mephenesin have been studied by examination of changes in membrane resistance and by voltage clamp analysis of neurons in *Aplysia*; pentylenetetrazol caused an increase in the inward (sodium) current in response to changes in membrane potential, resulting in bursts of action potentials (51), and mephenesin diminished the amplitude of the action potential and selectively reduced the early inward current caused by membrane depolarization (135). Whereas studies such as these provide an accurate description of the mechanisms underlying drug effects on invertebrate neurons, the assumption that similar mechanisms of action are involved in their effects on mammalian neurons may not be valid.

## METHODS

### I. INTRACELLULAR RECORDING IN VIVO

Young New Zealand white rabbits, weighing between 1.4 kg and 3.0 kg, were anesthetized with ethyl carbamate (urethan, Merck), 1.5 gm/kg injected intraperitoneally. Urethan was selected as the anesthetic of choice for these in vivo studies because it has been reported to depress the excitability and chemical sensitivity of neurons to a lesser extent than many other anesthetic agents (45,150) and because of its accepted use in similar situations (144,184,225). Cats, weighing between 2.5 kg and 3.5 kg were also anesthetized with urethan (1.5 gm/kg) injected intraperitoneally. Body temperature was maintained at  $37.5^{\circ}\text{C} \pm 1^{\circ}\text{C}$  with the aid of a D.C. heating lamp and, occasionally, by the use of a water circulating heating pad. Blood pressure was continuously measured with a Statham P23dc pressure transducer attached to a polyethylene catheter inserted into a femoral artery. End-tidal  $\text{CO}_2$  was monitored with a Beckman LB-1 infrared  $\text{CO}_2$  analyzer. Both arterial blood pressure and end-tidal  $\text{CO}_2$  were recorded on a Grass model 7 polygraph throughout the experiment.

The surgical procedure for exposing the nodose ganglion in both cats and rabbits was as follows. The animal was secured on its back to the operating table and its skull immobilized by means of a specially designed head holder. A midline incision was made extending from the chin to the thorax. Blunt dissection was utilized to separate superficial

from deep muscle layers. The skin and attached superficial muscle layer were retracted laterally to expose the deeper cervical structures. All bleeding points were either ligated or cauterized. A low cervical tracheostomy was performed and a "U"-shaped glass cannula was inserted into the trachea and tied securely in place. The trachea, esophagus and their associated musculature were doubly ligated near the point of tracheal cannulation, care being taken to assure that the common carotid arteries, and the vagal and sympathetic nerve trunks were not damaged during this procedure. The trachea, esophagus and their associated musculature were then cut between the ligatures and reflected cranially. The superior laryngeal nerves were transected near the larynx in order to prevent any tension on the vagus nerves. The carotid sheath on the right side was opened and the vagus nerve was carefully separated from surrounding structures. With the aid of a Ziess operating microscope, the nodose ganglion on the right side was exposed and separated from surrounding structures. The blood supply to the ganglion was kept intact. To stabilize the ganglion for intracellular recording, a small stainless steel platform was placed under the ganglion and firmly attached to the frame of the operating table. A solution of agar (4% in saline) was poured into neck, completely covering the ganglion, and allowed to harden. The hardened agar immediately above the ganglion was removed and, with the aid of the operating microscope, a small opening was made in the outer connective tissue capsule of the ganglion. Warmed and oxygenated

physiologic saline was poured over the ganglion. In order to further minimize the possibility of movement artifacts, the hydraulic microdrive (David Kopf) attached to a Narashige micromanipulator (model ME-5), the ganglion platform, and the operating microscope were all firmly mounted on the operating table which in turn rested on a vibration-free work bench (Serva-Bench Mark III).

The animal was paralyzed with gallamine triethiodide (8 mg/kg, i.v.) and ventilated artificially with a Harvard small animal respirator. The rate and depth of respiration were adjusted to minimize movement artifacts while adequate ventilation was maintained as determined by measurements of end-tidal  $\text{CO}_2$ . Periodically, samples of arterial blood were taken in order to determine the pH,  $\text{PO}_2$ , and  $\text{PCO}_2$ .

Glass microelectrodes, filled with either 3 M KCl or 5 M KAc were used to obtain intracellular recordings from neurons in the ganglion (see Methods: Intracellular Recording Apparatus). The electrodes were held in the carrier of the hydraulic microdrive and positioned directly above the opening in the connective tissue capsule of the ganglion. It was not possible to observe directly the cell bodies of the neurons in this type of preparation. Several problems were associated with in vivo intracellular recording. Because of the ganglion's close proximity to several major arteries and the jugular vein, movement artifacts associated with changes in blood pressure and ventilation were a constant problem. Only in some preparations, because of slight anatomical variations, could the movement artifact

be controlled adequately to permit stable intracellular penetrations. It is from these preparations that data will be reported.

## II. INTRACELLULAR RECORDING IN VITRO

New Zealand white rabbits, weighing between 1 kg and 3 kg were obtained from Hilltop Rabbitry, CA and kept in individual cages in a temperature controlled room with a 12 hr light/dark cycle until use. Anesthesia was induced in rabbits with a single rapid intravenous injection of sodium methohexital (Eli Lilly & Co.) in an approximate dose of 5 mg/kg, following which an endotracheal catheter was inserted and connected to a standard anesthetic machine. Occasionally succinylcholine chloride (Anectine, Burroghs Wellcome & Co.) was administered intravenously (0.5 mg/kg) to facilitate endotracheal intubation. Anesthesia was maintained with a mixture of methoxyflurane (Metofane, Pitman-Moore), nitrous oxide and oxygen.

Cats weighing between 1.7 kg and 4.6 kg were obtained from various private vendors and housed individually according to accepted standards. During the first two years of the study, cats were anesthetized with urethan injected intraperitoneally (ethyl carbonate, 1-1.5 gm/kg). During the third and final years of the study anesthesia was induced with sodium methohexital (Eli Lilly & Co.) in an approximate dose of 10 mg/kg injected intravenously. These animals were then intubated and anesthesia maintained as described for rabbits.

Two alternative surgical procedures were used for the removal of nodose ganglia from both cats and rabbits. The first procedure

closely resembled that used for the in vivo studies. The trachea was cannulated and the nodose ganglia were exposed through a midline incision in the neck, the esophagus, trachea and surrounding muscles being cut between ligatures and reflected cranially. With the aid of a dissecting microscope, tissue was carefully dissected away from the ganglion, its nerve trunks and their branches. The infranodose and supranodose vagus, superior laryngeal and, in rabbit, the aortic nerves were transected as far from the ganglion as possible, and the ganglion and its attached nerves were removed and immediately placed into a chamber containing an oxygenated buffer solution. The second method differed from the first only in that the trachea and esophagus were kept intact and merely displaced from the region of the ganglion by suitable retractors. Immediately after removal from the animal, the ganglion was examined and clotted blood and connective tissue remnants were carefully dissected away. The ganglion was next transferred to a specially designed recording chamber (see Methods, Section IV), where small pins could be used to anchor it securely to the cork bottom. With the aid of the operating microscope, a small opening was made in the tough outer capsule of the ganglion. Once in the recording chamber the ganglion was continuously superfused with an oxygenated buffer solution.

The ganglia were routinely exposed to a proteolytic enzyme in order to facilitate penetration by the glass microelectrodes. In the initial experiments a freshly prepared solution of chymotrypsin

(Sigma Chemical Co., St. Louis, MO), in a concentration of 10 mg/ml, was applied on a small cotton pledget placed over the opening in the outer connective tissue capsule. This was carried out at room temperature (21-23°C) for 30 min. The treatment was followed by replacement of the buffer solution with dialyzed calf serum (Microbiological Associates) at 37°C for 30 min. In later experiments, pronase (Streptomyces griseus protease, protease type VI, Sigma Chemical Co., St. Louis, MO) was used for the enzyme treatment. It was freshly prepared and applied to the ganglion in a concentration of 5 mg/ml at 37°C for 5 min in a manner similar to that used for the chymotrypsin. Dialyzed calf serum (5 vols %) was added to the superfusing buffer solution at the conclusion of the pronase treatment. Following either enzyme treatment, ganglia were superfused with normal buffer for at least 30 min prior to the first intracellular recording.

### III. SUPERFUSION MEDIA FOR IN VITRO EXPERIMENTS

The selection of a buffer solution with which to superfuse the ganglia proved to be a difficult problem. In an initial series of experiments three different Krebs'-Ringer solutions were used to superfuse the ganglia maintained in vitro. The composition of these solutions is described in Table 2. All three solutions were supplemented with glucose (11.2 mM) and eventually with dialyzed calf serum (5 vol %; Microbiological Associates). In the first group of

TABLE 2. Comparison of Serum Values and Buffer Compositions. Values for cat and rabbit serum obtained from Spector (114) and Coldman and Good (36). Concentrations are expressed in milliequivalents per liter unless otherwise noted. All buffers were supplemented with dialyzed calf serum (5 vol %).

<u>Component</u>	<u>Serum Values</u>		<u>Buffer I</u>	<u>Buffer II</u>	<u>Buffer III</u>
	<u>Rabbit</u>	<u>Cat</u>			
Na <sup>+</sup>	142-158	132-158	150.4	143	147.9
K <sup>+</sup>	4.1	4.6-6	5.9	5.9	4.1/5.0
Ca <sup>++</sup>	7.0	-	5.0	5.0	7.0
Mg <sup>++</sup>	2.0	2.2	2.4	2.4	2.0
Cl <sup>-</sup>	92-112	112	127.4	126.5	105.1/106
HCO <sub>3</sub> <sup>-</sup>	28	-	0	25	25
SO <sub>4</sub> <sup>--</sup>	2.8	-	34.8	2.4	4
Glutamate <sup>-</sup>	-	-	0	0	8
Fumarate <sup>-</sup>	-	-	0	0	8.5
Pyruvate <sup>-</sup>	-	-	0	0	8
Glucose (mM)	7.4	5.5	11.1	11.1	11.1



experiments, ganglia from both cats and rabbits were superfused with Krebs'-Ringer phosphate buffered solution (Buffer I; 33,53) at a pH of 7.4 adjusted by varying the monobasic to dibasic phosphate ratio. This solution was continuously equilibrated with 100% O<sub>2</sub>. The second group of ganglia was superfused with Krebs'-Ringer bicarbonate buffered solution (Buffer II; 34,53) at a pH of 7.40 and continuously equilibrated with 95% O<sub>2</sub> and 5% CO<sub>2</sub>. It was possible that the high chloride concentration present in these latter two buffers may affect normal electrophysiologic behavior, perhaps by altering the chloride equilibrium potential. Therefore, a third group of ganglia was superfused with Improved Krebs'-Ringer bicarbonate buffered solution in which the chloride concentration was reduced by substituting glutamate, fumarate and pyruvate salts for some of the chloride salts. At this time it was thought that perhaps the best superfusion media would be one which closely duplicated the normal ionic composition of cat or rabbit serum. Therefore, the Improved Krebs' buffer was modified for this purpose and designated Buffer III. Table 2 compares the ionic compositions reported for cat and rabbit serum with that of the modified buffer solution. Unfortunately the glutamate, fumarate and pyruvate salts caused difficulties in the adjustment and maintenance of the solution pH and further complicated the formulation of the superfusate. Various other ions were studied for their ability to act as impermeant substitutes for the excess chloride ions.

The use of sulfate, methylsulfate, or isethionate salts to replace the combination of glutamate, fumarate and pyruvate salts was

found to be without effect on the various parameters measured in this study. Thus sulfate ions were used to substitute for excess chloride ions in much of this study. The composition of this buffer solution (Buffer IV) is shown in Table 3. However, because it was subsequently learned that sulfate ions may form complexes with sodium and potassium ions (Woodbury, personal communication) and thus alter the effective concentration of these important cations in the superfusing buffer solution, the decision was made to replace the sulfate ions almost entirely by glutamate ions. Glutamate ions have been shown to be highly impermeant in other systems (227). In addition, because of difficulties associated with repeatably reproducing the pH of the buffer solution from experiment to experiment, and because of a desire to improve the stability of the buffer solution, N-2-hydroxyethylpiperazine-N'-2-ethane sulfonic acid (HEPES; 15 mM) and morpholinopropane sulfonic acid (MOPS; 5 mM), were added to the superfusion media in order to supplement the existing bicarbonate-CO<sub>2</sub> buffer system. This supplemented version of Buffer IV has been designated Buffer V. Various parameters such as membrane resting potential, stability, duration of impalement and action potential amplitude and configuration were compared for neurons maintained in each of the buffers (see results).

#### IV. THE RECORDING CHAMBER

The requirements for a recording chamber were that it permit the continuous superfusion of a ganglion without the introduction of

TABLE 3. Composition of Extracellular Bathing Media Used in This Study. Concentrations are expressed in milliequivalents per liter unless otherwise noted.

Component	Buffer IV	Buffer V
Na <sup>+</sup>	150	150
K <sup>+</sup>	4.1 (rabbits) 5.0 (cats)	4.1 (rabbits) 5.0 (cats)
Ca <sup>++</sup>	7	7
Mg <sup>++</sup>	2	2
Cl <sup>-</sup>	105.1 (rabbits) 106.0 (cats)	105.1 (rabbits) 106.0 (cats)
HCO <sub>3</sub> <sup>-</sup>	22.4	22.4
HPO <sub>4</sub> <sup>--</sup>	2	2
SO <sub>4</sub> <sup>--</sup>	35.6	2
Glutamate <sup>-</sup>	0	21.5
HEPES (mM)	0	15
MOPS (mM)	0	5
OH <sup>-</sup>	0	10.1
Glucose (mM)	11.1	11.1
Dialized Calf Serum (vol%)	5	5

movement artifacts and provide access to the ganglion and its attached nerves for recording and stimulation. The precise control of temperature and gas tensions were also important considerations in the design of the chamber. Although many different chambers were constructed and tested during the course of these experiments only the design of the recording chamber which proved to be most satisfactory will be described here.

The chamber was constructed from a single block of plexiglas. As shown in Figure 1 there were three compartments separated by thin partitions. Slots in these partitions served to interconnect the compartments. The round central compartment had a readily replaceable cork bottom to which the ganglion could be affixed with small pins. The nerves from the ganglion were led through the slots into the peripheral compartments which were filled with paraffin oil and contained stimulating electrodes. Connections between the compartments were sealed with bone wax and white petroleum jelly. All three compartments were surrounded by an integral water jacket.

The superfusing media were pumped from their gassing flasks to the recording chamber in water-jacketed nylon tubing. Water jacketing the tubing insured that the temperature of the buffer solution was the same as the ganglion before the solution entered the chamber. A series of valves near the gassing flasks were used to switch from one type of solution to another. Because of the pump rate and system dead space there was a significant delay between the switching of the

valves and the entry of the new solution into the recording chamber. This delay was approximately 1.5 min. A partition within the central compartment prevented the inflowing stream of fluid from disturbing the ganglion. The superfusate was pumped out of the chamber through a hole near the top of the central compartment in order to provide a constant fluid level above the ganglion. Periodically, samples of buffer from the recording chamber were taken in order to determine pH (7.32-7.36),  $PO_2$  (350-410 mm Hg), and  $PCO_2$  (36-40 mm Hg).

At the conclusion of each experiment the entire recording chamber, the pumping chambers and the nylon tubing were first flushed with distilled water, then with 70% ethanol followed by another rinse in distilled water. This procedure was found to be necessary in order to minimize microbial growth.

#### V. INTRACELLULAR RECORDING APPARATUS

Glass micropipets, filled with either 3 M KCl or 5 M potassium acetate and having resistances ranging from 20 to 50  $M\Omega$ , were used throughout this study. These microelectrodes, constructed from redrawn Pyrex glass capillary tubing (O.D. = 1 mm; I.D. = 0.6 mm), were formed on a 2-stage vertical micropipet puller (David Kopf), and filled with electrolyte using the glass fiber method (216). The capillary tubes and glass fibers were first cleaned by rinsing in acetone and then soaking in 1N HCl, finally rinsing in deionized, distilled water and drying in an oven at 60°C. A bundle of 3-6 glass

fibers was inserted into each capillary tube prior to pulling. The heater current and final pulling tension were empirically adjusted to provide electrodes of the desired resistance and tip shape. The settings of these controls required periodic adjustment in order to maintain the production of useful electrodes. The electrolyte filling solution was filtered through a 0.45  $\mu$  Millipore filter immediately before filling the pipet. A syringe with a 6" 30 gauge needle was used to deliver the filling solution directly into the micropipet.

The microelectrodes were coupled to a high impedance ( $10^{13} \Omega$ ) preamplifier (Winston Electronics, San Francisco, CA) via a short length of chlorided silver wire. The indifferent electrode located in the ganglion chamber was a pellet of silver chloride. For some experiments, the indifferent electrode was separated from the ganglion chamber by a saline agar bridge. The microelectrode preamplifier was designed to allow for compensation of electrode tip potential as well as for neutralization of electrode capacitance. The output of the preamp was attached to one input of a 5A22N differential amplifier on a Tektronix D12 storage oscilloscope (Tektronix, Beaverton, OR) The other input to the differential amplifier received a calibrating pulse (10 mV, 5 msec; CA5 Calibrator, Bioelectric Instruments) triggered by each sweep of the oscilloscope. A digital voltmeter (Hewlett-Packard, Palo Alto, CA) was also used to monitor the unity-gain output of the preamplifier thereby providing a means for the

precise measurement of the membrane potential. The vertical output of the D12 oscilloscope was used to drive both a second oscilloscope (Tektronix model 565) to which was attached a Grass C4 oscilloscope camera, and a limited bandwidth pen recorder (Grass model 7).

In order to pass current through the recording electrode, a constant current source and bridge circuit was utilized (Winston Electronics, San Francisco, CA). There have been several objections to the use of a single electrode for both potential recording and passing polarizing current. The passage of current can alter the resistance of an electrode and thus affect the results obtained (72). This problem was examined in order to determine to what extent it might affect the results of this study. Figure 2 shows the results of passing -5 to +5 nA of constant current through a recording microelectrode on the microelectrode's measured tip impedance. A group of 40 micropipets, 20 filled with 3 M KCl and 20 filled with 5 M KAC, each having resistances in the range of 20-50 M $\Omega$  were studied. Electrode resistance was determined by measuring the amplitude of a 1000 Hz, alternating current square wave signal adjusted so that each millivolt of amplitude was equivalent to 1 M $\Omega$  of electrode resistance. The current passing through the microelectrode was determined by measuring, on the second channel of the oscilloscope, the voltage drop across a 1000 M $\Omega$  1% precision resistor in series with the electrode and current source. The data indicate that the passage of as little as 2 nA of hyperpolarizing current can significantly alter the electrode's resistance characteristics.

## VI. DATA ANALYSIS

The reduction of the magnitude and time course of neural events to numerical data was accomplished in two ways. In both cases the event to be recorded and analyzed was triggered to occur within a single sweep of the oscilloscope trace. The sweep speed of the oscilloscope was always adjusted to provide maximum resolution for the particular parameter to be measured. In the first method each individual oscilloscope sweep, or in some cases several superimposed traces, were recorded on single frames of 35 mm film (Kodak Linagraph 2476). These individual frames were enlarged and projected onto graph paper. A calibration pulse of known duration and magnitude, occurring at the beginning of each sweep provided the information necessary to convert the scale measurements to milliseconds or millivolts. As many as 30 frames for each neuron were analyzed in this manner in order to provide the most accurate representation of its electrophysiological properties. The second method took advantage of the storage feature of the Tektronix D13 oscilloscope. In this case, individual traces were stored on the oscilloscope screen and measurements of magnitude and time course were made directly. This method suffers from the fact that data reduction cannot be deferred until a more convenient time. Stable intracellular recording conditions must be maintained for a minimum of 4-5 min in order to complete the analysis. The simple photographic recording of the unanalyzed wave forms can be accomplished



usually within 60 sec. In most cases a combination of these two methods were utilized for the complete data analysis. In those cases where both methods had been used, and duplicate measurements of a particular parameter obtained, no differences in the analyzed data were ever found.

The various properties were determined as follows:

1. Membrane potentials were measured directly by a Hewlett-Packard digital voltmeter (model 3440A) attached to the 1X output of the microelectrode preamplifier. The highest stable potential observed during the course of the impalement was recorded as the membrane potential.
2. Input resistance of the neuronal membrane was determined by passing known constant current hyperpolarizing pulses (20-30 msec duration) through the intracellular recording electrode and measuring the resulting change in the membrane potential. The application of Ohm's law permits the direct calculation of input resistance. By measuring input resistance with several current pulses of different magnitude it was possible to determine slope resistance. When depolarizing current pulses were used to determine input resistance the results were often complicated by local membrane responses. The problems associated with the single electrode determinations of membrane resistance have been discussed by Frank and Fuortes (72). In their study on the cat motoneuron they observed that the passage of current through some electrodes resulted in an apparent change in

electrode resistance which they referred to as electrode polarization. They further noted that the time course of this electrode polarization was approximately exponential. Thus, the direct measurement of membrane resistance and time constant with concurrent polarization of the electrode could result in serious error. They proposed several alternative methods for the determination of these parameters. The "spike height method" for membrane resistance was based upon measurement of the action potential amplitude with and without the simultaneous flow of polarizing current, membrane resistance being equal to the change in action potential amplitude caused by the polarizing current divided by the polarizing current (Ohm's Law). This calculation relies on the assumption that the membrane resistance approaches zero at the peak of the action potential. Therefore, the magnitude of the overshoot will not be significantly affected by polarizing current flow, and any changes in action potential amplitude must be due to the voltage drop across the resistance of the resting cell membrane. Because the resistance of the membrane is probably not zero at the peak of the action potential, values determined by this method are low estimates.

3. Time Constant. The time course of potential change during the passage of a hyperpolarizing current pulse can be assumed to approximate an exponential curve as predicted by the resistance-capacitance model of the nerve membrane. Time constants were determined from measurements made during the time course of hyperpolarizing current



pulses. Photographic records were enlarged and projected onto graph paper. The voltage change caused by the current pulse was measured. The time required for the membrane to change by 0.63 (i.e.  $1-1/e$ ) of its final value minus initial value was taken as the membrane time constant ( $\tau$ ). The determination of the membrane time constant using depolarizing current pulses was severely complicated by local membrane responses which altered the time course of potential change. Frank and Fuortes (72) proposed an alternative method for the measurement of the time constant. Their "strength-latency method" is based on the assumption that depolarizing current will cause the membrane potential to decrease exponentially to a steady-state value. The relationship between the intensity and duration of a threshold stimulus was described by the equation:

$$I_{rh} / I = 1 - e^{-t/\tau}$$

where  $I_{rh}$  = rheobasic current;  $I$  = stimulus current;  $t$  = stimulus duration;  $\tau$  = time constant. When  $t = \tau$ ,  $I = 1.58 I_{rh}$ . Therefore, the stimulus duration at 1.58 times the rheobasic current is equivalent to the membrane time constant. Unfortunately, accommodation and local responses may distort the value of  $\tau$  derived from this relationship.

4. Membrane capacitance was calculated from the following relationship:

$$C = \tau/R$$

where  $C$  = membrane capacitance,  $R$  = membrane input resistance, and  $\tau$  = membrane time constant.

5. The following properties were usually all directly measured from the oscilloscope trace:

Action potential amplitude, defined as the potential difference in millivolts between the resting potential and the peak of the overshoot; overshoot, defined as the maximum positive spike potential; and the afterhyperpolarization, defined as the difference in millivolts between the resting potential and maximum negative spike potential. The action potential duration was measured as the interval between the start of the rising phase of the action potential and the point where the falling phase crossed the level of the resting potential. The maximum rates of rise and fall of the action potential were directly measured from fast sweep speed, stored oscilloscope traces, and expressed in volts per second. Threshold current was measured as the minimum current, applied intracellularly for 30 msec, necessary to stimulate the neuron approximately 50% of the time. Threshold depolarization was determined in a similar manner, measured between the resting potential and the inflection marking the start of the rising phase of the action potential.

6. Latency was measured as the time between the orthodromic stimulus artifact and the beginning of the action potential. Because of the unknown length and complexity of the initial segment and axon leading to the soma, it was not possible to determine the conduction distance and it was, therefore, impossible to calculate the conduction velocity from the latency measurements. Conduction velocities were measured, however, in a separate set of experiments, using two pair of stimulating electrodes on the infranodose vagus. By dividing the precisely measured intercathode distance by the latency difference, conduction velocity could be calculated.

#### VII. IONIC CONTRIBUTIONS TO PASSIVE AND ACTIVE PROPERTIES

Two different methods were utilized to study the contributions of sodium, potassium, calcium, and chloride ions to various passive and active electrical properties of neurons in nodose ganglia, primarily from cat. In the first method each ganglion was alternately superfused with the normal control buffer solution and with an experimental solution in which the concentration of a particular ion had been changed. Thus, data from 3-5 cells would be obtained initially while the ganglion was in normal buffer, then 7-10 cells would be studied during the ganglion's exposure to the experimental solution, and finally the ganglion would again be superfused with normal buffer and data from an additional 2-3 cells would be obtained. This paradigm could be repeated with the same or different experimental solutions. After solutions had been switched, a minimum of

15 min was allowed to elapse, in order to insure complete replacement and to allow time for diffusion and equilibration, before any additional data were obtained. The switch from control to experimental solution or back again was always accomplished while continuously recording from a neuron thereby allowing that neuron to serve as its own control. Unfortunately the switching procedure was not without hazard and many intracellular recordings were abruptly terminated before all of the necessary data could be obtained.

The second method made use of compounds known to interfere with specific ionic conductances or transport mechanisms in other systems. Thus tetrodotoxin was added to the superfusing buffer solution ( $10^{-9}$  -  $10^{-7}$  gm/ml) in order to block sodium conductance (66). Tetraethylammonium chloride was used to interfere with changes in potassium conductance (102,103). Ouabain, a potent inhibitor of active sodium transport (30,218), was added to the superfusate in order to assess the role of sodium pumping in the maintenance of passive membrane properties. The effects of 2,4-dinitrophenol, sodium cyanide, and hypoxia, all known to inhibit oxidative phosphorylation were studied in order to determine if any energy requiring process directly contributed to the maintenance of the passive electrical properties of neurons in the nodose ganglion.

#### VIII. PHARMACOLOGICAL TECHNIQUES

Two different techniques were used to administer drugs to the nodose ganglion in vitro. The first was a stop-flow technique in

which the superfusion pump was turned off and the substance to be studied was gently injected directly into the central compartment of the recording chamber. Assuming reasonable mixing, and knowing the volume of fluid in that compartment and the amount of substance injected, it was a simple matter to calculate the concentration. This technique suffered from several disadvantages, not the least of which was the ganglion's susceptibility to hypoxia. For this reason the period of observation could not exceed 3-4 min before the pump was turned on and fresh perfusate arrived in the chamber. The drug injection itself was not without hazard, and on several occasions resulted in the untimely termination of an otherwise successful impalement. In order to control for any possible effects associated with stopping the flow of the buffer solution, and also to rule out any possible solvent effects, it was always necessary to bracket each test with injections of the drug solvent during 3-4 min periods of stopped flow.

The second technique for drug administration simply consisted of preparing a separate buffer solution which contained a known concentration of the drug to be studied. It was then possible to switch from control buffer to the test solution and back again as often as necessary. While this overcame many of the problems associated with the first technique, it presented new difficulties of its own. Many drugs are susceptible to inactivation by oxidation (e.g., dopamine) and since the oxygen tension of a buffer in its gassing flask may be



as high as 600 mm Hg it is quite possible that the concentration of active drug reaching the ganglion could be significantly different from that in the original ungasped buffer solution. In addition, there is a considerable delay (1.5 min) between the time of switching from one buffer solution to another and the time when the new solution actually reaches the ganglion. This problem of dead space could be reduced through the use of a multichannel pump with the switching valves located near to the recording chamber.

The superfusion technique was best suited to the study of populations of neurons. The usual protocol for this technique was identical with that used in the ionic studies (see preceding section). The stop-flow technique, however, proved to be most useful for studying the effects of rapidly acting, oxygen sensitive compounds and offered the advantage that each neuron studied could serve as its own control. The effects of several drugs were studied with this technique.

The nodose ganglion was exposed to each of the following compounds using the method indicated (S = stop-flow technique; P = superfusion technique). Sodium methohexital (Brevane, Eli Lilly & Co., S); sodium pentobarbital (Nembutal, Abbot Laboratories, S); lidocaine (Xylocaine, Astra Pharmaceutical, S); atropine sulfate (Eli Lilly & Co., S); tetraethylammonium chloride (Etamon chloride, Parke, Davis & Co., P); veratridine (K & K Laboratories, P); phenyldiguanide (Aldrich Chemical Co., P); sodium cyanide (J. T. Baker Chemical Co., P); tetrodotoxin, ouabain, 2,4-dinitrophenol, and 5-hydroxytryptamine (Sigma Chemical Co., P).

## RESULTS

### I. SUPERFUSION MEDIA SELECTION

The selection of a buffer and the composition of the in vitro extracellular medium were determined by a preliminary series of experiments. These experiments were designed to examine the effects of various buffered media (see Methods) on resting and action potentials in isolated nodose ganglia from both cats and rabbits. The solutions were judged for their ability to sustain neuronal function in vitro. The following criteria were used: 1. neuron-ganglion ratio: this was the total number of successful intracellular recordings in a particular buffer divided by the total number of ganglia tested in that buffer; 2. magnitude of resting and action potentials; 3. nerve conduction velocity as estimated from stimulus response latency; and 4. average duration of intracellular recording. The results obtained in buffer types I, II and III are summarized in Table 4.

The bicarbonate buffers (II and III) appear to be significantly better than the phosphate buffer (I). More cells were obtained per ganglion, having higher resting potentials and shorter latencies in the bicarbonate buffered solutions than in phosphate buffer. It is also important to note that the average time of intracellular recording was significantly longer in the bicarbonate solutions. There

TABLE 4. A Comparison of Preliminary Results Obtained In Vitro With Buffer Types I, II and III.

<u>Preparation</u>	<u>V<sub>m</sub> (mV)</u>	<u>APA (mV)</u>	<u>OVST (mV)</u>	<u>APD (msec)</u>	<u>L (msec)</u>	<u>T (min)</u>
Rabbit						
Buffer I	-42 ± 1.4 (35)	57 ± 4 (13)	16 ± 3.2 (13)	7.2 ± 1.0 (13)	24 ± 5.8 (11)	3.3 ± 0.36 (35)
Buffer II	-47 ± 0.9 (129)	75 ± 1.4 (57)	26 ± 1.4 (56)	-	10 ± 0.7 (49)	8.0 ± 1.6 (118)
Buffer III	-47 ± 0.6 (149)	75 ± 1.3 (92)	27 ± 1.1 (92)	-	17 ± 0.8 (92)	6.2 ± 1.0 (148)
Cat						
Buffer I	-43 ± 1.6 (31)	74 ± 7.0 (7)	27 ± 4.7 (7)	9.2 ± 2.6 (5)	23 ± 4.0 (5)	3.9 ± 1.1 (25)
Buffer II	-53 ± 1.0 (37)	73 ± 3.0 (23)	21 ± 3.0 (23)	-	12 ± 5.0 (3)	8.3 ± 2.0 (35)
Buffer III	(none tested)					

NOTE: Buffer compositions and recording methods are described in the Methods section. Values are the mean and standard error for each determination. The number of cells studied is indicated in parentheses.

V<sub>m</sub> = resting membrane potential

APA = action potential amplitude

OVST = overshoot

APD = action potential duration

L = latency

T = duration of impalement

were no significant differences between bicarbonate buffer II and the "improved" bicarbonate buffer III in which the extracellular chloride concentration had been reduced. Buffer IV featured sulfate or glutamate ions as the impermeant extracellular anion and a pH (7.34) which more closely approximated cat and rabbit arterial blood pH. This buffer solution allowed for stable and reproducible intracellular recordings and was the superfusion medium used throughout most of this study. Buffer V featured a complex buffer system (HEPES-MOPS-Bicarbonate) which yielded an extremely stable pH. This solution was used to superfuse a large number of cat ganglia. Data obtained with this buffer (see below) were identical to those obtained for cat in buffer IV.

## II. PASSIVE ELECTROPHYSIOLOGIC PROPERTIES

### A. Resting Membrane Potentials

Cells from which stable resting potentials were recorded were classified as neurons only if they generated action potentials in response to direct stimulation applied to the nerve or through the recording electrode. Occasionally, cells were impaled that, despite high resting potentials (-60 to -70 mV), could not be stimulated either directly through the electrode or indirectly by stimulation of the nerve. This type of cell could be depolarized through zero to a positive membrane potential without generating any detectable active response. The identity of these cells is not known.

To provide anatomical reference for the intracellular recording sites, the ganglion was topographically partitioned into nine areas following the pattern established by Mei (160). No differences in the passive electrical properties of cells from these different regions were found; during the course of an experiment, intracellular potentials were recorded from the cells in each of the different areas with equal facility. Measurements of resting potentials were obtained from cells whose recorded potentials either remained stable or did not decrease more than a few mV over a minimal period of 30 sec; the resting potential was taken to be the highest stable potential obtained during such a recording period. Among the cells from which stable recordings were obtained, the actual time of recording ranged from about 1 min to over 3 hrs, averaging 7.4 min in rabbit cells and 8.3 min in cat cells. Figure 3 shows the distribution of resting membrane potentials recorded in this study (buffer IV). The mean value for the resting membrane potential recorded from cat cells in vitro was -51 mV for buffer IV and -52 mV for buffer V, and that for rabbit neurons in buffer IV was -50 mV. Table 5a summarizes these data. There was no significant difference between in vivo and in vitro values for either of these species.

#### B. Membrane Resistance

Membrane resistance was determined by passing current pulses of known and constant amplitude (usually 0.1-1 nA) across the membrane

and measuring the potential change produced. Figure 4 shows responses of a neuron (from rabbit) to anodal and to subthreshold cathodal current pulses. The effectiveness of the bridge circuit and pre-amplifier in balancing out the nonmembrane resistive and capacitive elements is also clearly demonstrated. The analysis of the response to subthreshold depolarizing current pulses was often complicated by local membrane activity generated by the current. Typically, on obtaining a stable impalement, several different hyperpolarizing current pulses (between 0.1 and 1 nA) were applied intracellularly to permit the determination of slope resistance. Table 5a contains the mean values for the membrane resistance measured in cats and rabbits. Rabbit ganglion cells had a significantly higher input resistance than that found for cat cells ( $p < 0.01$ ). The input resistance determined in vitro did not differ from that determined in vivo for either rabbit or cat. Figure 5 shows examples of the current-voltage relations in nodose ganglion cells. Several cells were studied for possible voltage-dependent changes in membrane resistance. To accomplish this, we varied the resting membrane potential by applying polarizing currents of different intensities (current clamping); there was no significant constant relationship change in membrane resistance as a function of membrane potential (Figure 6). However, the membrane resistance was related to the condition of the cell. When this gradually deteriorated, as evidenced by changes in configuration of the action potential and decline in resting potential, the

membrane resistance of the cell decreased. If these damaged cells were current-clamped to their original resting potential, then their membrane resistance increased, often to the original value.

Although rectifying behavior was rarely observed when cells were tested with hyperpolarizing current pulses of less than 1.5 nA, on those occasions when the current pulse exceeded 1.5 nA, what appeared to be rectification was more frequently observed. With the application of these larger current pulses, the initial hyperpolarizing response decayed with time to a steady, less hyperpolarized level, suggesting that the resistance had decreased. Thus, in the record shown in Figure 7, a current pulse of 2 nA caused the membrane potential to hyperpolarize from the resting value of -50 mV to -94 mV. The potential then declined slowly over the next 55 msec to -82 mV. In other words, it appeared as though the input resistance had decreased from an initial value of 22 M $\Omega$  to the steady value of 15.5 M $\Omega$  in response to hyperpolarizing current of 2 nA. Rectifying behavior of this kind was seen in many neurons (approximately 60%) in both species when such relatively large currents were applied. The microelectrodes were always tested before and after impalement in order to insure that they did not exhibit rectification at these current levels. The presence of rectifying behavior could not be statistically correlated with any other neuronal property.

Frank and Fuortes (72) discussed problems associated with the use of a single microelectrode for both stimulating and recording.

Although the magnitude of the possible recording errors associated with electrode polarization (see Methods) were assessed and believed to be relatively insignificant in this experimental situation, an indirect method was also used to measure membrane resistance in a few cells. This method is based upon measuring changes in the action potential amplitude caused by the passage of polarizing current across the cell membrane. Details of this method have already been reviewed. No significant differences were found between the values for membrane resistance determined by either the direct or indirect methods.

### C. Membrane Time Constant

The time course of the changes in membrane potential at the beginning and end of a hyperpolarizing rectangular pulse (0.1-1 nA, 20-30 msec) closely resembled simple exponential curves. This would be expected from the resistance-capacitance (RC) network model for nerve membranes. Direct measurements of the time constant were made, as described in the Methods, and are reported in Table 5a. There was a statistically significant difference between the time constants measured in cat cells and those in rabbit cells ( $p \leq 0.01$ ).

The reliability of the single electrode method for determining membrane time constant has been questioned (41,72). Therefore, to validate our directly determined values we used the strength-latency relationship developed by Frank and Fuortes (72) as an indirect



method for determining time constant. When membrane time constants were determined by both methods for several cells, no significant differences were found between the two values. However, there was a considerable discrepancy between directly determined values derived from depolarizing pulses and those derived from hyperpolarizing pulses. This was probably caused by depolarization induced, sub-threshold local current flow that was sufficient to distort the time course for potential change.

#### D. Membrane Capacitance

Total input capacitance (C) was calculated for each cell in which measurements of input resistance (R) and time constant ( $\tau$ ) had been obtained. The means of these calculated values are reported in Table 5a. Neurons in cat had a significantly higher input capacitance than did those in rabbit ( $p < 0.03$ ); there was no difference between in vitro and in vivo values for either species.

#### E. Specific Membrane Resistance and Capacitance

The calculation of specific values for membrane resistance and capacitance requires a knowledge of the membrane surface area. Because it was not possible to observe and measure the surface areas of the impaled cells directly, an average value for surface area was assumed. To determine this, several ganglia were prepared histologically, and cell diameters were subsequently measured with an ocular

TABLE 5a. Passive Electrophysiologic Properties of Neurons in Mammalian Nodose Ganglia.

Preparation	$V_m$ (mv)	$R_m$ (M $\Omega$ )	$R_m'$ ( $\Omega/cm^2$ )	$C_m$ (nF)	$C_m'$ ( $\mu F/cm^2$ )	$\tau$ (msec)
Rabbit <u>in vivo</u>	$-50 \pm 0.4$ (10)	$19 \pm 5.0$ (4)	2150	$0.179 \pm 0.021$ (4)	1.6	$3.5 \pm 0.7$ (4)
Rabbit <u>in vitro</u> (Buffer IV)	$-49 \pm 0.4$ (397)	$21 \pm 0.9$ (142)	2370	$0.166 \pm 0.006$ (94)	1.5	$3.6 \pm 0.16$ (94)
Cat <u>in vivo</u>	$-53 \pm 4.0$ (12)	$20 \pm 4.0$ (5)	2260	$0.167 \pm 0.017$ (5)	1.5	$3.2 \pm 0.7$ (5)
Cat <u>in vitro</u> (Buffer IV)	$-51 \pm 0.7$ (180)	$17 \pm 0.8$ (70)	1920	$0.192 \pm 0.012$ (56)	1.7	$3.0 \pm 0.14$ (56)
Cat <u>in vitro</u> (Buffer V)	$-52 \pm 0.36$ (477)	$18 \pm 0.35$ (368)	2035	-	-	-

NOTE: Buffer compositions and recording methods are described in the Methods section. Values are the mean and standard error for each determination. The number of cells studied is indicated in parentheses.

$V_m$  = resting membrane potential  
 $R_m$  = input resistance  
 $R_m'$  = specific membrane resistance  
 $C_m$  = input capacitance  
 $C_m'$  = specific membrane capacitance  
 $\tau$  = membrane time constant

TABLE 5b. Active Electrophysiologic Properties of Neurons in Mammalian Nodose Ganglia.

<u>Preparation</u>	<u>APA (mV)</u>	<u>OVST (mV)</u>	<u>APD (msec)</u>	<u>RT (V/sec)</u>	<u>FT (V/sec)</u>	<u>AFHYP (mV)</u>
Rabbit <u>in vivo</u>	76 ± 5.0 (6)	25 ± 4.0 (6)	1.6 ± 0.24 (6)	179 ± 73.0 (6)	81 ± 15.0 (6)	15 ± 3.0 (6)
Rabbit <u>in vitro</u> (Buffer IV)	78 ± 0.7 (186)	28 ± 0.6 (187)	1.7 ± 0.05 (63)	151 ± 9.6 (63)	72 ± 2.4 (63)	18 ± 0.5 (170)
Cat <u>in vivo</u>	82 ± 4.0 (8)	30 ± 3.0 (8)	1.8 ± 0.35 (7)	186 ± 26.0 (7)	74 ± 18.0 (7)	13 ± 3.0 (8)
Cat <u>in vitro</u> (Buffer IV)	87 ± 1.1 (101)	35 ± 0.9 (101)	2.3 ± 0.10 (47)	155 ± 15.0 (47)	61 ± 8.0 (47)	16 ± 0.6 (78)
Cat <u>in vitro</u> (Buffer V)	87 ± 0.36 (462)	35 ± 0.3 (462)	1.7 ± 0.02 (392)	217 ± 3.1 (393)	75 ± 2.0 (392)	15 ± 0.2 (452)

NOTE: Buffer compositions and recording methods are described in the Methods section. Values are the mean and standard error for each determination. The number of cells studied is indicated in parentheses.

APA = action potential amplitude  
 OVST = overshoot  
 APD = action potential duration  
 RT = rate of rise of action potential  
 FT = rate of fall  
 AFHYP = afterhyperpolarization

micrometer. We also assumed that larger cells would be most readily impaled and that they were perfectly spherical. Based upon these assumptions and measurements, it was concluded that the "typical" cell had a diameter of 60  $\mu$ , although most of the cells in the ganglion were considerably smaller. Thus, the surface area was calculated to be  $113 \times 10^{-6} \text{ cm}^2$ , and values for specific membrane resistance and capacitance are based on this area. There are indications, however, that the cells are not perfectly spherical and may have a complex surface morphology which would tend to greatly increase their effective surface area (M. Grillo, personal communication). It is important to recognize the limitations of these specific values, which are reported for comparative purposes only.

### III. ACTIVE ELECTROPHYSIOLOGIC PROPERTIES

Table 5b summarizes the active membrane properties of nodose ganglion cells recorded in vitro and compares them with measurements of the same properties obtained in vivo. The different properties of the action potential are defined as stated in the Methods section. Because it was difficult to obtain stable intracellular recordings in vivo, it is possible to present data from only a relatively few cells. Nonetheless, there was no significant difference between action potentials recorded in vivo and those recorded in vitro.

#### A. Spontaneous and Repetitive Activity

In studies in which in vivo recordings were made, spontaneously occurring action potentials were recorded from many neurons impaled

during the course of the experiments in both cats and rabbits. In many cases, the pattern and frequency of discharge were easily correlated with some phase of the cardiac or respiratory cycles. Occasionally, however, recordings were made from a neuron which was silent or which fired in an apparently irregular manner. Another type of activity was often observed, both in vivo and in vitro on impalement of a ganglion cell. It consisted of a high frequency spiking discharge (occasionally greater than 100 Hz) beginning as soon as the electrode entered the cell. The frequency gradually decreased until it stopped. At the same time the resting membrane potential rapidly fell toward zero. This activity was probably caused by damage to the cell sustained at the time of impalement. Slight changes in the position of the electrode or the passage of steady polarizing currents through the electrode did not preserve the resting potentials. Rarely, high frequency discharges (50-100/sec) continued for several minutes, without changes in resting potential. In these cases, polarizing currents significantly altered the frequency of discharge. Hyperpolarization of the membrane to approximately -60 mV blocked these discharges, and depolarization generally augmented the rate of discharge at first and then depressed it as the resting membrane potential approached zero.

#### B. The Action Potential

Typical action potentials recorded in cat and rabbit nodose ganglion cells are shown in Figure 8. The action potential amplitude

ranged between 107 mV and 53 mV in cats and 114 mV and 48 mV in rabbits. All neurons exhibited an overshoot although in some, whether because of injury or deteriorating conditions, the overshoot eventually decreased or was completely eliminated. This change in overshoot was most often accompanied by a simultaneous decrease in resting membrane potential and membrane resistance. The values for overshoot and action potential amplitude measured in cat were significantly different from those measured in rabbit cells ( $p \leq 0.001$  and  $p \leq 0.002$ , respectively).

Although not apparent at normal oscilloscope sweep speeds and stimulation conditions, there were deflections in the rising phase that probably contributed to the normally recorded action potential. As the spike electrogenic mechanisms in the soma membrane begin to fail, a distinct inflection was frequently recorded. In addition, continuous repetitive stimulation at frequencies as low as 10-20 Hz, either directly through the recording electrode or indirectly via one of the nerve trunks, also often resulted in soma spike failure (Figure 9). The remaining active potential probably originated in the initial segment of the axon or axon hillock region, spreading electrotonically to the recording electrode. This is analagous to the IS spike (or NM) component recorded in other neurons.

A third smaller spike component was observed only rarely and after failure of the IS spike. This small local potential probably originated at a point more distant from the recording electrode than

the IS spike, possibly at the bifurcation of the nerve fiber or in the nerve fiber itself, and could be analagous to the M spike observed in motoneurons (24) and also described for toad spinal ganglion cells (119). Occasionally, intracellular action potentials were recorded that had a different configuration from that shown in Figure 8. These spikes were of short duration ( $<0.5$  msec) and exhibited no afterhyperpolarization. Their stimulus-response latencies were extremely short (always less than 1 msec), and there were no other components evident in these action potentials. We assumed that these recordings were obtained from axons.

The duration of the action potential ranged from 0.40 to 2.50 msec in cat ganglia, and from 0.75 to 2.40 msec in rabbit ganglia. The rate of rise ranged from 70 to 720 V/sec in cats and from 70 to 400 V/sec in rabbits. Mean values are presented in Table 5b. The falling phase of the somatic action potential recorded in rabbit neurons was normally smooth with no detectable inflection points. In neurons from cat ganglia, however, there was occasionally an inflection on the falling phase of the action potential, particularly evident when the latter was viewed at fast sweep speeds on the oscilloscope. In both species, the falling phase was always followed by a period of afterhyperpolarization, whose magnitude and duration ranged from 2 to 28 mV and 8 and 30 msec, respectively. The membrane potential returned to the pre-spike resting level without any evidence of a subsequent depolarizing phase. There was no period of afterhyperpolarization associated with the IS or M spikes.

All data on active membrane properties (Table 5b) were obtained by analyzing action potentials evoked indirectly by stimulation of the vagus nerve or one of its branches. In addition, all of the cells could be stimulated directly by brief depolarizing current pulses passed through the recording electrode. Typical action potentials were generated whenever the intracellularly applied current pulse exceeded a threshold level (Figure 10). The threshold depolarization for generating an action potential by direct intracellular stimulation ranged between 7 and 29 mV (mean of 299 cat cells, 14.8 mV; mean of 98 rabbit cells, 15.1 mV).

### C. Effects of Depolarizing and Hyperpolarizing Currents

A variety of responses was observed when neurons were stimulated by long (up to 10 sec) suprathreshold current pulses. A classification system for the various response types was established. Type 1 neurons were characterized by generating a burst of 1-3 action potentials in response to the current pulse (Figure 11a). Type 2 neurons generated a short train of impulses characterized by gradually decreasing spike amplitudes and increasing interspike intervals (Figure 11b). The duration of this response never exceeded 3 sec and rarely exceeded 1 sec. Types 3 and 4 were characterized by their ability to fire continuously for the duration of the suprathreshold current pulse, up to 10 sec. The type 3 response consisted of an initial burst of impulses followed by continuous activity at a lower



frequency (Figure 11c). The type 4 neuron fired continuously without significant change in frequency (Figure 11d). When type 4 neurons were current clamped to suprathreshold levels, spike frequency was found to be directly proportional to the magnitude of depolarization. As shown in Figure 12, stepwise changes in the stimulus strength caused stepwise changes in the response frequency. At the step transitions, off responses, similar to those observed in many slowly-adapting sensory receptors (52,156), were seen.

A population of 114 neurons, in ganglia removed from cat, was studied in order to determine if the adaptive response type of a particular neuron could be related to any of its other passive or active electrophysiologic properties. Of the 114 neurons examined, 24% were classified as type 1, 24% as type 2, 34% as type 3, and 18% as type 4. An analysis of the electrophysiologic properties of these neurons, showed that significant differences occurred only between the rapidly adapting type 1 neurons and the nonadapting type 4 neurons. In this case, the conduction velocity of the type 4 neurons was significantly ( $p \leq 0.01$ ) faster than that of the type 1 neurons. Discriminant analysis revealed that no single property, however, was sufficiently well correlated with adaptation type to permit its use as a predictor of adaptation type.

Invasion of the soma could be blocked by hyperpolarizing pulses. If an indirectly-evoked action potential was timed to occur during the passage of a hyperpolarizing current pulse, the somatic spike

could be blocked completely, clearly demonstrating an IS spike (Figure 13), but a further increase in the magnitude of the hyperpolarizing pulse did not block the IS spike or significantly affect its amplitude. Occasionally, cells generated action potentials at the termination of a hyperpolarizing current pulse. This "anodal break" excitation was considered to be a sign of deterioration, as it was usually associated with decreases in both resting potential and input resistance.

Alteration of the resting potential by the passage of steady polarizing current across the cell membrane usually caused significant changes in the magnitude and duration of the afterhyperpolarization (Figure 14). The afterhyperpolarization was increased by depolarization (Figure 14a) and reduced by hyperpolarization (Figures 14c-f) of the membrane. With anodal current, the cells could be hyperpolarized to the reversal potential for the afterhyperpolarization ( $E_{AH}$ ). At  $E_{AH}$ , the falling phase of the action potential terminated when the level of the prespike resting potential was reached and, thus, resembled an axon spike (Figure 14e). Further hyperpolarization of the membrane resulted in the appearance of an afterdepolarization (Figure 14f). The reversal potential was determined for 83 cells from both cats and rabbits and ranged between -62 and -86 mV (mean =  $-71.8 \text{ mV} \pm 0.5$ ).

Changes in the resting membrane potential, produced by the intracellular application of polarizing current, had little or no

effect on the magnitude of the action potential overshoot, thereby allowing the action potential amplitude to vary directly with changes in membrane potential. The rates of potential change for the rising and falling phases of the action potential were also found to be proportional to the resting membrane potential in any one cell.

#### D. Repetitive Stimulation

Many neurons could be stimulated to fire repetitively at rates as high as 50-100 spikes per second. Indirect (nerve) stimulation was as effective as direct (intracellular) stimulation even at these high frequencies. On many occasions, both in vivo and in vitro, recordings were made from cells that developed a distinct, persistent hyperpolarization when repetitive action potentials occurred (Figure 15). In contrast to post-tetanic hyperpolarization, this hyperpolarization began with the first action potential and persisted no longer than 5 sec after stimulation was stopped. The magnitude of this hyperpolarization was often as high as 10-15 mV and appeared to be dependent on the frequency of discharge, some hyperpolarization being observed at frequencies as low as 1-2 spikes per second. This persistent hyperpolarization only occurred if action potentials were generated in the cell body, and sometimes caused failure of somatic spike generation.

In several preliminary experiments, the effect of the resting membrane potential on the magnitude of this activity hyperpolarization

was investigated. Membrane potential was altered by the passage of steady polarizing currents (current clamping). The magnitude of activity hyperpolarization was found to be dependent upon the membrane potential, increasing during depolarization and decreasing during hyperpolarization. It appeared that the reversal potential for this process was approximately the same as the reversal potential for the afterhyperpolarization in the same cell.

#### E. Latency and Conduction Velocity

Anatomical uncertainties such as the exact location of the cell within the ganglion, and the length of the complex initial segment and intraganglionic conduction path, precluded the precise determination of the distance between the stimulating and recording electrodes. Values are reported for the latency, which is defined as the time (in msec) between the stimulus artifact and the onset of the action potential. Figure 16 shows the distribution of latencies measured in both cat and rabbit neurons in vitro. The design of the recording chamber and the fixed positions of the stimulating electrodes make it unlikely that the observed latency differences were significantly affected by the recording arrangement.

The measurement of latency cannot be considered a reliable way to determine conduction velocity. Accordingly, in a separate group of cat ganglia, conduction velocity was measured using two sets of stimulating electrodes separated by a precisely known distance.

Conduction velocities determined by this technique ranged between 0.4 to 30 M/sec (mean of 51 neurons, 4 M/sec). The latencies determined for this same population of neurons were negatively correlated with the conduction velocities ( $s \leq 0.001$ ) as would be expected. Figure 17 shows the distribution of conduction velocities and latencies measured in this population of neurons.

A statistical analysis of the distribution of individual values obtained for the passive and active electrophysiological properties (other than conduction velocity or latency) measured in both cat and rabbit nodose ganglion neurons indicated that they were unimodally distributed about their respective means. Tests for correlation among the various properties did not reveal any unexpected relationships.

#### IV. IONIC CONTRIBUTIONS

##### A. Potassium

The effect of varying the external potassium concentration between 0.25 mM and 98 mM on the resting membrane potential in cat neurons is shown in Figure 18. In all cases, potassium was exchanged for sodium in the bathing medium and measurements were taken at least 15 min after the solutions were changed. In those experiments in which the time course of the effect of potassium on a single neuron was observed, potassium-induced changes in the membrane potential were complete within 3-5 min.

The slope of the line relating the log of the external potassium concentration to the membrane potential is nonlinear at potassium concentrations below 2.5 mM (Figure 18). The maximum slope of the relation at potassium concentrations above 2.5 mM is 25 mV per 10-fold change in potassium concentration. Input resistance was determined for the same population of neurons and is shown in Figure 18.

An external potassium concentration greater than 10 mM usually blocked nerve conduction and this was rapidly followed by failure of the soma to generate action potentials. Consequently, little data are available from neurons exposed to high extracellular potassium. These blocking and other effects were usually reversible upon return to solutions containing normal potassium concentrations. The rate of potential change ( $dV/dt$ ) of the falling phase of the action potential was found to vary as a function of potassium concentration between 2.5 and 25 mM. As the external potassium concentration was increased within this range, the rate of fall decreased from 88 V/sec at 2.5 mM ( $\pm 2.4$ ,  $n=11$ ) to 40 V/sec at 25 mM ( $\pm 3.8$ ,  $n=5$ ). At concentrations of extracellular potassium below 2.5 mM, the rate of fall was not significantly affected, occasionally showing a slight tendency to increase. The rate of rise of the action potential was not significantly affected by changes in external potassium concentration ranging between 1 and 10 mM.

The magnitude of the afterhyperpolarization varied as a function of the external potassium concentration. The maximum slope of the

relation between log potassium concentration and afterhyperpolarization was, however, only 16 mV per decade (Figure 18). The reversal potential for the afterhyperpolarization ( $E_{AH}$ ) was not significantly changed in solutions containing potassium concentrations below 5 mM. At concentrations above 5 mM, however,  $E_{AH}$  decreased at the rate of 30 mV per ten-fold change in external potassium concentration.  $E_{AH}$  was equal to -72 mV ( $\pm 0.9$ ,  $n=30$ ) at the normal external potassium concentration of 5 mM, and decreased to -64 mV ( $\pm 0.8$ ,  $n=13$ ) at an external potassium concentration of 10 mM.

The amount of current necessary to bring the cell body to threshold and generate an action potential increased under conditions of low potassium concentration and decreased in high potassium. The threshold level itself also appeared to be dependent upon the external potassium concentration, varying inversely with it. Thus, the threshold potential was -51 mV ( $\pm 1.1$ ,  $n=14$ ) in 0.25 mM potassium, -37 mV ( $\pm 0.3$ ,  $n=299$ ) in normal buffer, and -30 mV ( $\pm 2.8$ ,  $n=5$ ) in 25 mM potassium.

## B. Sodium

External sodium concentration could not be increased without seriously affecting the osmotic equilibrium. Therefore, changes in sodium concentration were confined to a reduction from its normal 150 mM to 34.4 mM. The lower value was selected both because it represented a significant reduction in external sodium and because the buffer media could be prepared conveniently at that concentration.

Choline chloride or TRIS chloride was used to replace sodium chloride in most experiments. In some experiments an osmotically equivalent amount of sucrose was used to replace partially both sodium and chloride.

The replacement of all but 34.4 mM of sodium in the bathing medium with either choline or TRIS caused a slight but statistically significant decrease in resting membrane potentials (3-4 mV;  $n = 34$ ;  $p \leq 0.05$ ). Reducing extracellular sodium concentration to 34.4 mM and chloride concentration to 12.1 mM with sucrose replacement caused a slight (4 mV) but again, significant ( $p \leq 0.01$ ) depolarization in the 21 neurons tested. Membrane input resistance was unchanged in low sodium media containing choline or TRIS substituent ions. The input resistance was, however, significantly increased (average increase = 11  $M\Omega$ ;  $n = 14$ ;  $p \leq 0.02$ ) when an osmotically equivalent quantity of sucrose was used to replace all but 34.4 mM of sodium and 12.1 mM of chloride ions.

The overshoot and absolute amplitude of the action potential were both reduced in the low sodium media. The amplitude of the overshoot was found to change by 23 mV per 10-fold change in extracellular sodium concentration. The rates of potential change ( $dV/dt$ ) for both the rising and falling phases of the action potential were reduced in low sodium media. The rate of rise was decreased by an average of 74% from control values and the rate of fall was decreased by an average of 36%. The magnitude of the afterhyperpolarization



was unaffected in choline substituted low sodium media, but was usually reduced by up to 50% in low sodium solutions containing either TRIS or sucrose. These effects on the action potential are shown in Figure 19.

The average current necessary to bring the soma membrane to threshold was significantly reduced in sucrose-substituted low sodium media but unchanged when either TRIS or choline were used to replace sodium. The threshold potential was decreased in low sodium media by an average of +8 mV ( $n=17$ ,  $p \leq 0.02$ ) from its normal value of -37 mV.

The effects of replacing most of the extracellular sodium with lithium were examined in 5 neurons from 2 cat nodose ganglia. The lithium substitution had no effect on either the resting membrane potential or input resistance. The overshoot, action potential amplitude, and afterhyperpolarization were variably but often significantly reduced in the lithium substituted medium as were the rate of rise and, to a lesser extent, the rate of fall of the action potential.

### C. Calcium

The extracellular concentration of calcium was reduced to zero by elimination of calcium-containing salts from the superfusing solution and by the addition of the calcium chelating agent EGTA (1 mM), the calcium ions being replaced by sodium ions. Resting membrane potentials were unchanged from control in zero calcium

media. The input resistance, however, was reduced by 40% (6-8 M $\Omega$ , n = 13; p  $\leq$  .02) in the absence of calcium. The overshoot and, therefore, the action potential amplitude were slightly (2-7 mV) but significantly (n = 14, p  $\leq$  .05) reduced. Although the rate of rise of the action potential was unaffected, the rate of fall and the afterhyperpolarization were both significantly reduced in zero calcium media. The rate of fall was decreased by 30% (n = 13, p  $\leq$  .02) and the afterhyperpolarization was decreased by 37% (n = 13, p  $\leq$  .02). The elimination of extracellular calcium had no effect on threshold current but did cause a slight increase in threshold potential (increased excitability).

In a second group of experiments, the extracellular calcium concentration was increased from its normal value of 3.5 mM to a final value of 25 mM. The sodium concentration was correspondingly reduced to maintain osmotic balance. This increased calcium concentration had no effect on the resting membrane potential and caused a slight increase (average 30%; n=5, not statistically significant) in the input resistance. The overshoot and therefore the action potential amplitude were slightly (5-10 mV) but significantly (n=5, p  $\leq$  0.05) reduced by the high calcium concentration. It should be noted that the extracellular sodium concentration was slightly reduced in the high calcium media. Although the rate of rise of the action potential was unaffected, the rate of fall was increased by an average of 50% (n=5, p  $\leq$  0.01). Both the magnitude of the afterhyperpolarization and the threshold current were unaffected by the increased calcium concentration.

#### D. Chloride

The presumably impermeant anions glutamate and methylsulfate were used to replace chloride ions in the chloride-free media. The effect of glutamate was identical to the effect of methylsulfate. The resting membrane potential was unaffected while the input resistance was increased by 7-12 M $\Omega$  (n = 26, p  $\leq$  0.02). Because the sudden changes in chloride concentration usually resulted in electrode polarization artifacts, transient effects on the membrane potential occurring within 60 sec of the solution change may have been undetected. The threshold current appeared to be slightly reduced. All other parameters were unaffected by exposure to a chloride-free environment.

An increase in the external chloride concentration from 106 mM to 127.5 mM caused a significant (n=11, p  $\leq$  0.03) 5 mV hyperpolarization of the resting membrane potential. The input resistance was reduced by an average of 35%, and there was a slight increase in the current required to bring the cell body to threshold. No other parameters were significantly affected by this increase in chloride concentration.

#### V. PHARMACOLOGIC PROPERTIES

Neurons in nodose ganglia of both cat and rabbit were exposed to a variety of pharmacologically active compounds. The purpose of these experiments was to provide a qualitative indication of the existence of chemical sensitivity in mammalian nodose ganglion neurons.

As these experiments were regarded as preliminary in nature, no attempt was made to precisely quantify all drug effects or to determine underlying mechanisms.

#### A. Tetrodotoxin

Several ganglia removed from cat were exposed to tetrodotoxin (TTX) at concentrations from  $10^{-9}$  to  $10^{-7}$  gm/ml in the superfusing medium. At TTX concentrations of  $5 \times 10^{-8}$  gm/ml or less, the action potential remained unaffected for the duration of the exposure, up to 32 min. During this same period of time, however, the resting membrane potential appeared to hyperpolarize slightly and progressively, reaching a maximum hyperpolarization of 3-5 mV. At TTX concentrations greater than  $5 \times 10^{-8}$  gm/ml action potential generation was blocked within 4.5 - 7 min. Prior to spike failure, the configuration of the action potential underwent certain characteristic changes. The spike became progressively prolonged, and its rate of rise and overshoot were markedly reduced. Nerve conduction block occurred first and was shortly followed by soma spike failure. In all cases (n=8), complete spike failure was followed by a general deterioration of the neuron, characterized by a decrease in membrane potential and input resistance, and associated with increased difficulty in maintaining a stable intracellular impalement. This eventually led to a total inability to obtain intracellular recordings.

### B. Tetraethylammonium Ions

Nodose ganglia removed from both cat and rabbit were exposed to external bathing media containing tetraethylammonium chloride (TEA) at a concentration of  $10^{-3}$  -  $5 \times 10^{-4}$  gm/ml. As shown in Figure 20 the falling phase of the action potential always developed a distinct plateau. This effect of TEA was associated with a slight but significant depolarization of the membrane (2-5 mV;  $n=6$ ,  $p \leq 0.02$ ). All of the effects of TEA were readily and completely reversible upon return to normal external media.

### C. Ouabain

Neurons in cat nodose ganglia exposed to ouabain, for more than 1 hr, at concentrations of  $10^{-7}$  M or less were unaffected except for the membrane potentials which occasionally showed a slight hyperpolarizing tendency, an effect which was reversible after return to normal media. At concentrations higher than  $10^{-7}$  M, ouabain appeared to cause relatively rapid and irreversible damage to the ganglion. The following sequence of events was typical when recording from a neuron suddenly exposed to ouabain at this concentration or greater. Within 5 min the neuron hyperpolarized by 3-7 mV, followed within 30 min by a complete loss of excitability. Shortly thereafter the impalement was lost and subsequent attempts to obtain other intracellular recordings were unsuccessful. These effects were not reversible within the period of observation up to 2 hrs ( $n=25$ ).

#### D. Metabolic Inhibitors

Both cyanide (CN) and 2,4-dinitrophenol (2,4-DNP) are potent inhibitors of oxidative metabolism. Cat and rabbit nodose ganglion neurons were superfused with media containing CN (100  $\mu\text{g}/\text{ml}$ ) or 2,4-DNP (1  $\mu\text{g}/\text{ml}$ ). Both agents had effects similar to those observed under hypoxic conditions. That is, over a period of 5-15 min both the membrane potential and input resistance gradually decreased. The configuration of the action potential changed to resemble that of an obviously deteriorating neuron. In a manner reminiscent of TTX and ouabain, the intracellular impalement was eventually lost and subsequent attempts to obtain other stable intracellular records were unsuccessful. These effects were not reversible upon return to control for up to 3 hrs of observation (CN, n=6; DNP, n=1).

#### E. Local and General Anesthetics

The local anesthetic lidocaine (2  $\mu\text{g}/\text{ml}$ ) and the general anesthetics sodium pentobarbital (30-300  $\mu\text{g}/\text{ml}$ ) and sodium methohexital (50  $\mu\text{g}/\text{ml}$ ) all had similar effects on nodose ganglion neurons. A typical example of these effects is shown in Figure 21. At the concentrations indicated, these agents all rapidly and reversibly blocked generation of somatic spikes. The IS spike and, therefore, presumably nerve conduction remained unaffected. Exposure to these anesthetics at slightly higher concentrations or for longer periods of time, however, resulted in nerve conduction block. As shown in

Figure 22 the effects of atropine (10  $\mu\text{g/ml}$ ) closely resembled those of the anesthetic agents.

F. Veratridine, Phenyldiguanide, and 5-Hydroxytryptamine

Veratridine, phenyldiguanide (PDG), and 5-hydroxytryptamine (5-HT) were all reported to produce action potentials in cat nodose ganglion neurons (198) when injected into the common carotid artery while simultaneously recording activity in small nerve bundles dissected from either the supra- or infranodose vagus. In the present study, the effects of these agents on intracellularly recorded potentials in nodose ganglion neurons of both cat and rabbit were examined.

Veratridine produced several significant effects on both cat and rabbit neurons at a concentration of 1  $\mu\text{g/ml}$ . Whereas resting membrane potentials in both species were unaffected, the membrane input resistance of cat neurons was decreased by 3-15  $M\Omega$  ( $n=15$ ,  $p \leq 0.01$ ), and in rabbit neurons was increased by 5-19  $M\Omega$  ( $n=18$ ,  $p \leq 0.02$ ). The most prominent effect of veratridine was its ability to produce a large and long-lasting after-depolarization following the generation of an action potential either by direct intracellular stimulation or by stimuli applied to the nerve trunk. The nature and magnitude of this after-depolarization is clearly shown in Figure 23. The depolarizing response often gave rise to a train of action potentials as shown in the same figure. The duration of this repetitive activity was frequently quite prolonged. In the example

shown in Figure 24, a stimulus pulse applied to the nerve caused a single action potential to be generated (indicated by the arrow) in the cell body. The subsequent after-depolarization resulted in the repetitive generation of action potentials for approximately the next 5 sec. The generation of spike trains in response to a single action potential was observed in about one-third of the neurons tested. For technical reasons it was not possible to make correlations between veratridine response and adaptation type. Blackman et al. (13) have recently confirmed many of these findings.

Neither 5-HT (1-3  $\mu\text{g/ml}$ ) nor PDG (0.5-2  $\mu\text{g/ml}$ ) had any effect on action potential generation in nodose ganglion neurons of either cat or rabbit. PPG caused a slight, 3-4 mV hyperpolarization ( $n=9$ ,  $p \leq 0.005$ ) associated with a 4-10  $M\Omega$  increase in membrane resistance ( $n=12$ ,  $p \leq 0.01$ ); 5-HT had no effect on either of these properties.



## DISCUSSION

The passive and active membrane properties recorded from neurons in rabbit and cat nodose ganglia maintained in vitro were indistinguishable from those obtained in vivo. This indicates that the neurons did not deteriorate appreciably while in vitro, and that the data represent a reasonable description of these properties of adult mammalian sensory neurons. The values obtained in this study were similar to those reported for other peripheral sensory neurons under different recording conditions (Table 1), despite the fact that cells in other studies were often selected on the basis of high resting membrane potentials. In this study, properties were analyzed for all cells that had stable resting membrane potentials and were able to generate action potentials, and there were no additional criteria for selection. Another indication of the viability of the neurons maintained in vitro is that stable recordings were routinely made for upwards of 20-30 min, and, when specific attempts were made, intracellular recordings could be obtained for as long as 2-3 hrs with no decline in either passive or active properties. The ease with which such recordings can be made in this in vitro preparation, and the ability to vary and control the extracellular medium, provided an opportunity to examine the role of different ions in the maintenance of passive properties of mammalian nerve cells and in the generation of their action potentials.

## I. PASSIVE ELECTROPHYSIOLOGIC PROPERTIES

The resting membrane potentials of nodose ganglion cells of both rabbit and cat had unimodal distributions about their respective means, indicative of a uniform population of neurons within the ganglion even though different sensory modalities are carried by their afferent fibers and there is a wide range of cell diameters (20-60  $\mu$ ). Although neurons in cat differed from those of rabbit with regard to certain specific properties, such as membrane resistance, time constant, overshoot and action potential amplitude, the physiological significance of these differences is unknown.

Within the range of changes in membrane potential used in this study (+10 to -110 mV), voltage-dependent changes in membrane resistance were not observed. Indeed, the only time such changes occurred was when the neurons were deteriorating as indicated by a relatively slow decline in the membrane potential. Under these conditions, the membrane resistance was also decreasing, and the application of hyperpolarizing current caused the resistance to increase toward the control value. On studies in similar neurons, Ito (119) reported that the membrane resistance of toad spinal ganglion cells was decreased by depolarization and increased by hyperpolarization.

A significant decrease (50-60%) in membrane resistance associated with hyperpolarization of the membrane potential has been reported to occur in cat motoneuron (123,167) and rabbit sympathetic ganglion cells (34). This "anomalous rectification" has also been observed in the

ganglion cells of Helix aspersa (129), frog muscle cells (2,163) and in the horizontal cells in the retina of the mudpuppy (224). The physiological significance of this voltage dependent conductance change has been related to possible effects on synaptic transmission. Anomalous rectification has also been used to explain the nonlinear relationship between membrane potential and EPSP amplitude observed in some neurons.

Anomalous rectification has not been reported in primary sensory neurons, (e.g., dorsal root or spinal ganglia). This study demonstrated that some neurons in nodose ganglia of both cat and rabbit do exhibit some form of rectifying behavior (Figure 6). This delayed decrease in membrane resistance is identical with that reported for other rectifying neurons (123,224). The anomalous rectification in nodose ganglion cells occurred only when the membrane was hyperpolarized beyond the reversal potential for the afterhyperpolarization ( $E_{AH}$ ). Because  $E_{AH}$  is believed to be near the potassium equilibrium potential, a delayed increase in potassium conductance may account for the rectification as was suggested in sympathetic neurons (34). The physiologic role of anomalous rectification is thought to be the modification of postsynaptic potentials. Further studies will be necessary in order both to characterize fully the rectifying behavior of nodose ganglion neurons and to determine the physiological significance of anomalous rectification in neurons devoid of synaptic inputs.

The input resistance of neurons in the nodose ganglion is considerably higher than that reported for many other neurons (Table 1). With

the exception of sympathetic neurons, low values of input resistance appear to be associated with neurons whose cell bodies possess dendrites and receive multiple synaptic inputs. The apparent low input resistance of these neurons may be due to the current sinking capabilities of the dendritic arborization or to special conductance properties of sub-synaptic membrane areas. Nodose ganglion neurons are uncomplicated by these factors, and values for their input resistance (both in vivo and in vitro) compare favorably with those reported for other vertebrate sensory neurons (Table 1a).

The calculated values for time constant, specific membrane resistance and specific membrane capacitance of sensory neurons in nodose ganglia from both cat and rabbit are similar to those reported for sensory neurons of other species, as well as to spinal motoneurons of both toad and cat. However, all calculations were based on the assumption that nodose ganglion neurons were 60  $\mu$  in diameter and possessed smooth spherical surfaces. These assumptions, made only for convenience of calculation, must be seriously questioned. For example, electron microscopic studies have shown that sensory neurons in nodose ganglia of monkey (30) and cat (Grillo, personal communication) are not spherical and that the membrane appears irregular and convoluted. The actual surface area of these cells, therefore, may be considerably greater than that derived from their assumed spherical diameter. Thus, the true values for specific membrane resistance and capacitance are likely to differ from those reported here.

## II. ACTIVE ELECTROPHYSIOLOGIC PROPERTIES

Prior to this study, there had been no report of action potentials recorded intracellularly from cell bodies in mammalian nodose ganglia (see note 1), although they have been from dorsal root ganglion cells of cat and rat (59,68,151,199). A consideration of the morphological features of sensory neurons in the nodose ganglion raises a question as to whether action potentials in afferent fibers of the vagus nerve and its branches actually invade the soma. In contrast to the majority of neurons in dorsal root ganglia, a larger proportion of those in nodose ganglia give rise to long, thin and often convoluted initial complexes before bifurcating into central and peripheral projections (190; M. Grillo, personal communication). This initial complex is of smaller diameter than either the central or peripheral branches of the afferent fibers, and may range from 50 to 170  $\mu$  in length. The length and small diameter of these initial complexes suggest that action potentials are propagated actively in them to the soma from the afferent fibers, as electronic spread would seem to be insufficient to generate a spike in the soma from a site so distant in the axon.

Sato and Austin (199) reported that there was no inflection on the rising phase of the action potential in cat dorsal root ganglion neurons, and they postulated that the threshold for spike generation in the soma was similar to that in the initial segment. Although we normally

---

Note 1. During the preparation of this manuscript, however, Blackman et al. (13), studying the effects of veratrum alkaloids, have published figures of action potentials recorded intracellularly from neurons in guinea pig nodose ganglia.

observed a smooth rising phase of the somatic spike in nodose ganglion neurons, a clear inflection could be demonstrated under certain circumstances such as high frequency stimulation. This indicates that the threshold is higher in the soma of the neuron than in the initial complex. Inflections on the rising phase of the action potential have been reported for a variety of other neurons (24,119,151,214). With the exception of the somatic spike, we are uncertain as to the origins of the other potentials. On analogy with other neurons (24), it might be assumed that the IS component arises from the region of the axon hillock and beginning initial complex. However, because of the unusual morphology of the initial complex in mammalian peripheral sensory neurons (190; Grillo, personal communication), it is possible that this component originates from a site more distant from the soma than the axon hillock.

Cell bodies of nodose ganglion neurons, whether in vitro or in vivo, generated action potentials in response to impulses occurring in their afferent fibers. These somatic spikes may be of functional importance in the modulation of afferent nerve activity. Thus, Tagini and Camino (214) reported that trains of stimuli, at frequencies of 20-100 Hz to the nerve trunk of the 9th or 10th dorsal root ganglion of frog, often produced additional action potentials ("anomalous" spikes) in fibers in the dorsal roots, so that the number of action potentials recorded from single units in the dorsal root exceeded the number of stimuli applied to the trunk. A similar phenomenon occurred when the

dorsal roots were stimulated and recordings were made from single fibers in the nerve trunk. As repetitive stimulation caused a progressive delay in the generation of the S-spike recorded in ganglion cells, these investigators concluded that the "anomalous" spikes were generated as a consequence of the delayed spikes invading the axon after its refractory period had terminated. Although this phenomenon was not examined in detail in this study, repetitive stimuli were found to cause a progressive delay in the generation of somatic spikes while IS spikes were continuously generated. It is possible that this phenomenon could alter the number of nerve impulses in afferent fibers central to the sensory ganglion. For example, the delayed somatic spikes could propagate preferentially into the peripheral branches of the axons because of the longer refractory period in smaller diameter central branches (82, 91,199), and thereby alter the number of impulses reaching the central nervous system. Further experiments, using single or few-fiber recording techniques, and designed to measure the input-output relationship of a single neuron, will be necessary in order to determine the role of these peripheral sensory neurons in the modulation of afferent input to the brain.

In a number of neurons in both cat and rabbit nodose ganglia, repetitive action potentials generated in the cell body caused a persistent hyperpolarization (Figure 15). There are several examples of this activity-induced hyperpolarization in other neurons. Ito and Oshima (122) reported that repetitive activity in cat spinal motoneurons

could result in a long-lasting hyperpolarization, which they attributed to a summation of the changes in potassium conductance associated with the afterhyperpolarizations. Gage and Hubbard (81) accounted for the post-tetanic hyperpolarization in rat phrenic nerve terminals by assuming a post-tetanic increase in potassium conductance. In many cases, however, the major component of the hyperpolarization has been attributed to an activity induced increase in an electrogenic sodium pump (203). In leech neurons, Jansen and Nicholls (126) reported evidence that the hyperpolarizing effect of an electrogenic pump is combined with a specific increase in potassium conductance. A similar dual mechanism is believed to account for the activity hyperpolarization observed in mammalian nonmyelinated nerve fibers (188,196). The possibility that the increase in potassium conductance is mediated by an influx of calcium ions has also been considered. Krnjević and Lisiewicz (149) showed that the intracellular injection of calcium ions into spinal motoneurons caused a potassium-dependent hyperpolarization, and Meech (159) demonstrated that the post-tetanic hyperpolarization in Aplysia neurons is directly dependent upon the influx of calcium ions. He theorized that this "calcium-mediated negative feedback process" may be an important feature of information processing.

The mechanism by which repetitive activity induces hyperpolarization in nodose ganglion neurons is not known. The possibility that it is simply a summation of afterhyperpolarizations seems unlikely, because the duration of the afterhyperpolarization rarely exceeded 30 msec while



activity hyperpolarization was seen with somatic spikes occurring as infrequently as 1-2 per second (Figure 15). Since the interspike interval then ranged between 500-1000 msec, it is difficult to imagine how summation could have occurred. There have been no published reports of activity-induced hyperpolarization occurring at such low stimulus frequency levels. It is interesting to note that the amplitude of the afterhyperpolarization decreased as the activity-induced hyperpolarization increased (Figure 15). Other experiments in this study demonstrated that the magnitude of the hyperpolarization is dependent on the membrane potential. Thus, it appears that the hyperpolarization following repetitive activity in nodose ganglion neurons could, in large part, be accounted for by specific changes in membrane conductance. Further studies will be necessary to confirm this hypothesis and to determine which species of ion are involved.

The sensory endings of many vagal afferent fibers are categorized according to their adaptive properties, as for example slowly-adapting and rapidly-adapting bronchopulmonary receptors (181). The mechanisms responsible for these differences in adaption are not fully understood, but it is believed that mechanical characteristics of the tissue surrounding the sensory ending or the electrical properties of the sensory ending itself are important (3). The slowly and rapidly adapting stretch receptor neurons of crayfish have been the subject of extensive study (H. Fields, in press; 162,164), and it has been concluded that differences in specific properties of the electrically excitable nerve

membrane account for the slowly or rapidly adapting characteristic of crayfish stretch receptor. Mechanical adaptation in the generator region is believed to play only a minor role. When a slowly adapting crayfish stretch receptor was stimulated by intracellularly applied constant current, it always produced long-lasting trains of action potentials, whereas neurons characterized as rapidly adapting were never able to produce sustained, repetitive spikes. Nakajima (162) reported that there was no correlation between adapting type and membrane resistance, capacitance, rectifying properties, or characteristics of the action potential. He suggested that many factors including unique (non-Hodgkin-Huxley) ionic mechanisms may be responsible for the observed differences in spike adaptation.

It has been demonstrated that motoneurons in cat spinal cord differ in their adaptive properties, many neurons responding to intracellularly applied constant current with sustained repetitive discharges (188); the discharge frequency being linearly related to the stimulus strength over a wide range. Differences in the accommodative properties of cat motoneurons have also been found (202). This suggests the possibility that the accommodative properties of the nerve membrane may account for the neuron's adaptation characteristic. Thus, one might expect that slowly adapting cells would show little or no accommodation. Since accommodation has been shown to be related to sodium inactivation and potassium conductance changes (202,221), it is possible that these same mechanisms may underlie the differences in adaptation to prolonged stimulation.

In the present study, cell bodies of neurons in nodose ganglia of both cat and rabbit were found to differ in their abilities to adapt to prolonged suprathreshold depolarization. These differences in adaptation could not be correlated with any specific active or passive membrane property, including the ability to hyperpolarize in response to repetitive activity. For purposes of classification, 4 different adaptation types were recognized, with responses ranging from cells which fired continuously for up to 10 sec (type IV), to those cells which could respond with only 1-3 spikes at the start of depolarization (type I). All neurons could be readily classified into one of the 4 possible categories (see Results). This, however, is not meant to suggest that there are 4 distinct subpopulations of neurons within the nodose ganglion. The intermediate adaptation types II and III may simply be normal physiologic variants of the rapidly (I) or slowly (IV) adapting neurons.

It is generally agreed that the different types of adaptation in vertebrate mechanoreceptors depend primarily on the mechanical properties of the receptor and surrounding tissue, and to a lesser extent, on the electrical properties of the sensory ending itself (3,67). With the exception of the pacinian corpuscle, no studies on "spike adaptation", that is, adaptation occurring at the level of the spike generating membrane, in vertebrate sensory neurons, have been reported. This may, in part, account for the bias toward mechanical explanations of sensory adaptation. Data reported in this study suggest that fundamental properties of the nerve membrane itself, and not the mechanical

relations of the surrounding tissue, may be of primary importance in determining the adaptation characteristic of mammalian vagal mechanoreceptors. Thus, if it is possible to extrapolate the properties of the soma membrane to the nerve ending, neurons in the nodose ganglion will provide an opportunity to examine the specific mechanisms underlying receptor adaptation.

### III. IONIC CONTRIBUTIONS

The effects of changing extracellular potassium concentration were most apparent on the resting membrane potential, although the maximum change in membrane potential (25 mV/decade) was far less than the 61 mV predicted from the Nernst equation for a 10-fold change in external potassium concentration. In addition, the relation between log external potassium concentration and membrane potential was not linear at potassium concentrations less than 2.5 mM. Both of these findings appear to indicate that the soma membrane of nodose ganglion neurons does not behave simply as a potassium electrode, and that it must be significantly permeable to other ion species at rest. For example, Hodgkin and Horowicz (107) demonstrated that similar but significantly smaller deviations are to be expected if the membrane is slightly permeable to sodium ions at rest ( $P_{Na} = 0.01 P_K$ ). Alternatively, it has been shown that changes in extracellular potassium concentration can cause changes in membrane permeability (90,211,131) associated with changes in membrane resistance. Potassium related changes in the membrane resistance

of nodose ganglion neurons appear to be minor (Figure 18) but may, nonetheless, contribute to the observed deviations from predicted behavior. Finally, in any experiment where external ion concentrations are changed, it is important to consider possible effects on the intracellular ionic composition. Hodgkin and Horowicz (107) suggested that deviations from the Nernst equation may be caused by changes in the internal ionic composition occurring during the course of an experiment. The possibility that any or all of these factors are operating in mammalian nodose ganglion neurons cannot be excluded, and significantly complicates the analysis of experimental results.

Armett and Ritchie (8) demonstrated that the relative sodium permeability of mammalian C fibers is significantly greater than that reported for any other excitable membranes. They reported a value of 0.25 for  $P_{Na}/P_K$  in rabbit vagal C fibers and a value of 0.10 for cat hypogastric nerve. In their experiments, they observed a 28 mV change in membrane potential for a 10-fold change in external potassium concentration and accounted for this low slope on the basis of the high resting sodium permeability. Several other authors have reported lower values than expected for the potassium-potential slope (see Introduction), and have suggested a high resting sodium permeability to account for it. In these cases, one would anticipate that changes in external sodium concentration would cause a significant change in membrane potential. This has not been reported (16,105,139,140,176,217). The sodium-dependent changes in membrane potential that have been reported

were usually characterized as "small and transient" or "insignificant", a finding that may be common to all mammalian neurons.

The afterhyperpolarization phase of an action potential is believed to be caused by a transient increase in potassium conductance (130). Thus, it would be expected that changes in external potassium concentration would exert their greatest effect on the afterhyperpolarization. Indeed, Blackman et al. (16) have shown that while the resting potential in frog sympathetic ganglion cells changes only 43 mV per 10-fold potassium change, the afterhyperpolarization changes by about 75 mV. They do not comment on this deviation from the Nernst predicted change of 59 mV, assuming that the membrane behaves as a potassium electrode at the peak of the afterhyperpolarization. In the present study, the afterhyperpolarization in nodose ganglion neurons was found to change by 16 mV per 10-fold change in external potassium concentration. This appears to indicate that the nerve membrane is considerably less sensitive to potassium at the peak of the afterhyperpolarization than it is at rest. This unexpected finding is supported by data which indicate that the reversal potential for the afterhyperpolarization ( $E_{AH}$ ) changes by only 30 mV per 10-fold change in external potassium. The physiological significance of these results must be interpreted with caution because recent studies have demonstrated that glial cells may function to buffer effectively the potassium concentration in the perineuronal space (99,219). For example, the sodium-potassium pump in glial cell membranes has been shown to be markedly more sensitive to

changes in extracellular potassium concentration than was the neuronal membrane pump (99). Thus, assuming that the dense glial cell layer covering each neuron may be an effective diffusion barrier, it is conceivable that the potassium concentration in the microenvironment immediately surrounding a neuron may be significantly different than that in the extracellular bathing medium. Therefore, the apparent insensitivity of the resting potential and afterhyperpolarization of nodose ganglion neurons to changes in potassium concentration could be accounted for, at least in part, by the potassium buffering capacity of their dense glial cell covering.

If, the resting membrane of neurons in the nodose ganglion is significantly permeable to sodium ions, as has been assumed for other neurons (130), then a marked reduction in external sodium concentration would be expected to cause hyperpolarization of the resting membrane potential. Data in this study clearly indicate, however, that the reduction of external sodium ion concentration is associated with a slight but significant depolarization. This decrease in resting potential cannot be explained by the generally accepted ionic theory of the origin of the membrane potential. Although several other studies have reported similar findings (16,105,140), no satisfactory explanations have been offered. It is quite possible that the impermeant substituent cations (usually choline or TRIS) may alter the membrane permeability to other ions and thus be responsible for the induced depolarization. Further studies, perhaps using more sophisticated techniques, will be necessary in order to explain these results.

At the peak of the action potential the nerve membrane becomes maximally permeable to sodium ions. Thus, the overshoot should change with changes in the external sodium concentration in a manner predicted by the Nernst equation. In nodose ganglion neurons the maximum slope of the relation between log external sodium concentration and overshoot potential was found to be 23 mV/decade. Because this is significantly less than the 61 mV change predicted by the Nernst equation, it may be reasonable to assume that the membrane is significantly permeable to other ion species even at the peak of the overshoot. These findings are supported by similar results obtained from frog sympathetic neurons (16) and dorsal root neurons (139,140).

As expected, the rate of rise of the action potential was extremely sensitive to changes in the external sodium concentration. This agrees well with the ionic theory which attributes the rising phase to a sudden increase in sodium conductance (130). Results in the present study also showed that both the rate of fall of the action potential and the after-hyperpolarization were decreased by a reduction in external sodium concentration. These components of the action potential are normally associated with changes in potassium conductance (130). Recent studies by Brismar (20), and Brismar and Frankenhauser (21,22) on frog myelinated nerve, have demonstrated that the external concentration of specific ions can affect the permeability properties of the nerve membrane. Of particular interest are experiments which indicated that a decrease in external sodium concentration caused a decrease in potassium



permeability. It is important to consider the possibility that similar complex interactions between the ionic composition of the external medium, and the permeability properties of the nerve membrane may occur in mammalian neurons. This may be a possible explanation for the effect of low sodium on the falling phase of the action potential, the after-hyperpolarization, and the resting membrane potential.

When lithium was used to replace most of the sodium in the superfusing medium, both the rate of rise and overshoot of the action potential were reduced, but the passive properties of the nerve membrane were unaffected. These results suggest that during activation the membrane of the nodose ganglion neuron, in contrast to other nerve membranes, is not as permeable to lithium ions as it is to sodium ions. The best documented effect of lithium is its impairment of the sodium-potassium pump, an effect known to occur even at low therapeutic concentrations (186), but it is difficult to imagine how this effect could account for the rapid changes in action potential configuration reported here. Lithium has been shown to increase potassium permeability in snail neurons (182), but there is no evidence to indicate that this occurs in mammalian sensory neurons. Thus, it appears that lithium was able to substitute effectively for sodium as a carrier of transient inward current but not as well as in other neurons that have been studied. The precise mechanism by which lithium affects the action potential configuration in nodose ganglion neurons must await further study.

The importance of calcium ions for normal neural function is well known (3,48,130). In many tissues, the reduction of extracellular

calcium concentration increases membrane excitability, even to the point of causing spontaneous repetitive activity, whereas in other tissues, such as frog myelinated nerve, the elimination of external calcium causes a complete loss of excitability without significantly affecting the resting membrane potential (73). Koketsu (138), in reviewing the effects of calcium on excitable membranes, stated that the extracellular concentration of calcium controls both the intracellular ionic composition and the membrane permeability. It is apparent, however, that the specific effects of calcium and their magnitudes are different in different tissues.

Nodose ganglion neurons were exposed to a calcium-free superfusate containing 1 mM EGTA. Although the resting membrane potential was not affected, input resistance was markedly reduced. Thus, the complete removal of extracellular calcium appeared to cause an increase in membrane conductance. The slight but significant reduction in overshoot indicates that calcium ions may function as a minor charge carrier for the transient inward current of the action potential. Alternatively, the decrease in overshoot may simply be attributed to the short-circuiting effect of the increased membrane conductance. Both the rate of fall and the afterhyperpolarization of the action potential were significantly reduced in zero calcium, findings that suggest that the intracellular calcium concentration may directly affect potassium conductance. Support for this interpretation is provided by studies in which it was found that the intracellular injection of calcium ions into cat motoneurons (149), or into *Aplysia* neurons (157), caused a

significant increase in potassium conductance. It is not unreasonable to assume that the internal calcium concentration varies as a function of the external concentration. Hence, the effects of calcium removal on the rate of fall and afterhyperpolarization may be due primarily to changes in the active potassium conductance.

When external calcium concentration was increased, the most significant effect was to increase the rate of fall of the action potential. This is consistent with the suggestion that calcium affects active potassium permeability. Voltage-clamp studies to characterize the effects of external calcium ion concentration on the late steady-state current will be necessary to substantiate this theory.

The only effect of reducing extracellular chloride concentration to zero was a significant 7-12 M $\Omega$  increase in input resistance. This effect was the same whether glutamate or methylsulfate were used as the impermeant anion substitute. Increasing the external chloride concentration caused a 35% reduction in input resistance associated with a significant 5 mV hyperpolarization of the resting potential. These results suggest that chloride conductance contributes significantly to the overall membrane conductance at rest. This demonstrates the importance of controlling chloride concentration in in vitro bathing media, a point that is often overlooked because of assumptions based on data from nonmammalian neurons.

The origin and maintenance of the resting membrane potential and the mechanisms underlying spike electrogenesis can be explained in terms

of ionic gradients and permeabilities (93). The Goldman equation has been very useful for predicting the membrane potential if the internal and external ionic compositions and permeability ratios are known. Unfortunately, most of this information is not available for the mammalian nodose ganglion. Several studies, however, have reported values for the intracellular ionic concentration in other mammalian nervous tissue. The results of these studies are summarized in Table 6. It is reasonable to assume that the intracellular ionic concentrations in neurons of the nodose ganglion lie somewhere within the range of values given in Table 6. Equilibrium potentials for each ion species may then be calculated from the Nernst equation.

If the internal sodium concentration is 40 mM, then the sodium equilibrium potential ( $E_{Na}$ ) is calculated to be +35 mV. Similarly, if intracellular potassium is 140 mM, then  $E_K$  is calculated to be -89 mV. In the present study, the calculated value for  $E_K$  is significantly higher than the measured reversal potential for the afterhyperpolarization ( $E_{AH} = -69$  mV). As indicated in previous discussion, other ions, in addition to potassium, may contribute to the membrane conductance at the peak of the afterhyperpolarization. Thus,  $E_{AH}$  cannot be considered to be a reliable measure of  $E_K$ . Based on an internal chloride concentration of 30 mM,  $E_{Cl}$  equals -33 mV, suggesting the existence of an active chloride pump. The equilibrium potential for calcium ( $E_{Ca}$ ) cannot be calculated as there are no measurements of intracellular ionized calcium concentration available. Because the internal concentration of ionized calcium is believed to be quite small (191), the value for  $E_{Ca}$  is probably positive.

TABLE 6. Intracellular Ionic Concentrations in Mammalian Neurons

<u>Reference</u>	<u>Tissue</u>	<u>Intracellular Concentration (mM)</u>		
		<u>Na<sup>+</sup></u>	<u>K<sup>+</sup></u>	<u>Cl<sup>-</sup></u>
134	Rabbit Vagus	63	145	39
188	Rabbit Vagus	77	166	40
228	Rabbit Sympathetic Ganglion	37.4	163	23.5
225	Rabbit Vagus	42	98	-

These same values for the intracellular ionic composition can be used with the Goldman equation to predict the resting membrane potential. Armett and Ritchie (8) report that the sodium-potassium permeability ratio for cat hypogastric nerve is 0.10. Using this value and assuming the chloride permeability to be approximately one-half that of sodium, the Goldman equation becomes:

$$\begin{aligned} \text{resting membrane potential} &= 61 \log \frac{1 (5) + 0.10 (150) + 0.05 (30)}{1 (140) + 0.10 (40) + 0.05 (106)} \\ &= -51 \text{ mV} \end{aligned}$$

which is in good agreement with the results obtained in this study. Moreover, this equation predicts that a 10-fold change in external potassium concentration will cause a 29.5 mV depolarization, which compares favorably with the 25 mV/decade change observed experimentally. It is important, however, to consider the limitations of the Goldman equation as used in this situation. Although the results with metabolic inhibitors do not suggest the presence of electrogenic pumps, the possibility that they do exist and contribute significantly to the resting membrane potential cannot be excluded. The fact that the Goldman equation does not take into account active ion fluxes may thus represent a significant limitation.

#### IV. PHARMACOLOGIC PROPERTIES

Tetrodotoxin (TTX) is well known for its ability to block the regenerative, voltage-dependent increase in membrane permeability to sodium ions (66,165). In some tissues, TTX also appears to block the resting membrane permeability to sodium (79) without measurably affecting the membrane resistance. Completely blocking the membrane permeability to sodium ions would be expected to cause effects similar to those predicted for sodium-free media, that is, the membrane potential should hyperpolarize. Freeman (79) reported that TTX ( $3 \times 10^{-7}$  M) caused an average 5 mV hyperpolarization in squid axon. Since, in our study, TTX induced a 3-5 mV hyperpolarization in the resting potential of nodose ganglion neurons, while a reduction in extracellular sodium ion concentration caused a slight depolarization in these same neurons, it would seem safe to assume that the mechanisms responsible for the polarization are not the same. This indirectly supports a previous suggestion that alterations in the extracellular ionic composition may have complex, and therefore, not easily predicted effects on the permeability properties and electrical behavior of the mammalian nerve membrane.

It has been shown that the tetraethylammonium ion (TEA) inhibits the voltage-dependent changes in membrane permeability to potassium (102) in a manner complimentary to that of TTX on sodium. Hille (102) demonstrated that the selectivity of TEA for potassium conductance is as complete as that of TTX for sodium conductance in frog myelinated nerve.

In the present experiments, the falling phase of the action potential in nodose ganglion neurons was found to be markedly affected by TEA in the external bathing medium. This suggests that TEA may inhibit potassium conductance changes in these mammalian neurons. In addition, the results have shown that TEA causes a depolarization of the resting membrane potential associated with an increase in membrane resistance. Thus, it is possible that TEA may also reduce the resting potassium permeability of the membrane.

The possibility that a ouabain-sensitive electrogenic ion pump directly contributes to the resting membrane potential in nodose ganglion neurons is not supported by the results of the ouabain experiments. The slight hyperpolarization that was occasionally observed may be caused by an intracellular effect of ouabain, indirectly acting to increase potassium permeability, as suggested by Gorman and Marmor (88) or possibly by inhibiting a depolarizing electrogenic pump. Similarly, the loss of excitability and general deterioration which occurs during exposure to ouabain may be due to other as yet unknown intracellular effects. 2,4-Dinitrophenol (DNP) has been shown to severely depress electrical excitability in cat cortical neurons (86). Godfraind et al. (86) suggest that this depression of excitability may be due to an inhibition of mitochondrial activity leading to the release of energy-dependent stores of intramitochondrial calcium. The increase in intracellular free-calcium ions could then affect membrane permeability properties to reduce excitability. In addition to this indirect effect



on the nerve membrane, Barker and Levitan (11) have recently demonstrated that DNP has a direct effect on the membrane permeability of certain molluscan neurons. Neither DNP nor cyanide appears to have any effect on membrane permeability, at least as evidenced by changes in membrane potential, in nodose ganglion neurons. However, the rapid general deterioration caused by these agents may be due to interference with mitochondrial functions and may have masked more subtle changes occurring at the membrane. Perhaps iontophoretic application or direct intracellular injection of these compounds will permit a thorough and detailed examination of their actions.

The membrane stabilizing effects of anesthetic agents are well known (204). The exact mechanisms by which these agents produce their effects, however, are still a subject of investigation. Interference with membrane conductances is thought to be a principle effect of many anesthetics (204,45,166). In the preliminary experiments on neurons in the nodose ganglion, the anesthetic agents (pentobarbital and lidocaine) rapidly and reversibly blocked invasion of the cell bodies by action potentials, long before nerve conduction itself was blocked. This effect was probably due to an impairment of conduction at the regions of low safety factor; primarily at the initial axon-soma junction, and also at the junction of the afferent fiber and initial axon. In order to determine what effect, if any, these anesthetics may have on afferent impulse traffic through the ganglion, it will be necessary to perform an input-output type analysis using single nerve fiber recording techniques.

The anesthetic effect of atropine deserves special mention. Atropine is known to block cholinergic transmission at many different synapses (46) and is a widely used clinical and experimental drug. For example, Eyzaguirre (173) has applied atropine to the cat carotid body and reported that it caused an inhibition of chemoreceptor activity. For this and other reasons he has concluded that acetylcholine was the excitatory transmitter in the carotid body. These results and conclusions must be interpreted with caution, however, because of the demonstrated local anesthetic properties of atropine, which could account for the reduction in chemoreceptor activity. It has also been reported that high doses of atropine are capable of blocking transmission at non-muscarinic synapses, suggesting that the different receptors for acetylcholine exhibit only a quantitative difference in their susceptibility to atropine (46). Again, the local anesthetic effects of atropine, especially at high doses, must be given careful consideration.

In a previous study (198), it was reported that veratridine, phenyldiguanide (PDG) and 5-hydroxytryptamine (5-HT) all stimulated neurons in the nodose ganglion to produce action potentials, which were recorded in small nerve bundles dissected from the supra- or infranodose vagus. Several other reports have demonstrated that PDG and 5-HT (125), the veratrum alkaloids (17,18,19,31), and a cardiac glycoside (32) produce at least some of their systemic effects by an action on the nodose ganglion. In the present study, using intracellular microelectrodes to record activity, none of these substances (with the possible exception of acetylstrophanthidin, which was not tested) were capable of

causing the spontaneous generation of action potentials in nodose ganglion neurons. 5-HT had no significant effect on any passive or active membrane property and PDG was found to cause only a slight hyperpolarization associated with an increase in membrane resistance. The apparently contradictory results can be explained in several ways. As pointed out by Sampson and Jaffe (198), not all neurons are capable of responding to any particular agent. They report that of 50 fibers tested, only 34 responded to 5-HT, and only 18 of those 34 were stimulated by PDG. Thus, because of the small number of neurons tested (5-HT = 12; PDG = 9) it is possible that responsive cells exist but were not encountered. The ease of obtaining stable intracellular recordings is probably dependent on neuron size and location. It is also possible that the primary site of action for these agents is not the cell body but some peripheral structure or receptor. Finally, the possibility that the in vitro maintenance of the nodose ganglion may alter the pharmacologic responsiveness of the cell bodies must be taken into consideration.

The effects of veratridine, while not directly causing the production of spontaneous action potentials were, nevertheless, quite dramatic. The production of a prolonged afterdepolarization which often caused the generation of long-lasting trains of action potentials may account for the hypotensive action of veratridine. In the presence of veratridine, a single impulse in the infranodose vagus may give rise to a train of impulses in the supranodose vagus. It is not difficult to

imagine the effect of such an impulse multiplier on normal afferent discharges from, for example, baroreceptor endings. Thus, the production of bradycardia and hypotension by veratridine may arise reflexly because of the increased vagal afferent activity arising from two sites, the peripheral sensory endings and a sensitive region on or near the cell body.

## CONCLUSIONS

The results presented in this study have demonstrated that, under carefully controlled and defined conditions, adult mammalian neurons can be maintained in vitro at least 10 hours without deterioration. Furthermore, it was shown that these in vitro neurons were capable both of maintaining stable resting membrane potentials and generating action potentials that were identical with those measured in vivo. Thus, an important goal of this project has been achieved. The utility and importance of an in vitro preparation of adult mammalian sensory neurons is large, matched only by the present need for such a preparation. For example, it will now be possible to study the neurophysiologic effects on mammalian neurons of drugs and other agents, under precisely defined conditions. Theories or mechanisms of action previously deduced from studies of invertebrate neurons can now be tested directly on mammalian neurons.

The basic passive and active electrophysiologic properties of neurons in nodose ganglia of cat and rabbit have been characterized. A total of more than 1400 neurons were studied with the aid of intracellular microelectrodes in order to obtain this data. Rectifying and accommodative properties of the soma membrane were described. The roles of the cations: sodium, potassium and calcium; and the anion: chloride, were investigated and several inconsistencies with similar studies on invertebrate neurons were repeatedly demonstrated, most notably, the

depolarization upon reduction of external sodium concentration, the low sensitivity of both the resting potential and spike afterhyperpolarization to changes in external potassium concentration, and the effect on membrane potential and resistance caused by a small increase in external chloride concentration. A limited examination of the pharmacologic properties of these mammalian sensory neurons was conducted. The significance of many of the findings must await further analysis and experimentation with more sophisticated techniques such as micro-iontophoresis and voltage clamping.

The results of this study have raised several fundamental questions concerning the electrophysiologic properties of mammalian sensory neurons. For example, experiments to measure the passive membrane properties have demonstrated the existence of anomalous rectification, a phenomenon usually associated with synaptic elements, and whose role in the normal function of the nodose ganglion remains unknown. Study of the active properties has revealed the existence of physiologically distinct subpopulations of neurons within the ganglion. Neurons differ both according to their adaptive type and their ability to hyperpolarize during low frequency stimulation. The possibility that these characteristics may be correlated with the sensory modality subserved by the intact neuron should be the subject of future investigation. Measurements of the specific ion contributions to the resting and action potentials have revealed several differences between these mammalian neurons and the neurons of nonmammalian species. These differences need

to be studied in more detail before any definitive conclusions can be reached. Many of the findings can be explained, however, if one postulates the existence of a glial cell barrier capable of buffering changes in the extracellular fluid, and thus maintaining the constancy of the neuronal microenvironment. The need for experiments on the physiological role of glial cells in the nodose ganglion is clearly indicated. Finally the possibility that the neuron cell bodies in the nodose ganglion may be more than simple food processing plants, functioning only to sustain distant receptor and transmitter endings, needs careful consideration. This study has demonstrated that peripherally generated action potentials can invade the cell body and that these cell bodies are capable of responding to a variety of pharmacologic agents. It is not unreasonable to speculate that the nerve cell bodies in the nodose ganglion normally are able to, or through pharmacologic treatment can be induced to, alter the pattern of afferent impulse traffic through the ganglion. A detailed examination of this peripheral information processing may provide an insight into the complexities of central information processing.

### SUMMARY

1. The passive and active electrical properties of the soma membrane of neurons in nodose ganglia removed from cats and rabbits were studied. The ganglia were maintained in vitro and were superfused at 37°C with a solution formulated to approximate the extracellular fluid of each species. The solution was buffered to pH 7.34, continuously equilibrated with 95% O<sub>2</sub> and 5% CO<sub>2</sub>, and contained dialyzed calf serum and glucose. These properties were also examined in nodose ganglion neurons in vivo. Intracellular recordings were obtained with glass micropipettes filled with either 3 M KCl or 5 M K acetate.

2. Mean values for a variety of passive and active electrophysiologic properties were determined. Values obtained in vitro did not differ significantly from those obtained in vivo. Based on the passive electrical properties of the soma membrane, neurons in the nodose ganglion appear to be a uniform population, despite the different sensory modalities conveyed by the afferent fibers.

3. Cell bodies of neurons generated action potentials in response to impulses in their afferent fibers. Somatic spikes could be evoked by stimulation of either the supranodose or infranodose vagus nerve, and an inflection point could be seen on their rising phase. When the vagus nerve was stimulated at frequencies greater than 10-20 Hz, the generation of somatic spikes often became progressively delayed and then



failed completely, leaving a smaller potential (IS spike) which was apparently generated in the initial complex. The afterhyperpolarization was associated only with the somatic spike.

4. Many neurons, both in vitro and in vivo developed a persistent hyperpolarization when repetitive action potentials occurred in the soma. This hyperpolarization was apparent at frequencies as low as 1-2 Hz, persisted for up to 5 s after the occurrence of the last somatic spike, and sometimes caused failure of somatic spikes to be generated.

5. Neurons in both species differed in their responses to supra-threshold depolarization applied through the recording electrode. Some neurons produced a train of action potentials which lasted for the duration of the depolarizing pulse, the frequency of the train being related to the magnitude of depolarization. The trains were characterized by gradually decreasing spike amplitudes and increasing interspike intervals. Other neurons responded with only a single spike or brief burst of action potentials at the beginning of depolarization to threshold.

6. It is suggested that the adaptive properties of the soma membrane of a peripheral sensory neuron are similar to those of its sensory ending, and the electrophysiological studies of the soma membrane may provide an opportunity to examine mechanisms of receptor adaptation.

7. The ionic contributions to the resting and action potentials in neurons in cat nodose ganglia were studied. Ganglia were initially superfused with a solution approximating the ionic composition of cat extracellular fluid. The solution was equilibrated with 95%  $O_2$  and 5%  $CO_2$ , and its pH,  $P_{CO_2}$  and  $P_{O_2}$  were measured periodically and maintained constant throughout the experiment. In order to study ionic contributions, special solutions of altered ionic composition were also used to superfuse the ganglia. Data on passive and active membrane properties were obtained from 5-10 neurons in the normal superfusate, then the ganglion was superfused with the experimental solution, data being obtained from 5-10 additional neurons after a minimum exposure time of 15 min. Finally, the ganglion was returned to normal solution where data from 3-5 more neurons were obtained. This procedure was repeated with several different ganglia for each experimental solution.

8. As expected, the membrane potential of neurons in cat nodose ganglia was dependent upon the external potassium concentration. The maximum slope of the potassium-potential curve (25 mV/decade), however, was significantly less than the Nernst predicted value of 61 mV/decade and was significantly less than the values predicted for most nonmammalian species. Moreover, the amplitude of the afterhyperpolarization in these cat sensory neurons was less affected by changes in external potassium concentration than was the resting potential.

9. The results with sodium are of particular interest because of the observation that the membrane potential depolarized when the external sodium concentration was reduced from 150 to 34.4 mM. This is in marked contrast to similar studies in other species which reported either no change or slight hyperpolarization of the resting potential upon removal of extracellular sodium.

10. Increases and decreases in the concentration of extracellular calcium ions associated with similar directional changes in the rate of fall and afterhyperpolarization of the action potential. A non-selective effect on membrane conductance may be indicated by the insensitivity of the resting membrane potential to similar changes in external calcium ion concentration.

11. A small rise in external chloride ion concentration (from 106 to 127.5 mM) increased the resting membrane potential by 5 mV while significantly reducing the membrane resistance by an average of 35%. This is of particular importance when one considers that the normal chloride concentration used in this study corresponds to the chloride concentration measured in the extracellular fluid of cats while the high chloride concentration is equivalent to that found in typical mammalian Ringer's solution.

12. Measurements of the specific ion contributions to the resting and action potentials have revealed several differences between these mammalian neurons and the neurons of nonmammalian species. These differences need to be studied in more detail before any definitive conclusions can be reached. Many of the findings can be explained, however, if one postulates the existence of a glial cell barrier capable of buffering changes in the extracellular fluid, and thus maintaining the constancy of the neuronal microenvironment. The need for experiments on the physiologic role of glial cells in the nodose ganglion is clearly indicated.

13. The pharmacologic actions of a variety of drugs were tested on neurons in cat and rabbit nodose ganglia. Results suggest that the cell bodies possess receptors for drugs, and that drug-induced effects may result in the initiation of action potentials or the modification of pre-existing activity. Thus, the nodose ganglion may be an important site of action for the autonomic effects of some drugs.

REFERENCES

1. Adelman, W. J., Jr. (Ed.). Biophysics and Physiology of Excitable Membranes. Van Nostrand Reinhold Co., New York, 1971.
2. Adrian, R. H. and W. H. Freygang. The potassium and chloride conductance of frog muscle membrane. *J. Physiol. (London)*, 163:61-103, 1962.
3. Aidley, D. J. The Physiology of Excitable Cells. Cambridge University Press, 1971.
4. Agostoni, E., J. E. Chinnock, M. DeBurgh Daly and J. G. Murray. Functional and histological studies of the vagus nerve and its branches to the heart, lungs and abdominal viscera in the cat. *J. Physiol. (London)*, 135:182-205, 1957.
5. Albano, J. P. Etude de l'activite electrique des neurones du ganglion jugulaire. *J. Physiol. (Paris)*, 1:77, 1969.
6. Araki, T. and T. Otani. Response of single motoneurons to direct stimulation in toad's spinal cord. *J. Neurophysiol.*, 18:472, 1955.

7. Araki, T., T. Otani and T. Furukawa. The electrical activities of single motoneurons in toad's spinal cord, recorded with intracellular electrodes. *Jap. J. Physiol.*, 3:254-267, 1953.
8. Armett, C. J. and J. M. Ritchie. On the permeability of mammalian non-myelinated fibres to sodium and to lithium ions. *J. Physiol. (London)*, 165:130-140, 1963.
9. Asano, T. and W. P. Hurlbut. Effects of potassium, sodium, and azide on the ionic movements that accompany activity in frog nerves. *J. Gen. Physiol.*, 60:588-608, 1958.
10. Baker, P. F., M. P. Blaustein, A. L. Hodgkin and R. A. Steinhardt. The influence of calcium on sodium efflux in squid axons. *J. Physiol. (London)*, 200:431-458, 1969.
11. Barker, J. L. and H. Levitan. Phenols: Effects on membrane permeability of molluscan neurons. *Brain Res.*, 67:555-561, 1974.
12. Barrett, J. N. and W. E. Crill. Specific membrane properties of cat motoneurons. *J. Physiol. (London)*, 239:301-324, 1974.

13. Blackman, J. G., H. L. Borison and R. J. Milne. Intracellular recording of after-discharge induced by veratrum alkaloids in the guinea-pig nodose ganglion. *Brain Res.*, 98:369-372, 1975.
14. Blackman, J. G., P. J. Crowcroft, C. E. Devine, M. E. Holman and K. Yonemura. Transmission from preganglionic fibres in the hypogastric nerve to peripheral ganglia of male guinea-pigs. *J. Physiol. (London)*, 201:723-743, 1969.
15. Blackman, J. G., B. L. Ginsborg and C. Ray. Synaptic transmission in the sympathetic ganglion of the frog. *J. Physiol. (London)*, 167:355-373, 1963.
16. Blackman, J. G., B. L. Ginsborg and C. Ray. Some effects of changes in ionic concentration on the action potential of sympathetic ganglion cells in the frog. *J. Physiol. (London)*, 67:374-388, 1963.
17. Blackman, J. G. and R. D. Purves. Intracellular recordings from ganglia of the thoracic sympathetic chain of the guinea-pig. *J. Physiol. (London)*, 203:173-198, 1969.
18. Borison, H. L. and V. F. Fairbanks. Mechanism of veratrum-induced emesis in the cat. *J. Pharmacol. Exp. Therap.*, 105:317-325, 1952.

19. Borison, H. L., V. F. Fairbanks and C. A. White. Afferent reflex factors in veriloid-induced hypotension. Arch. Int. Pharmacodyn., 101:189-199, 1955.
20. Brismar, T. Effects of ionic concentration on permeability properties of nodal membrane in myelinated nerve fibres of Xenopus laevis. Potential clamp experiments. Acta Physiol. Scand., 87:474-484, 1973.
21. Brismar, T. and B. Frankenhaeuser. Effects of ionic concentration on sodium permeability properties of myelinated nerve fibres of Xenopus laevis. J. Physiol. (London), 249:549-559, 1975.
22. Brismar, T. and B. Frankenhaeuser. The effect of calcium on the potassium permeability in the myelinated nerve fibre of Xenopus laevis. Acta Physiol. Scand., 85:237-241, 1972.
23. Brock, L. G., J. S. Coombs and J. C. Eccles. Recording potentials from motoneurons with an intracellular electrode. J. Physiol. (London), 117:431-460, 1952.
24. Brock, L. G., J. S. Coombs and J. C. Eccles. Intracellular recording from antidromically activated motoneurons. J. Physiol. (London), 122:429-461, 1953.



25. Brown, D. A. and C. N. Scholfield. Changes of intracellular sodium and potassium ion concentrations in isolated rat superior cervical ganglia induced by depolarizing agents. *J. Physiol. (London)*, 242:307-319, 1974.
26. Burnstein, J. Untersuchungen zur thermodynamie der bioelektrischen ströme. *Pflüg. Arch. Ges. Physiol.*, 92:521-562, 1902.
27. Byck, R. and J. M. Ritchie.  $\Delta^9$ -Tetrahydrocannabinol: Effects on mammalian non-myelinated nerve fiber. *Science*, 180:84-85, 1973.
28. Cajal, S. R. *Histologie du système nerveux de l'homme et des vertébrés*, Volume 1. (Translated by L. Azoulay, 1952). Instituto Ramón y Cajal, Madrid, 1911.
29. Caldwell, P. C. Factors governing movement and distribution of inorganic ions in nerve and muscle. *Physiol. Rev.*, 48:1-64, 1968.
30. Carmel, P. W. and B. M. Stein. Cell changes in sensory ganglia following proximal and distal nerve section in the monkey. *J. Comp. Neurol.*, 135:145-166, 1969.

31. Chai, C. Y. and S. C. Wang. Mechanisms of sinus bradycardia induced by veratrum alkaloids - protoveratrine A. *J. Pharmacol. Exp. Therap.*, 154:546-557, 1966.
32. Chai, C. Y., H. H. Wang, B. F. Hoffman and S. C. Wang. Mechanisms of bradycardia induced by digitalis substances. *Amer. J. Physiol.*, 212:26-34, 1967.
33. Chalazonitis, A., L. A. Greene and M. Nirenberg. Electrophysiological characteristics of chick embryo sympathetic neurons in dissociated cell culture. *Brain Res.*, 68:235-252, 1974.
34. Christ, D. D. and S. Nishi. Anomalous rectification of mammalian sympathetic ganglion cells. *Exp. Neurology*, 40:806-815, 1973.
35. Christoffersen, G. R. J. Chloride conductance and the effect of extracellular calcium concentration on resting neurons in the snail, Helix pomatia. *Comp. Biochem. Physiol.*, 46A:371-389, 1973.
36. Coldman, M. F. and W. Good. The distribution of sodium, potassium and glucose in the blood of some mammals. *Comp. Biochem. Physiol.*, 21:201-206, 1967.

37. Cole, K. S. and H. J. Curtis. Membrane potential of the squid giant axon during current flow. *J. Gen. Physiol.* 24:551-563, 1941.
38. Coleridge, H. M., J. C. G. Coleridge, A. Dangel, C. Kidd, J. C. Luck, and P. Sleight. Impulses in slowly conducting vagal fibers from afferent endings in the veins, atria, and arteries of dogs and cats. *Circ. Res.*, 33:87-97, 1973.
39. Connor, J. A. and C. F. Stevens. Prediction of repetitive firing behavior from voltage clamp data on an isolated neuron soma. *J. Physiol. (London)* 213:31-53, 1971.
40. Coombs, J. S., D. R. Curtis and J. C. Eccles. The generation of impulses in motoneurons. *J. Physiol. (London)*, 139:232-249, 1957.
41. Coombs, J. S., D. R. Curtis and J. C. Eccles. The electrical constants of the motoneurone membrane. *J. Physiol. (London)*, 145:505-528, 1959.
42. Coombs, J. S., J. C. Eccles and P. Fatt. The electrical properties of the motoneurone membrane. *J. Physiol. (London)*, 130:291-325, 1955.

43. Crain, S. M. Resting and action potentials of cultured chick embryo spinal ganglion cells. *J. Comp. Neurol.*, 104:285-329, 1956.
44. Crain, S. M. Intracellular recordings suggesting synaptic functions in chick embryo spinal sensory ganglion cells isolated in vitro. *Brain Res.*, 26:188-191, 1971.
45. Crawford, J. M. Anesthetic agents and the chemical sensitivity of cortical neurones. *Neuropharmacol.*, 9:31-46, 1970.
46. Cullumbine, H. Cholinergic blocking drugs. In: Drill's Pharmacology in Medicine, 4th ed., J. R. DiPalma (Ed.), McGraw-Hill, New York, 1971.
47. Curtis, H. H. and Cole, K. S. Membrane action potentials from the squid giant axon. *J. Cell. Comp. Physiol.* 15:147-157, 1940.
48. Cuthbert, A. W. (Ed.). Calcium and Cellular Function. St. Martin's Press, Inc., New York, 1970.
49. Dalton, J. C. Effects of external ions on membrane potentials of a lobster giant axon. *J. Gen. Physiol.*, 41:529-542, 1958.

50. Dambach, G. E. and S. D. Erulkar. The action of calcium at spinal neurones of the frog. *J. Physiol. (London)*, 228:799-817, 1973.
51. David, R. J., W. A. Wilson and A. V. Escueta. Voltage clamp analysis of pentylenetetrazol effects on Aplysia neurons. *Brain Res.*, 67:549-554, 1974.
52. Davis, H. Some principles of sensory receptor action. *Physiol. Rev.* 41:391-416, 1961.
53. Dawson, R. M. C., D. C. Elliott, W. H. Elliott and K. M. Jones. Data for Biochemical Research, 2nd Ed., Oxford University Press, NY, 1969.
54. DeGroat, W. C. The actions of  $\gamma$ -aminobutyric acid and related amino acids on mammalian autonomic ganglia. *J. Pharmacol. Exp. Therap.*, 172:384-396, 1970.
55. DeGroat, W. C. GABA - Depolarization of a sensory ganglion: Antagonism by picrotoxin and bicuculline. *Brain Res.* 38:429-432, 1972.
56. DeGroat, W. C., P. M. Lalley and W. R. Saum. Depolarization of dorsal root ganglia in the cat by GABA and related amino acids: Antagonism by picrotoxin and bicuculline. *Brain Res.*, 44:273-277, 1972.

57. Dodge, F. A. and Frankenhaeuser, B. Membrane currents in isolated frog nerve fibre under voltage clamp conditions. *J. Physiol. (London)*, 143:76-90, 1958.
58. Dodge, F. A. and B. Frankenhaeuser. Sodium currents in the myelinated nerve fibre of Xenopus laevis investigated with the voltage clamp technique. *J. Physiol. (London)*, 148:188-200, 1959.
59. Downes, H. and D. N. Franz. Effects of a convulsant barbiturate on dorsal root ganglion cells and dorsal root discharges. *J. Pharmacol. Exp. Therap.*, 179:660-670, 1971.
60. Dun, F. T. The delay and blockage of sensory impulses in the dorsal root ganglion. *J. Physiol. (London)*, 127:252-264, 1955.
61. Eccles, J. C. The electrophysiological properties of the motoneurone. *Cold Spr. Harb. Symp. Quant. Biol.*, 17:175-183, 1952.
62. Eccles, J. C., B. Libet and R. R. Young. The behaviour of chromatolysed motoneurons studied by intracellular recording. *J. Physiol. (London)*, 143:11-40, 1958.
63. Eccles, R. M. Intracellular potentials recorded from a mammalian sympathetic ganglion. *J. Physiol. (London)*, 130:572-584, 1955.

64. Eccles, R. M. Orthodromic activation of single ganglion cells. *J. Physiol. (London)*, 165:387-391, 1963.
65. Erulkar, S. D. and J. K. Woodward. Intracellular recording from mammalian superior cervical ganglion in situ. *J. Physiol. (London)*, 199:189-203, 1968.
66. Evans, Martin H. Tetrodotoxin, saxitoxin, and related substances: Their applications in neurobiology. *Int. Rev. Neurobiol.*, 15:83-166, 1972.
67. Ezyaguirre, C. and S. J. Fidone. Physiology of the Nervous System. (2nd ed.), Year Book Medical Publishers, Inc., Chicago, 1975.
68. Feltz, P. and M. Rasminsky. A model for the mode of action of GABA on primary afferent terminals: Depolarizing effects of GABA applied iontophoretically to neurones of mammalian dorsal root ganglia. *Neuropharmacol.*, 13:533-563, 1974.
69. Fischbach, G. D. and M. A. Dichter. Electrophysiologic and morphologic properties of neurons in dissociated chick spinal cord cell cultures. *Dev. Biol.*, 37:100-116, 1974.

70. Frank, K. and M. G. F. Fuortes. Potentials recorded from the spinal cord with microelectrodes. *J. Physiol. (London)*, 130:625-654, 1955.
71. Frank, K. and M. G. F. Fuortes. Unitary activity of spinal interneurons of cats. *J. Physiol. (London)*, 131:424-435, 1956.
72. Frank, K. and M. G. F. Fuortes. Stimulation of spinal motoneurons with intracellular electrodes. *J. Physiol. (London)*, 134:451-470, 1956.
73. Frankenhaeuser, B. The effect of calcium on the myelinated nerve fibre. *J. Physiol. (London)*, 137:245-260, 1957.
74. Frankenhaeuser, B. Sodium permeability in toad nerve and in squid nerve. *J. Physiol. (London)*, 152:159-166, 1960.
75. Frankenhaeuser, B. Instantaneous potassium currents in myelinated nerve fibres of Xenopus laevis. *J. Physiol. (London)*, 160:46-53, 1962.
76. Frankenhaeuser, B. Potassium permeability in myelinated nerve fibres of Xenopus laevis. *J. Physiol. (London)*, 160:54-61, 1962.



77. Frankenhaeuser, B. A quantitative description of potassium currents in myelinated nerve fibres of Xenopus laevis. J. Physiol. (London), 169:424-430, 1963.
78. Frankenhaeuser, B. and A. F. Huxley. The action potential in the myelinated nerve fibre of Xenopus laevis as computed on the basis of voltage clamp data. J. Physiol. (London), 171:302-315, 1964.
79. Freeman, A. R. Electrophysiological activity of tetrodotoxin on the resting membrane of the squid giant axon. Comp. Biochem. Physiol., 40A:71-82, 1971.
80. Freeman, Alan R. Electrophysiological analysis of the actions of strychnine, bicuculline, and picrotoxin on the axonal membrane. J. Neurobiol., 4:567-582, 1973.
81. Gage, P. W. and J. I. Hubbard. The origin of the post-tetanic hyperpolarization of mammalian motor nerve terminals. J. Physiol. (London), 184:335-352, 1966.
82. Gasser, H. S. Properties of dorsal root unmyelinated fibers on the two sides of the ganglion. J. Gen. Physiol., 38:709-728, 1955.

83. Geduldig, D. and D. Junge. Sodium and calcium components of action potentials in the Aplysia giant neurone. J. Physiol. (London) 199:347-365, 1968.
84. Gerschenfeld, H. M. and D. Paupardin-Tritsch. Ion mechanisms and receptor properties underlying the responses of molluscan neurones to 5-hydroxytryptamine. J. Physiol. (London), 243:427-456, 1974.
85. Gillis, R. A., J. A. Quest, H. Thibodeaux, M. M. Clancy and D. E. Evans. Neural mechanisms involved in acetylcholinesterase-induced bradycardia. J. Pharmacol. Exp. Therap., 193:336-345, 1975.
86. Godfraind, J. M., H. Kawamura, K. Krnjevic and R. Pumain. Actions of dinitrophenol and some other metabolic inhibitors on cortical neurones. J. Physiol. (London), 215:199-222, 1971.
87. Goldman, D. E. Potential, impedance and rectification in membranes. J. Gen. Physiol., 27:37-60, 1943.
88. Gorman, A. L. F. and M. F. Marmor. Long-term effect of ouabain and sodium pump inhibition on a neuronal membrane. J. Physiol. (London), 242:49-60, 1974.

89. Grillo, M. A., L. Jacobs and J. H. Comroe, Jr. A combined fluorescence histochemical and electron microscopic method for studying special monoamine-containing cells (SIF cells). *J. Comp. Neurol.*, 153:1-14, 1974.
90. Grossmann, W. and I. Jurna. The effects of diphenylthiohydantoin on the membrane potentials of rat sensory nerve fibre bundles. *Neuropharmacol.*, 13:819-827, 1974.
91. Grossman, Y., M. E. Spira and I. Parnas. Differential flow of information into branches of a single axon. *Brain Res.*, 64:379-386, 1973.
92. Grutizit, C. C., W. A. Fruyberger and G. K. Moe. The action of veriloid on carotid presso receptors. *J. Pharmacol. Exp. Therap.* 109:261-267, 1953.
93. Grundfest, H. Ionic mechanisms in electrogenesis. *N.Y. Acad. Sci., Annals*, 94:405-457, 1961.
94. Haapanen, L., G. M. Kolmodin and C. R. Skoglund. Membrane and action potentials of spinal interneurons in the cat. *Acta Physiol. Scand.*, 43:315-348, 1958.

95. Hagiwara, S. and N. Saito. Membrane potential change and membrane current in supramedullary nerve cell of puffer. *J. Neurophysiol.*, 22:204-221, 1959.
96. Hagiwara, S., K. Toyama and H. Hayashi. Mechanisms of anion and cation permeations in the resting membrane of a barnacle muscle fiber. *J. Gen. Physiol.*, 57:408-434, 1971.
97. Hashimura, W. and E. B. Wright. Effect of ionic environment on excitability and electrical properties of frog single nerve fiber. *J. Neurophysiol.*, 21:24-44, 1958.
98. Hays, E. A., M. A. Lang and H. Gainer. A re-examination of the Donnan distribution as a mechanism for membrane potentials and potassium and chloride ion distributions in crab muscle fibers. *Comp. Biochem. Physiol.*, 26:761-792, 1968.
99. Henn, F. A., H. Haljamäe and A. Hamberger. Glial cell function: Active control of extracellular  $K^+$  concentration. *Brain Res.*, 43:437-443, 1972.
100. Hild, W. and I. Tasaki. Morphological and physiological properties of neurons and glial cells in tissue culture. *J. Neurophysiol.*, 25:277-304, 1962.

101. Hillarp, N.-Å. Peripheral autonomic mechanisms. (J. Field, Ed.), American Physiological Society, Washington, D.C., Handbook of Physiology, Section 1, Chapter 38, 1960.
102. Hille, B. The selective inhibition of delayed potassium currents in nerve by tetraethylammonium ion. J. Gen. Physiol., 50:1287-1302, 1967.
103. Hille, B. Potassium channels in myelinated nerve. Selective permeability to small cations. J. Gen. Physiol., 61:669-686, 1973.
104. Hillman, H., W. J. Campbell and H. McIlwain. Membrane potentials in isolated and electrically stimulated mammalian cerebral cortex. J. Neurochem., 10:325-339, 1963.
105. Hillman, H. and H. Hydén. Membrane potentials in isolated neurones in vitro from Deiter's nucleus of rabbit. J. Physiol. (London), 177:398-410, 1965.
106. Hirst, G. D. S and I. Spence. Calcium action potentials in mammalian peripheral neurones. Nature New Biol., 243:54-56, 1973.

107. Hodgkin, A. L. and P. Horowicz. The influence of potassium and chloride ions on the membrane potential of single muscle fibres. *J. Physiol. (London)*, 148:127-160, 1959.
108. Hodgkin, A. L. and A. F. Huxley. Action potentials recorded from inside a nerve fibre. *Nature*, 144:710-711, 1939.
109. Hodgkin, A. L. and A. F. Huxley. A quantitative description of membrane current and its application to conduction and excitation in nerve. *J. Physiol. (London)* 117:500-544, 1952.
110. Hodgkin, A. L. and A. F. Huxley. Movement of radioactive potassium and membrane current in a giant axon. *J. Physiol. (London)* 121:403-414, 1953.
111. Hodgkin, A. L. and B. Katz. The effect of sodium ions on the electrical activity of the giant axon of the squid. *J. Physiol. (London)*, 108:37-77, 1949.
112. Hodgkin, A. L. and R. D. Keynes. Active transport of cations in giant axons from Sepia and Loligo. *J. Physiol. (London)* 128:28-60, 1955.
113. Honerjäger, P. Electrophysiological effects of various ceveratrum alkaloids on single nerve axons. *Naunyn-Schmiedeberg's Arch. Pharmacol.*, 280:391-416, 1973.

114. Huizar, P., M. Kuno and Y. Miyata. Electrophysiological properties of spinal motoneurons of normal and dystrophic mice. *J. Physiol. (London)*, 248:231-246, 1975.
115. Hunt, C. C. and M. Kuno. Properties of spinal interneurons. *J. Physiol. (London)*, 147:346-363, 1959.
116. Hunt, C. C. and P. G. Nelson. Structural and functional changes in the frog sympathetic ganglion following cutting of the presynaptic nerve fibres. *J. Physiol. (London)*, 177:1-20, 1965.
117. Huxley, A. F. and R. Stämpfli. Effect of potassium and sodium on resting and action potentials of single myelinated nerve fibres. *J. Physiol. (London)*, 122:496-508, 1951.
118. Ichioka, M. The effects of calcium ions upon the size of the action current of single myelinated nerve fibres of the toad. *Jap. J. Physiol.*, 7:20-28, 1957.
119. Ito, M. The electrical activity of spinal ganglion cells investigated with intracellular microelectrodes. *Jap. J. Physiol.*, 7:297-323, 1957.

120. Ito, M. An analysis of potentials recorded intracellularly from the spinal ganglion cell. *Jap. J. Physiol.*, 9:20-32, 1959.
121. Ito, M., T. Hongo, M. Yoshida, Y. Okada and K. Obata. Intracellularly recorded antidromic responses of Deiters' neurones. *Experientia*, 20:295-296, 1964.
122. Ito, M. and T. Oshima. Temporal summation of after-hyperpolarization following a motoneurone spike. *Nature*, 195:910-911, 1962.
123. Ito, M. and T. Oshima. Electrical behaviour of the motoneurone membrane during intracellularly applied current steps. *J. Physiol. (London)*, 180:607-635, 1965.
124. Ito, M. and M. Saiga. The mode of impulse conduction through the spinal ganglion. *Jap. J. Physiol.*, 9:33-42, 1959.
125. Jacobs, L. and J. H. Comroe, Jr. Reflex apnea, bradycardia and hypotension produced by serotonin and phenyldiguanide acting on the nodose ganglia of the cat. *Circ. Res.*, 29:145-155, 1971.
126. Jansen, J. K. S. and J. G. Nicholls. Conductance changes, an electrogenic pump and the hyperpolarization of leech neurones following impulses. *J. Physiol. (London)*, 229:635-655, 1973.



127. Julien, R. M. and L. M. Halpern. Stabilization of excitable membrane by chronic administration of diphenylhydantoin. *J. Pharmacol. Exp. Therap.*, 175:206-212, 1970.
128. Kandel, E. R., W. A. Spencer and F. J. Brinley, Jr. Electrophysiology of hippocampal neurons. I. Sequential invasion and synaptic organization. *J. Neurophysiol.*, 24:225-242, 1961.
129. Kandel, E. R. and L. Tauc. Anomalous rectification in the metacerebral giant cells and its consequences for synaptic transmission. *J. Physiol. (London)*, 183:287-304, 1966.
130. Katz, B. Nerve, Muscle, and Synapse. McGraw-Hill Book Co., New York, 1966.
131. Kerkut, G. A. and R. W. Meech. The effect of ions on the membrane potential of snail neurones. *Comp. Biochem. Physiol.*, 20:411-429, 1967.
132. Kernell, D. The adaptation and the relation between discharge frequency and current strength of cat lumbosacral motoneurons stimulated by long-lasting injected currents. *Acta Physiol. Scand.*, 65:65-73, 1965.

133. Keynes, R. D. Chloride in the squid giant axon. *J. Physiol.* (London), 169:690-705, 1963.
134. Keynes, R. D. and J. M. Ritchie. The movements of labelled ions in mammalian non-myelinated nerve fibres. *J. Physiol.* (London), 179:333-367, 1965.
135. Klee, M. R. and D. S. Faber. Mephenesin blocks early inward currents and strychnine-induced multiple discharges of aplysia neurons. *Pflügers Arch.*, 346:97-106, 1974.
136. Kleinhaus, A. L. and J. W. Prichard. Calcium dependent action potentials produced in leech retzius cells by tetraethylammonium chloride. *J. Physiol.* (London), 246:351-361, 1975.
137. Koike, H., Y. Okada and T. Oshima. Accommodative properties of fast and slow pyramidal tract cells and their modification by different levels of their membrane potential. *Exp. Brain Res.*, 5:189-201, 1968.
138. Koketsu, K. Calcium and the excitable cell membrane. *Neuroscience Res. Program*, 2:1-39, 1969.
139. Koketsu, K., J. A. Cerf and S. Nishi. Effect of quaternary ammonium ions on electrical activity of spinal ganglion cells in frogs. *J. Neurophysiol.*, 22:177-194, 1959.

140. Koketsu, K., J. A. Cerf and S. Nishi. Further observations on electrical activity of frog spinal ganglion cells in sodium-free solutions. *J. Neurophysiol.*, 22:693-703, 1959.
141. Koketsu, K. and I. Koyama. Membrane responses of frog's spinal ganglion cells in calcium-free solutions. *J. Physiol. (London)*, 163:1-12, 1962.
142. Koketsu, K., S. Nishi and H. Soeda. Effects of calcium ions on prolonged action potentials and hyperpolarizing responses. *Nature*, 200:786-787, 1963.
143. Koketsu, K., S. Nishi and H. Soeda. Calcium and acetylcholine-potential of bullfrog sympathetic ganglion cell membrane. *Life Sciences*, 7:955-963, 1968.
144. Kosterlitz, H. W., G. M. Lees and D. I. Wallis. Resting and action potentials recorded by the sucrose-gap method in the superior cervical ganglion of the rabbit. *J. Physiol. (London)*, 195:39-53, 1968.
145. Kosterlitz, H. W. and D. I. Wallis. The action of morphine-like drugs on impulse transmission in mammalian nerve fibres. *Br. J. Pharmacol.*, 22:499-510, 1964.

146. Krebs, H. A. Untersuchungen über den stoffwechsel der aminosäuren im tierkörper. Höpfe-Seyler's Z. Physiol. Chem., 217:191-227, 1933.
147. Krebs, H. A. and K. Henseleit. Untersuchungen über die harnstoffbildung im tierkörper. Höpfe-Seyler's Z. Physiol. Chem., 210:33-66, 1932.
148. Kriz, N., E. Sykova, E. Ujec and L. Vyklicky. Changes of extracellular potassium concentration induced by neuronal activity in the spinal cord of the cat. J. Physiol. (London), 238:1-15, 1974.
149. Krnjevic, K. and A. Lisiewicz. Injections of calcium ions into spinal motoneurons. J. Physiol. (London), 225:363-390, 1972.
150. Larrabee, M. G. and J. M. Posternak. Selective action of anaesthetics on synapses and axons in mammalian sympathetic ganglia. J. Neurophysiol. 15:91-114, 1952.
151. Letbetter, W. D., and W. D. Willis. Electrophysiological characteristics of cat dorsal root ganglion cells. Physiologist, 12:283, 1969.

152. Levitan, H. and J. L. Barker. Effect of non-narcotic analgesics on membrane permeability of molluscan neurons. *Nature New Biol.*, 239:55-57, 1972.
153. Ling, G. and R. W. Gerard. The normal membrane potential of frog sartorius fibers. *J. Cell. Comp. Physiol.*, 34:383-396, 1949.
154. Llinas, R., R. Baker and W. Precht. Blockage of inhibition by ammonium acetate action on chloride pump in cat trochlear motoneurons. *J. Neurophysiol.*, 37:522-532, 1974.
155. Lux, H. D. and D. A. Pollen. Electrical constants of neurons in the motor cortex of the cat. *J. Neurophysiol.*, 29:207-220, 1966.
156. Lowenstein, W. R. (ed.). *Handbook of Sensory Physiology: Principles of Receptor Physiology*, Vol. 1. Springer-Verlag, New York, 1971.
157. Martin, A. R. and G. Pilar. Dual mode of synaptic transmission in the avian ciliary ganglion. *J. Physiol. (London)*, 168:443-463, 1963.

158. Meech, R. W. Intracellular calcium injection causes increased potassium conductance in Aplysia nerve cells. *Comp. Biochem. Physiol.*, 42A, 493-499, 1972.
159. Meech, R. W. Calcium influx induces a post-tetanic hyperpolarization in Aplysia neurones. *Comp. Biochem. Physiol.*, 48A:387-395, 1974.
160. Mei, N. Disposition anatomique et propriétés électro-physiologiques des neurones sensitifs vagues chez le chat. *Exp. Brain. Res.*, 11:465-479, 1970.
161. Murray, M. R. and Stout, A. P. Adult human sympathetic ganglia cells cultivated in vitro. *Am. J. Anat.*, 80:225-273, 1947.
162. Nakajima, S. Adaptation in stretch receptor neurons of crayfish. *Science*, 146:1168-1170, 1964.
163. Nakajima, S., S. Iwasake and K. Obata. Delayed rectification and anomalous rectification in frog's skeletal muscle membrane. *J. Gen. Physiol.*, 46:97-115, 1962.

164. Nakajima, S. and K. Onodera. Membrane properties of the stretch receptor neurones of crayfish with particular reference to mechanisms of sensory adaptation. *J. Physiol. (London)*, 200:161-185, 1969.
165. Narahashi, T., H. G. Haas and E. F. Therrien. Saxitoxin and tetrodotoxin: comparison of nerve blocking mechanism. *Science*, 157:1441-1442, 1967.
166. Narahashi, T., J. W. Moore and R. N. Poston. Anesthetic blocking of nerve membrane conductances by internal and external applications. *J. Neurobiol.*, 1:3-22, 1969.
167. Nelson, P. G. and K. Frank. Anomalous rectification in cat spinal motoneurons and effect of polarizing currents on excitatory postsynaptic potential. *J. Neurophysiol.*, 30:1097-1113, 1967.
168. Nelson, P. G. and H. D. Lux. Some electrical measurements of motoneuron parameters. *Biophysical J.*, 10:55-73, 1970.
169. Nelson, P. G. and J. H. Peacock. Electrical activity in dissociated cell cultures from fetal mouse cerebellum. *Brain Res.*, 61:163-174, 1973.

170. Nelson, P. G., J. H. Peacock and T. Amano. Responses of neuroblastoma cells to iontophoretically applied acetylcholine. *J. Cell. Physiol.*, 77:353-362, 1971.
171. Nelson, P. G., J. H. Peacock, T. Amano and J. Minna. Electrogenesis in mouse neuroblastoma cells in vitro. *J. Cell. Physiol.*, 77:337-352, 1971.
172. Nernst, W. Zur theorie des elektrischen reizes. *Pflügers Arch.*, 122:275-314, 1908.
173. Nishi, K. and C. Eyzaguirre. Effects of atropine on chemoreceptor discharges in the carotid body of the cat. *Brain Res.*, 23:292-297, 1970.
174. Nishi, K. and C. Eyzaguirre. The action of some cholinergic blockers on carotid body chemoreceptors in vivo. *Brain Res.*, 33:37-56, 1971.
175. Nishi, S. and K. Koketsu. Electrical properties and activities of single sympathetic neurons in frogs. *J. Cell. Comp. Physiol.*, 55:15-30, 1960.



176. Nishi, S., S. Minota and A. G. Karczmar. Primary afferent neurones: the ionic mechanism of GABA-mediated depolarization. *Neuropharmacol.*, 13:215-219, 1974.
177. Nishi, S. and H. Soeda. Hyperpolarization of a neurone membrane by barium. *Nature*, 204:761, 1964.
178. Nishi, S., H. Soeda and K. Koketsu. Effect of alkali-earth cations on frog spinal ganglion cell. *J. Neurophysiol.*, 28:457-472, 1965.
179. Ohta, M., T. Narahashi and R. F. Keeler. Effects of veratrum alkaloids on membrane potential and conductance of squid and crayfish giant axons. *J. Pharmacol. Exp. Therap.*, 184:143-154, 1973.
180. Okun, L. M. Isolated dorsal root ganglion neurons in culture: cytological maturation and extension of electrically active processes. *J. Neurobiol.*, 3:111-151, 1972.
181. Paintal, A. S. Vagal afferent fibers. *Ergebn. Physiol.*, 52:74-156, 1963.
182. Partridge, L. D. and R. C. Thomas. Effect of intracellular lithium on snail neurones. *Nature*, 249:578-580, 1974.

183. Peacock, John H., P. G. Nelson and M. W. Goldstone. Electro-physiologic study of cultured neurons dissociated from spinal cords and dorsal root ganglia of fetal mice. *Developmental Biology*, 30:137-152, 1973.
184. Perri, V., O. Sacchi and C. Casella. Electrical properties and synaptic connections of the sympathetic neurons in the rat and guinea-pig superior cervical ganglion. *Pflügers Arch.*, 314:40-54, 1970.
185. Phillips, C. G. Intracellular records from Betz cells in the cat. *Quart. J. Exp. Physiol.*, 41:58-84, 1956.
186. Ploeger, E. J. and A. Den Hertog. The effects of lithium on excitable cell membranes. II. The effect on the electrogenic sodium pump of non-myelinated nerve fibres of the rat. *Eur. J. Pharmacol.*, 21:24-29, 1973.
187. Rang, H. P. and J. M. Ritchie. On the electrogenic sodium pump in mammalian non-myelinated nerve fibres and its activation by various external cations. *J. Physiol. (London)*, 196:183-221, 1968.

188. Rang, H. P. and J. M. Ritchie. The ionic content of mammalian non-myelinated nerve fibres and its alteration as a result of electrical activity. *J. Physiol. (London)*, 196:223-236, 1968.
189. Rall, W. Membrane time constant of motoneurons. *Science*, 126:454, 1957.
190. Ranson, S. W., J. O. Foley and C. D. Alpert. Observations on the structure of the vagus nerve. *Amer. J. Anat.*, 53:289-315, 1933.
191. Rasmussen, H. Cell communication, calcium ion and cyclic adenosine monophosphate. *Science*, 170:404-412, 1970.
192. Richens, A. The action of general anesthetic agents on root responses of the frog isolated spinal cord. *Br. J. Pharmacol.*, 36:294-311, 1969.
193. Richens, A. Microelectrode studies in the frog isolated spinal cord during depression by general anaesthetic agents. *Br. J. Pharmacol.*, 36:312-328, 1969.
194. Richter, D. W., F. Heyde and M. Gabriel. Intracellular recordings from different types of medullary respiratory neurons of the cat. *J. Neurophysiol.*, 38:1162-1171, 1975.

195. Richter, D. W., R. W. Schlue, K.-H. Mauritz and A. C. Nacimiento. Comparison of membrane properties of the cell body and the initial part of the axon of phasic motoneurons in the spinal cord of the cat. *Exp. Brain Res.*, 21:193-206, 1974.
196. Ritchie, J. M. and R. W. Straub. The hyperpolarization which follows activity in mammalian non-medullated fibres. *J. Physiol. (London)*, 136:80-97, 1957.
197. Rubio, R. and G. Zubieta. The variation of the electric resistance of microelectrodes during the flow of current. *Acta Physiol. Latino Amer.*, 11:91-94, 1961.
198. Sampson, S. R. and R. A. Jaffe. Excitatory effects of 5-hydroxytryptamine, veratridine and phenyldiguanide on sensory ganglion cells of the nodose ganglion of the cat. *Life Sci.*, 15:2157-2165, 1974.
199. Sato, M. and G. Austin. Intracellular potentials of mammalian dorsal root ganglion cells. *J. Neurophysiol.*, 24:569-582, 1961.
200. Sawa, M., Maruyama, N., S. Kaji and T. Hanai. Action of stimulation to medullary pyramids on single neurons in cat's motor cortex. *Folia Psychiatr. Jap.*, 14:315-346, 1960.

201. Schauf, C. L., F. A. Davis and R. L. Kesler. Actions of the antidepressant drug imipramine on the voltage-clamped Myxicola giant axon. J. Pharmacol. Exp. Therap., 193:669-675, 1975.
202. Schlue, W. R., D. W. Richter, K.-H. Mauritz and A. C. Nacimiento. Mechanisms of accommodation to linearly rising currents in cat spinal motoneurons. J. Neurophysiol., 37:310-315, 1974.
203. Scott, B. S., V. E. Engelbert and K. C. Fisher. Morphological and electrophysiological characteristics of dissociated chick embryonic spinal ganglion cells in culture. Exp. Neurol., 23:230-248, 1969.
204. Seeman, P. The membrane actions of anesthetics and tranquilizers. Pharmacol. Rev., 24:583-655, 1974.
205. Somjen, G. G. and M. Gill. The mechanism of the blockade of synaptic transmission in the mammalian spinal cord by diethyl ether and by thiopental. J. Pharmacol. Exp. Therap., 140:19-30, 1963.
206. Somjen, G. G., S. P. Herman and R. Klein. Electrophysiology of methyl mercury poisoning. J. Pharmacol. Exp. Therap., 186:579-592, 1973.

207. Spector, William S. (ed.) Handbook of Biological Data.  
W. B. Saunders Co., Philadelphia, 1956.
208. Spencer, W. A. and E. R. Kandel. Electrophysiology of hippocampal neurons. III. Firing level and time constant.  
J. Neurophysiol., 24:260-271, 1961.
209. Spencer, P. S., C. S. Raine and H. Wisniewski. Axon diameter and myelin thickness - unusual relationships in dorsal root ganglia. Anat. Rec., 176:225-243, 1973.
210. Spyropoulos, C. S. and I. Tasaki. Nerve excitation and synaptic transmission. Ann. Rev. Physiol., 22:407-432, 1960.
211. Stämpfli, R. Is the resting potential of Ranvier nodes a potassium potential? Ann. N.Y. Acad. Sci. 81:265-284, 1959.
212. Svaetichin, G. Electrophysiological investigation on single ganglion cells. Acta Physiol. Scand. Suppl., 24:23-57, 1951.
213. Svaetichin, G. Component analysis of action potentials from single neurons. Exp. Cell Res., Suppl. 5:234-261, 1958.

214. Tagini, G. and E. Camino. T-Shaped cells of dorsal ganglia can influence the pattern of afferent discharge. *Pflügers Arch.*, 344:339-347, 1973.
215. Tasaki, I., S. Hagiwara, and A. Watanabe. Action potentials recorded from inside a Mauthner cell of the catfish. *Jap. J. Physiol.*, 4:79-90, 1954.
216. Tasaki, K., Y. Tsukahara, S. Ito, M. J. Wayner and W. Y. Yu. A simple, direct and rapid method for filling microelectrodes. *Physiol. Behav.*, 3:1009-1010, 1968.
217. Tashiro, N. and S. Nishi. Effects of alkali-earth cations on sympathetic ganglion cells of the rabbit. *Life Sci.*, 11:941-948, 1972.
218. Thomas, R. C. Electrogenic sodium pump in nerve and muscle cells. *Physiol. Rev.*, 52:563-594, 1972.
219. Trachtenberg, M. C. and P. A. Pollen. Neuroglia: biophysical and physiologic function. *Science*, 167:1248-1252, 1970.
220. Tsiquaye, K. N. and A. J. Zuckerman. Maintenance of adult Rhesus monkey motor neurons in tissue culture. *Cytobios*, 9:207-215, 1974.

221. Vallbo, Å. B. Accommodation related to inactivation of the sodium permeability in single myelinated nerve fibres from Xenopus laevis. Acta Physiol. Scand., 61:429-444, 1964.
222. Van Essen, D. C. The contribution of membrane hyperpolarization to adaptation and conduction block in sensory neurones of the leech. J. Physiol. (London), 230:509-534, 1973.
223. Varon, S. and C. Raiborn. Excitability and conduction in neurons of dissociated ganglionic cell cultures. Brain Res., 30:83-98, 1971.
224. Werblin, F. S. Anomalous rectification in horizontal cells. J. Physiol. (London), 244:639-657, 1975.
225. Wespi, H. H. Active transport and passive fluxes of K, Na, and Li in mammal non-myelinated nerve fibres. Pflügers Arch., 306:262-280, 1969.
226. Woodbury, J. W. and H. D. Patton. Electrical activity of single spinal cord elements. Cold Spr. Harb. Symp. Quant. Biol., 17:185-188, 1952.



227. Woodbury, J. W. and P. R. Miles. Anion conductance of frog muscle membranes: one channel, two kinds of pH dependence. *J. Gen. Physiol.* 62:324-353, 1973.
228. Woodward, J. K., C. P. Bianchi and S. D. Erulkar. Electrolyte distribution in rabbit superior cervical ganglion. *J. Neurochem.*, 16:289-299, 1969.
229. Zollman, J. R. and H. Gainer. Electrophysiological properties of nerve cell bodies in the sixth abdominal ganglion of the Maine lobster, Homarus americanus. *Comp. Biochem. Physiol.* 38A:407-433, 1971.

FIGURE 1. Diagram of perfusion chamber. Upper figure, top view; lower figure, side view. A: perfusate input tube; B: water jacket input; C: central well for superfusion of nodose ganglion; D: oil-filled stimulating well for infranodose vagus and branches; E: oil-filled stimulating well for supranodose vagus; F: channel for temperature-monitoring thermistor; G: water jacket output; H: water jacket; I: pin jacks attached to platinum stimulating electrodes; J: perfusate output. Chamber dimensions: 8 cm x 6 cm x 2.5 cm

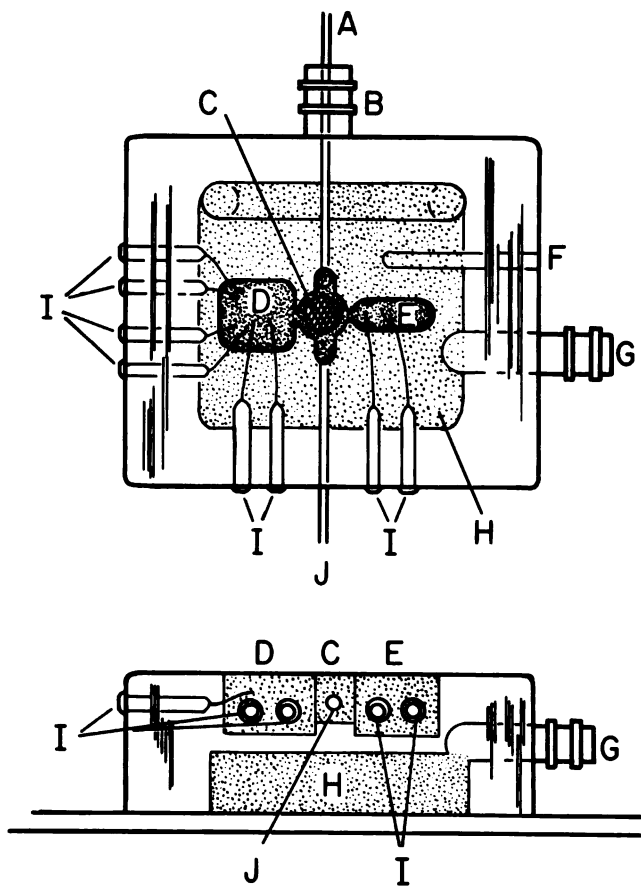


FIGURE 2. The effect of current passage on electrode resistance. The points represent the values (mean  $\pm$  S.E.) for changes in electrode resistance, expressed as a percentage of the original resistance (ordinate), for 30 electrodes (15 filled with 3M KCl and 15 filled with 5M KAc) during the passage of current (I, in nA; abscissa). Negative values = hyperpolarizing current.

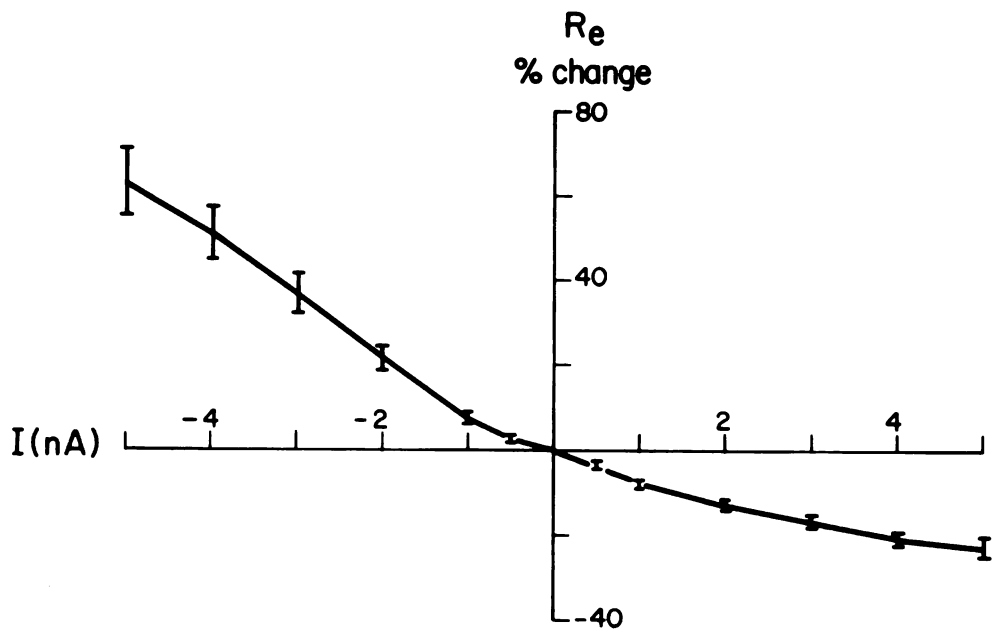


FIGURE 3. Distribution of resting membrane potentials recorded in vitro from neurons in nodose ganglia of rabbits (A) and cats (B).

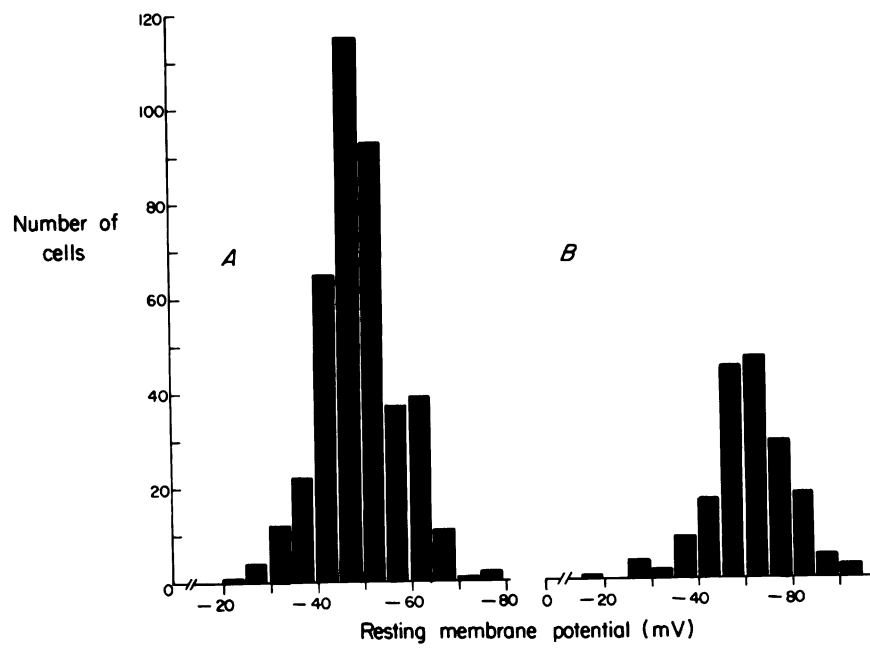


FIGURE 4. Responses of a neuron in the rabbit nodose ganglion to 2 depolarizing and 7 hyperpolarizing current pulses (25 msec duration) applied through the recording electrode. Upper traces, current pulses; lower traces, membrane potentials. The records were photographically superimposed. Current was applied in 0.2 nA steps to a maximum of 1.4 nA. Resting membrane potential was approximately -50 mV. Horizontal bar = 5 msec. Vertical bar = 20 mV.



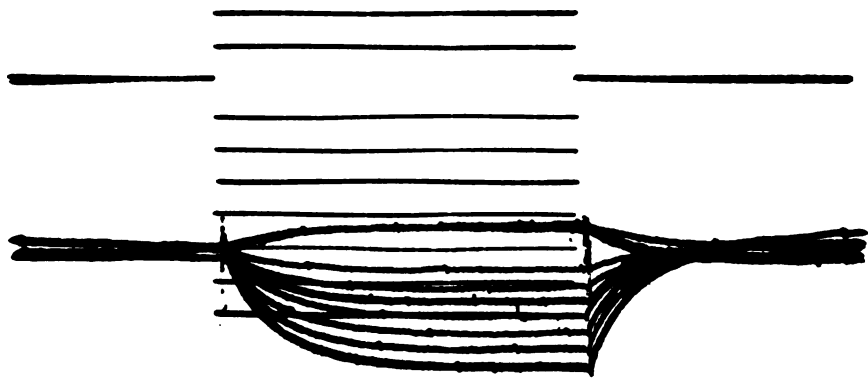


FIGURE 5. Examples of current - voltage relations in neurons from cat (A) and rabbit (B) nodose ganglia. The points represent the change in membrane potential (mV, ordinate) in response to 20-30 msec current pulses (nA, abscissa) passed intracellularly through the recording electrode. The input resistance of the neuron in A was calculated to be  $17 \text{ M}\Omega$ , and that of the neuron in B was  $30 \text{ M}\Omega$ .

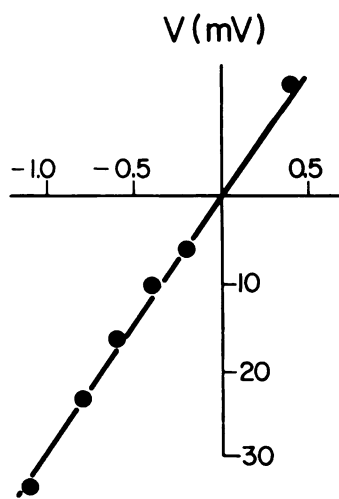
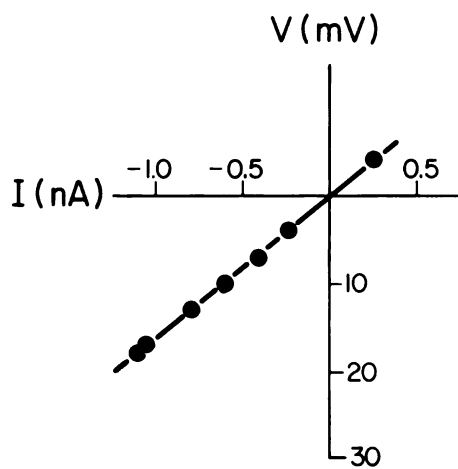


FIGURE 6. Plot of input resistance ( $M\Omega$ ) as a function of membrane potential of a neuron in the nodose ganglion of the cat. The control resting membrane potential was -50 mV. Input resistance was calculated from the change in membrane potential in response to a 20 msec current pulse (1 nA), while the membrane potential was clamped to each level along the abscissa by the passage of steady current through the electrode. Input resistance decreased during steady depolarization but was essentially unchanged during steady hyperpolarization.

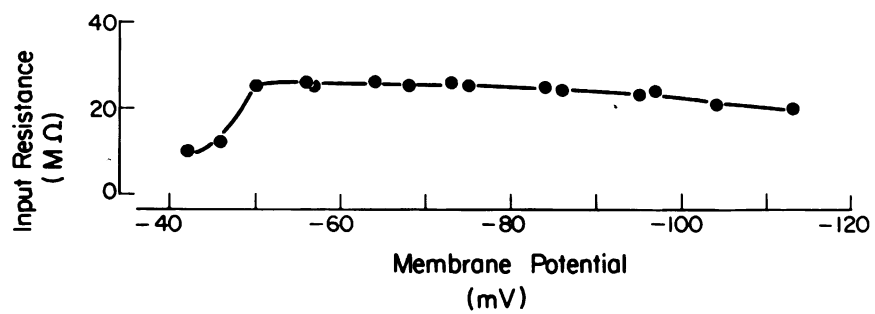


FIGURE 7. Example of rectifying behavior in a cat sensory neuron. The membrane responds to a square-wave hyperpolarizing current pulse of 2 nA magnitude and 80 msec duration with a delayed decrease in membrane resistance. Calibration pulse at beginning of trace: 5 msec duration, 10 mV amplitude. Resting membrane potential = -50 mV.



FIGURE 8. Examples of action potentials recorded intracellularly from neurons in the nodose ganglion of cat (A) and rabbit (B). In vitro preparation. Each action potential was evoked by electrical stimulation of the infranodose vagus nerve (stimulus artifact). Transmembrane resting potential was -53 mV in A, and -48 mV in B. Calibration pulse at beginning of each trace = 10 mV and 5 msec.



A



B

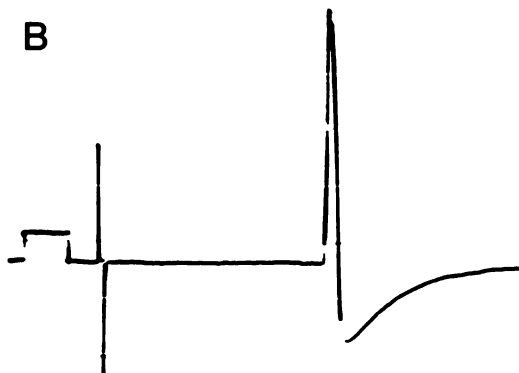


FIGURE 9. Three superimposed traces of action potentials recorded intracellularly from a neuron (resting potential = -51 mV) in the cat nodose ganglion in vitro. The traces show delay and subsequent failure of the generation of somatic spikes in response to repetitive stimulation of the infranodose vagus nerve at a frequency of 10 Hz. Note that afterhyperpolarizations occur with somatic spikes but not with the IS spike. Upper trace represents 0 mV. Calibration pulse at the beginning of the lower trace = 10 mV and 5 msec.

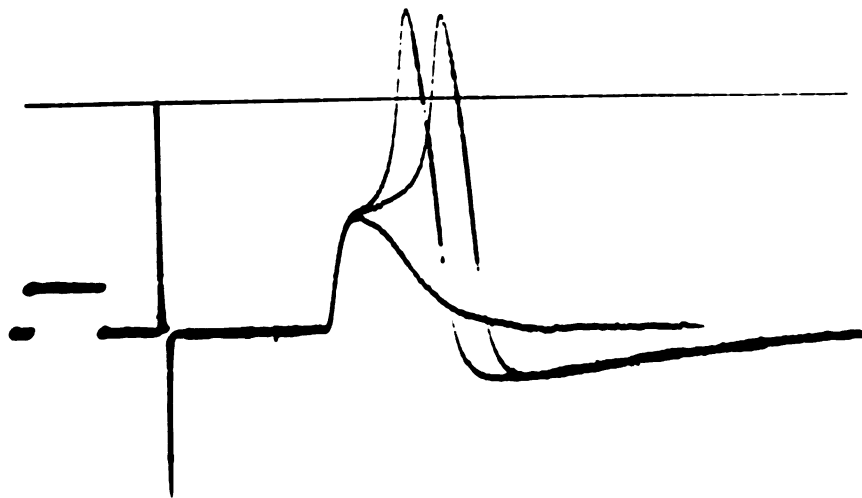


FIGURE 10. An example of an action potential evoked in a nodose ganglion neuron (rabbit) by depolarizing current applied through the recording electrode. Resting potential = -55 mV. Two superimposed traces are shown. The depolarizing pulse was just at threshold for spike generation. Calibration pulse = 10 mV and 5 msec.

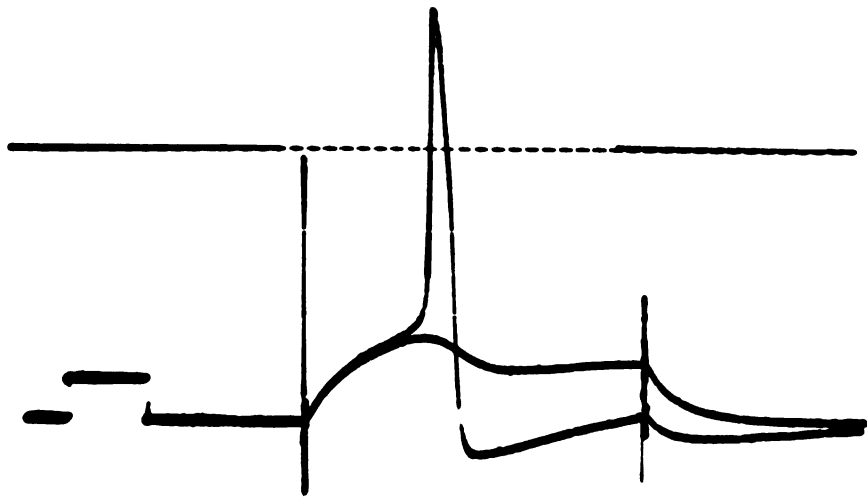
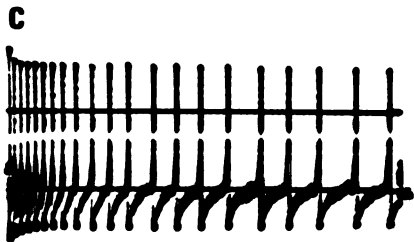
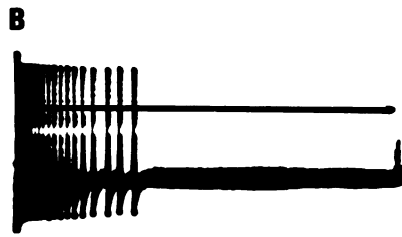
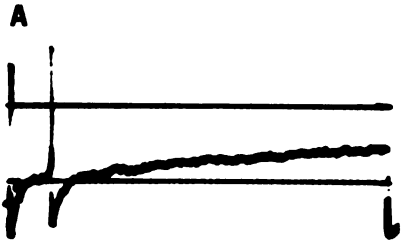


FIGURE 11. Adaptation types. A. Type I neuron; B. Type II neuron; C. Type III neuron; D. Type IV neuron. Stimulus duration (trace duration) = 1 sec in A and 5 sec in B-D. Cat nodose ganglia. Upper horizontal trace is the zero reference line and the lower horizontal trace is the -40 mV reference line. Stimulus strength = 3-10 times rheobasic current.



1977

WILSON DOCUMENTS

1977

1977



FIGURE 12. The effect of stimulus intensity on spike frequency in a slowly adapting (type IV) neuron from a cat nodose ganglion. Stimulus intensity was changed in a stepwise manner (upper trace). A typical "off-response" can be seen at some of the step transitions. Horizontal bar = 1 sec; vertical bar = 50 mV.

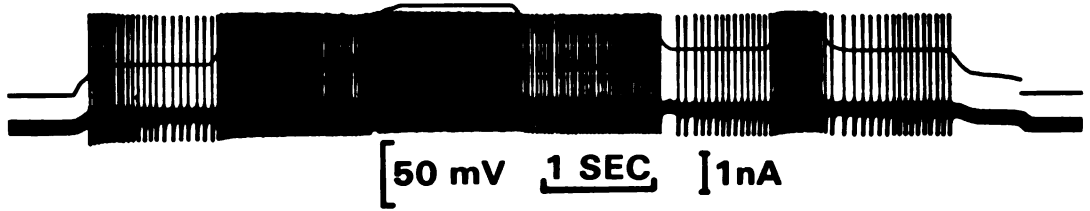


FIGURE 13. Blockade of somatic spike in a cat nodose ganglion neuron by passage of hyperpolarizing current (1.0 nA) through the recording electrode. The somatic action potential was evoked by stimulation of the infranodose vagus. Calibration pulse = 10 mV and 5 msec. (The horizontal traces represent 0, -40 and -80 mV).



FIGURE 14. Effects of steady changes in membrane potential on the afterhyperpolarization of a cat nodose ganglion neuron. The control afterhyperpolarization is shown in B (resting potential = -50 mV). In A, the neuron was depolarized and in C-F progressively hyperpolarized. The reversal potential for the afterhyperpolarization was -70 mV (D). Calibration pulse in each record = 10 mV and 5 msec.

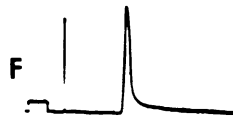
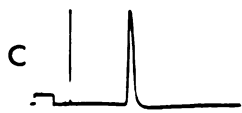
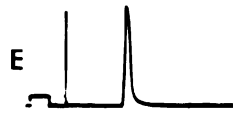
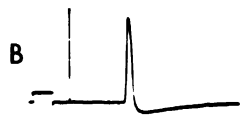
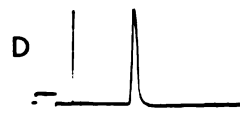
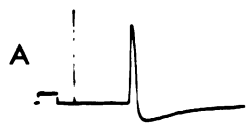


FIGURE 15. Examples of activity-induced hyperpolarization in rabbit nodose ganglion neurons. A, in vitro; during stimulation of the infranodose vagus at a frequency of 10 Hz, the membrane potential hyperpolarized from a resting level of -48 mV to -60 mV, and returned to the resting level 4 sec after stimulation was stopped. (There is a gap of 1.5 sec between the upper and lower film records of A). B, in vivo; intracellular recording of spontaneous action potentials in a nodose ganglion neuron from an unidentified peripheral receptor. With activity, the transmembrane potential hyperpolarized from -50 mV at rest to -57 mV. Note that there was occasional somatic failure, which may have been due to the hyperpolarization. Membrane potential returned to the resting level about 2.5 sec after the end of spontaneous activity. Upper horizontal line is the 0 mV reference and lower horizontal line is the -40 mV reference. C, an example of activity hyperpolarization in a cat nodose ganglion neuron recorded on a Grass polygraph. Stimulus frequency = 2 Hz changing to 1 Hz at the arrow; horizontal bar = 10 sec; vertical bar = 10 mV. Resting membrane potential = -42 mV; membrane potential at 1 Hz = -46 mV.

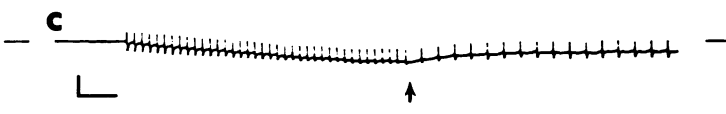
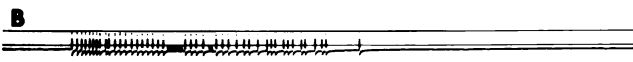
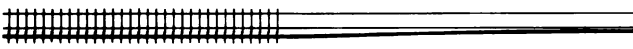




FIGURE 16. Histogram of latency to onset of somatic spikes induced by electrical stimulation of the infranodose vagus nerve in vitro.

Number of cells

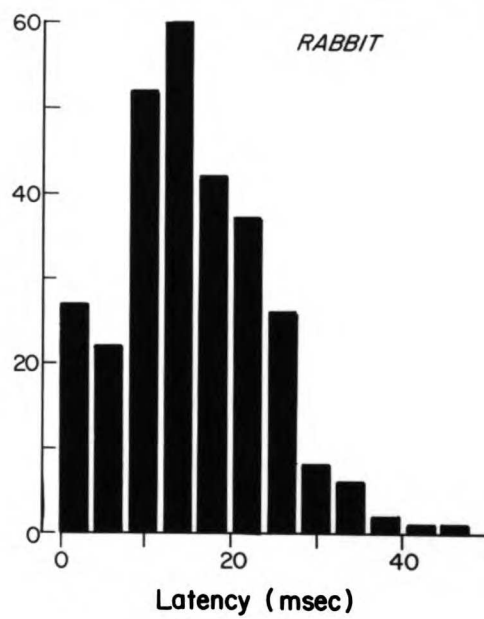
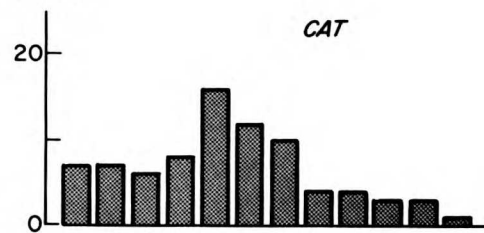


FIGURE 17. Histogram comparison of latency and conduction velocity distributions in cat nodose ganglion neurons. The conduction velocity bin intervals were selected to correspond to the opposite latency intervals, assuming a total conduction distance of 12 mm.

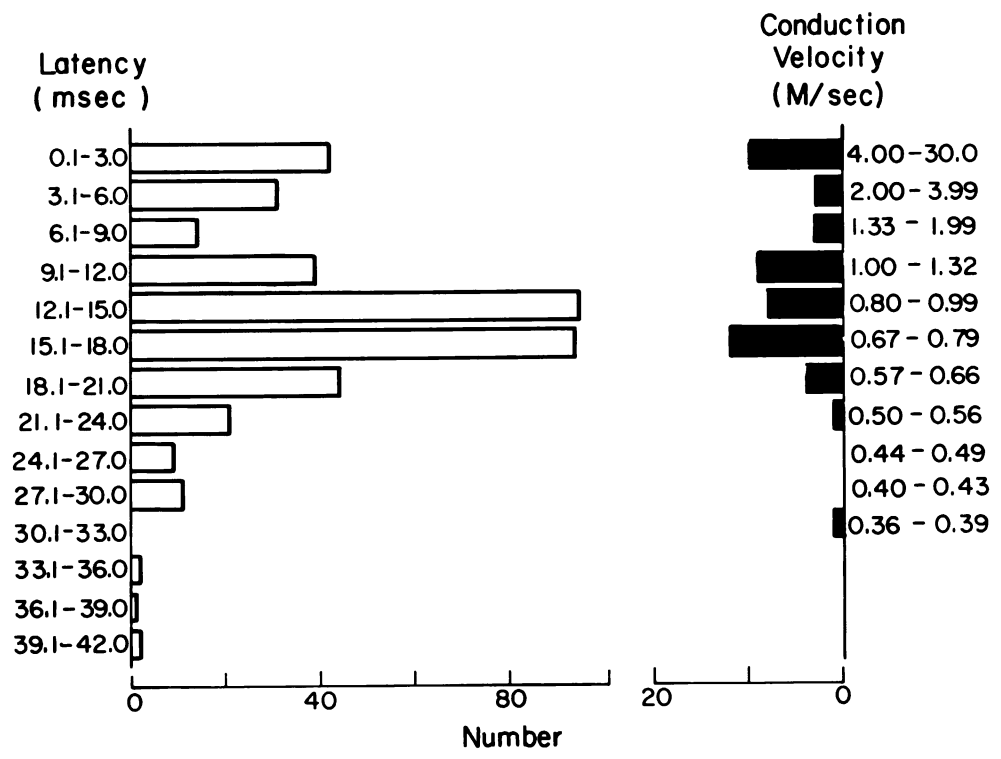


FIGURE 18. Effects of varying external potassium concentration on the resting membrane potential, afterhyperpolarization, and membrane resistance in cat nodose ganglion neurons. Each point shows the mean and standard error of the mean. See methods and results sections for complete details. Arrow indicates normal external potassium concentration.

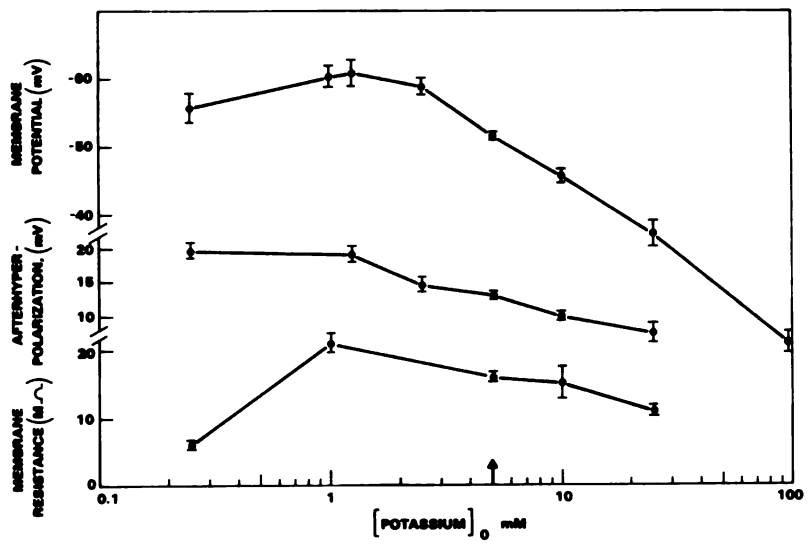
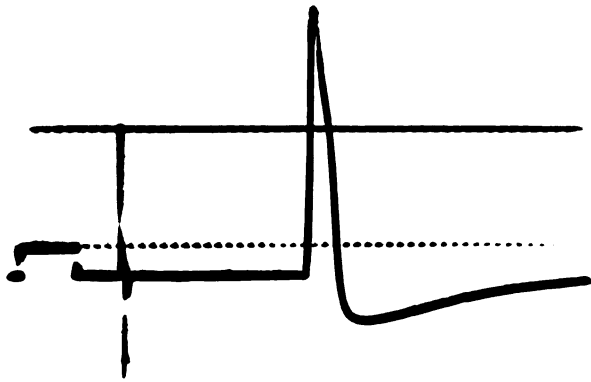
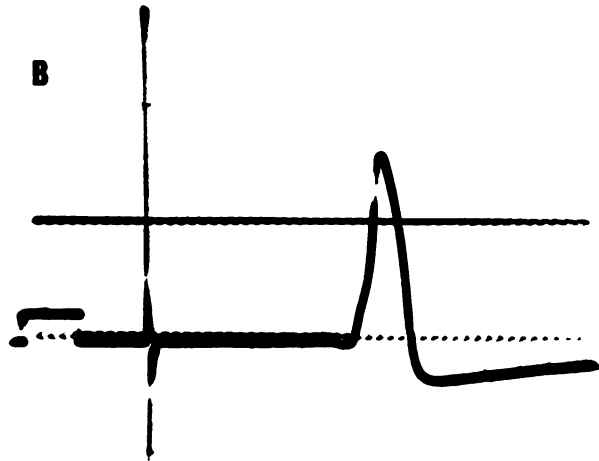


FIGURE 19. Effects of low external sodium ion concentration on action potential configuration in a cat nodose ganglion neuron. A. normal sodium concentration (150 mM);  $V_m = -49$  mV. B. low sodium concentration (34.4 mM);  $V_m = -42$  mV. Calibration pulse = 10 mV and 5 msec.

**A**



**B**





73072-7

FIGURE 20. Effects of TEA. A. Control spike; B. 24 sec after exposure to TEA ( $1 \times 10^{-5}$  gm/ml); C. 2 min 6 sec of exposure; D. Removal of TEA from external medium begins after 2 min 32 sec total exposure; E. 24 sec after wash-out begins; F. 5 min 12 sec spike nearly back to control configuration. Calibration pulses = 10 mV and 5 msec. Upper trace = 0 mV reference; lower trace = -40 mV reference.

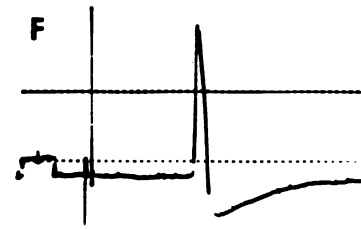
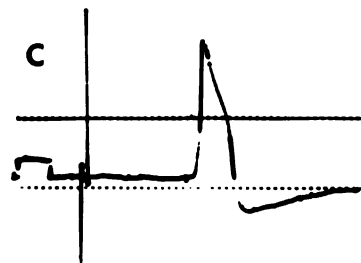
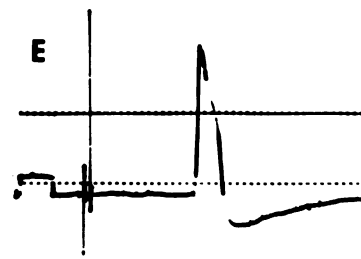
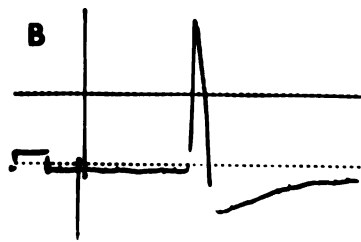
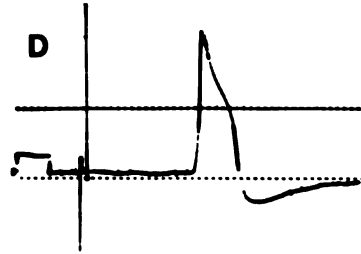
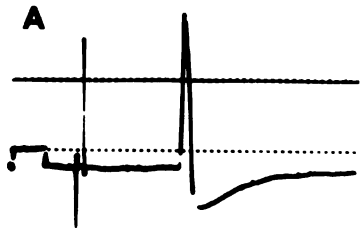


FIGURE 21. Effects of Lidocaine. A. Control spike; B. 25 sec after exposure to lidocaine ( $2 \times 10^{-6}$  gm/ml, the first sign of spike failure develops; C. At 27 sec soma spike failure is complete; D. 1 min 27 sec after removal of lidocaine; E. 2 min 25 sec: soma spike recovery begins; F. 3 min 55 sec after return to normal bathing medium. Calibration pulses = 10 mV and 5 msec. Upper trace = 0 mV reference; lower trace = -40 mV reference.

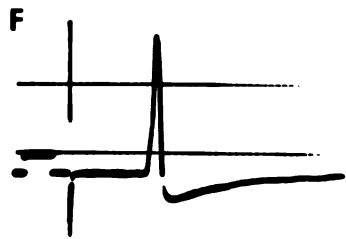
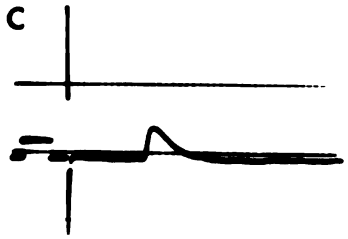
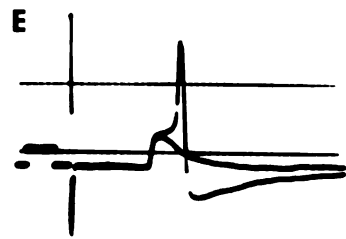
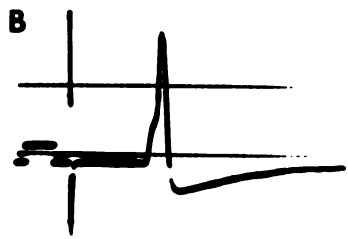
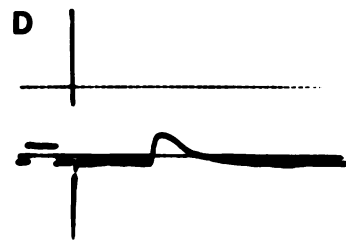
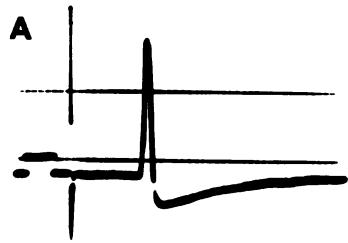


FIGURE 22. Effects of Atropine. A. Control spike; B. Spike failure occurs 2 min 15 sec after start of atropine ( $10^{-5}$  gm/ml) exposure; C. Complete soma spike failure occurs at 2 min 44 sec; D. 20 sec after atropine removal recovery is nearly complete. Calibration pulses = 10 mV and 5 msec. Upper trace = 0 potential reference; lower trace = -40 mV reference.

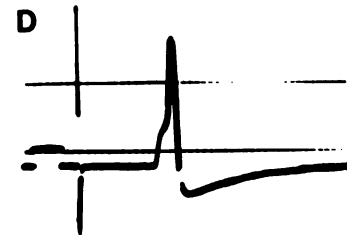
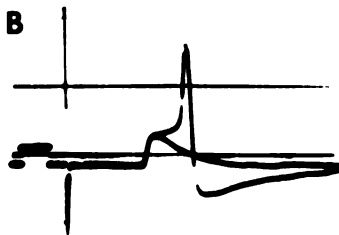
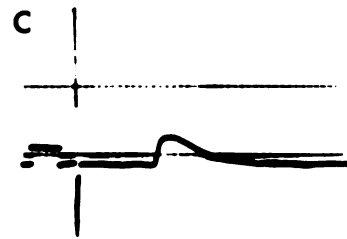
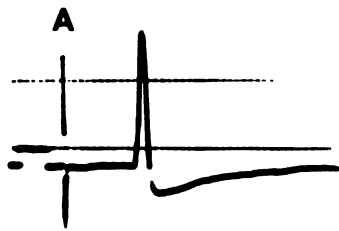


FIGURE 23. Effects of veratridine in the external perfusing medium. This figure consists of three superimposed traces each showing a calibration pulse (10 mV; 5 msec) followed by an intracellularly stimulated action potential with its associated afterpotential. In the first two traces the large depolarizing afterpotential failed to cause the generation of additional spikes. The third time that the cell was stimulated, however, the afterdepolarization was associated with the generation of a train of action potentials lasting several seconds. Upper trace = -40 mV reference line;  $V_m$  = -57 mV; cat.



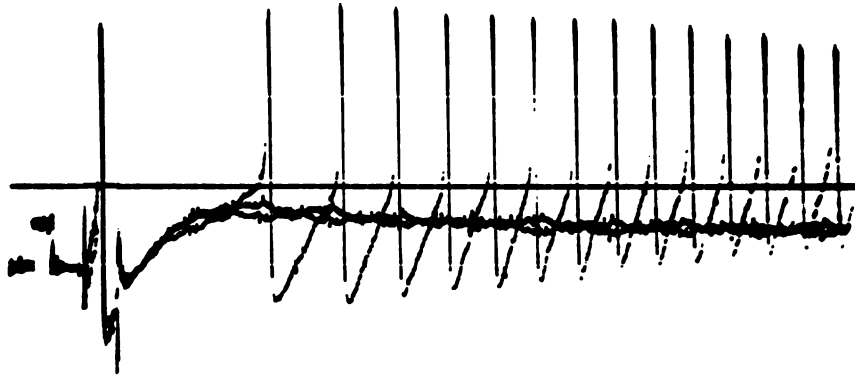


FIGURE 24. A train of action potentials generated in the presence of veratridine and in response to a single action potential (arrow) evoked by a stimulus applied to the infranodose vagus nerve. The subsequent spontaneous activity lasted 4.5 sec and was followed by a gradual repolarization of the resting potential.

